JRC Scientific and Technical Reports

# NEMEA-5
# Neutron measurements, Evaluations and Applications

Nuclear data for sustainable nuclear energy
Proceedings of the CANDIDE workshop
27-29 October 2008

**Edited by Arjan Plompen**

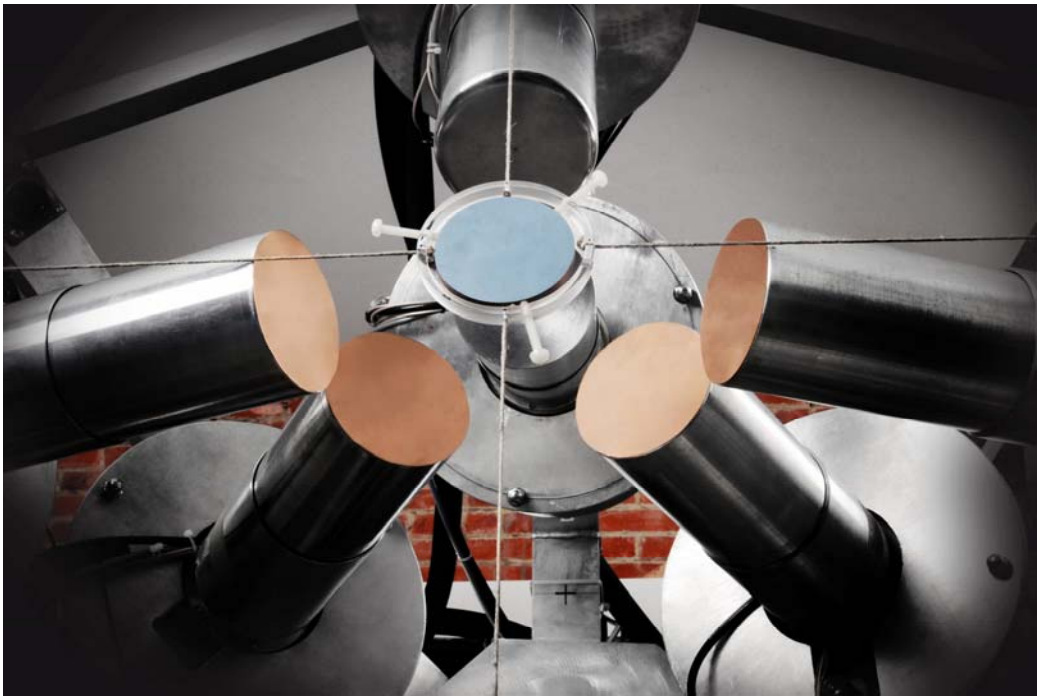

EUR 24692 EN - 2011

JRC
EUROPEAN COMMISSION

irmm
Institute for Reference Materials and Measurements

The mission of the JRC-IRMM is to promote a common and reliable European measurement system in support of EU policies.

European Commission
Joint Research Centre
Institute for Reference Materials and Measurements

**Contact information**
Address: A.J.M. Plompen, European Commission, Joint Research Centre, Institute for Reference Materials and Measurements, Retieseweg 111, 2440 Geel, Belgium
E-mail: Arjan.Plompen@ec.europa.eu
Tel.: +32 (0) 14 571 381
Fax: +32 (0) 14 584 273

http://irmm.jrc.ec.europa.eu/
http://www.jrc.ec.europa.eu/



JRC 62727

EUR 24692 EN
ISBN 978-92-79-19067-4
ISSN 1018-5593
doi:10.2787/36236

Luxembourg: Publications Office of the European Union



*Printed in Luxemburg*

# NEMEA-5
# Neutron measurements, Evaluations and Applications

Nuclear data for sustainable nuclear energy
Proceedings of the CANDIDE workshop
27-29 October 2008

**Edited by Arjan Plompen**

# Foreword

October 27-29, 2008, the workshop NEMEA-5 was held at the M-hotel in Ljubljana, Slovenia. The fifth edition of this workshop on Neutron Measurements, Evaluations and Applications was organised on behalf of the European coordination action CANDIDE by the Institute for Reference Materials and Measurements of the Joint Research Centre. CANDIDE is the Coordination Action for Nuclear Data for Industrial Development in Europe that focusses at establishing nuclear data needs from an industry point of view for the near and midterm future. It has a strong networking component to mobilise researchers to address those needs. As such, the workshops NEMEA-4 and NEMEA-5 are important vehicles of CANDIDE networking activities. In particular, NEMEA-5 addresses the state-of-the-art in nuclear data production methods.

NEMEA-5 has "Nuclear data for sustainable nuclear energy" as subtitle. In particular, its purpose was to comment on the way forward in addressing the nuclear data needs identified by Subgroup 26 of the Nuclear Energy Agency of the Organisation for Economic Cooperation and Development in the context of advanced reactor development. Of course in the context of CANDIDE and this workshop a wider range of data needs is considered than addressed by the subgroup; the fuel cycle, the need for ADS and the interest in fusion were addressed, as well.

The NEMEA series of workshops were initiated as an enlargement initiative of the Joint Research Centre. They have been organised in Candidate Countries and New Member States of the European Union and facilitated attendance of scientists from these new parts of the EU. Also on this occasion the enlargement aspect was important, as witnessed by the venue of and attendance to the workshop. This time the main support for this aspect is from CANDIDE and the ensuing sponsorship of the Research Directorate General of the European Commission.

I would hereby like acknowledge the support of the program advisory committee, H. Aït Abderrahim of SCK-CEN, Belgium, E. Bauge of CEA/Bruyères-le-Châtel, G. Barreau of CENBG CNRS/IN2P3, Bordeaux, J. Blomgren of the University of Uppsala, Sweden, F. Gunsing of CEA/Saclay, H. Harada of JAEA, Tokai-mura, Japan, R.C. Haight of LANL, USA, R. Jacqmin of CEA, France, A. Koning of NRG, The Netherlands, R.W. Mills of Nexia Solutions, UK, A. Nichols of the IAEA, M. Salvatores of CEA, France, FZK, Germany and ANL, USA. I would also like to thank the workshop secretary C. Cabanillas Platero and the team of the IRMM Management support unit responsible for NEMEA-5 for their contributions to the organisation of this workshop.

Arjan Plompen
December 2010

# Contents

# Integral measurement of $^{235}$U isomer activation by inelastic fission neutron scattering

*G.Bélier[1)], N.Authier[4)], J.A.Becker[3)], E.Bond[2)],* D.Hyneck[4)], *X.Jacquet[4)], Y.Jansen[4)], J.Legendre[4)], R.Macri[3)], V.Méot[1)], D.J.Vieira[2)], J.B.Wilhelmy[2)]*

1) CEA, DAM DIF, F-91297 Arpajon, France
2) Los Alamos National Laboratory, Los Alamos, NM 87545, USA
3) Lawrence Livermore National Laboratory, Livermore, CA 94550, USA
4) CEA, DAM, VALDUC, F-21120 Is-sur-Tille, France
gilbert.belier@cea.fr

***Abstract:*** The integral measurement of the $^{235}$U isomer activation cross section in a fission-like neutron spectrum is presented. The experiment has been performed at a pulsed reactor with a dedicated electron detector, and by using the activation technique. The samples preparation, efficiency measurements, irradiations and isomer decay measurement will be presented. Preliminary results on the activation cross section will be given and compared to evaluations performed at Bruyères le Châtel and at Los Alamos.

## Introduction

The uranium 235 first excited state has an uncommonly low excitation energy which is 76.5 eV (Fig. 1). Hence the isomeric transition to the ground state is highly converted. The measurement of its activation by (n,n') reaction gives the opportunity to test $\gamma$ cascade models since it's spin is very different from the ground state one. Moreover the isomer fission cross section is known to be different from that of the ground state at thermal neutron energy [1]. Hence the knowledge of its population by inelastic neutron scattering can be important for practical applications where high neutron fluxes are involved. For the same reason its excitation by electromagnetic processes in hot dense plasmas was investigated from an experimental point of view [2] as well as from a theoretical one [3].
This presentation reports on the measurement of the integral inelastic neutron scattering $^{235}U^{m}$ activation cross section. The experiment was performed at the pulsed critical reactor CALIBAN (CEA/VALDUC laboratory in France), that has a fission-like neutron spectrum. The isomer detection was done with a dedicated electron detector which was built for an experiment aiming at measuring the $^{235}U^{m}$ activation by the NEET effect in a plasma[2,3].

## Detection system

The $^{235}$U $1/2^{+}$ isomer decay to the $7/2^{-}$ ground state by an E3 transition, and due to this high multipolarity and to its very low excitation energy, the transition is completely converted. The outmost electron shells are implied in this decay with binding energies ranging from 4.6 to 44 eV. Finally the outgoing electrons have energies of no more than 71.9 eV. Since the outmost electron shells are involved the isomer half-life is very dependant on the chemical environment. Reference [4] has shown a 10% effect on it, depending on the oxidation state of the atom. It has also been shown that it depends on the metal in which the isomer is implanted[5]. The common adopted value for this half-life is 26 minutes. In such a situation the measurement of the $^{235}$U isomer activation is very peculiar. One has to detect electrons with very low energies, and for cross section measurements, when a minimum mass is needed no spectroscopy can be done on these electrons. Hence the only observable that can be used to identify the isomer is the half-life. The knowledge of this parameter is of prime importance, together with the control of the background.
The detector that has been built for measuring this activation is depicted in the left part of Figure 1. It is based on an electrostatic deviator and a channeltron electron multiplier (photonis X9551BL). The electrostatic part deflects and accelerates the electrons from few electronvolts to 1.5 keV. It also allows focusing the electrons from a 5 cm$^2$ sample on the channeltron whose entrance area is 2.5 cm$^2$.

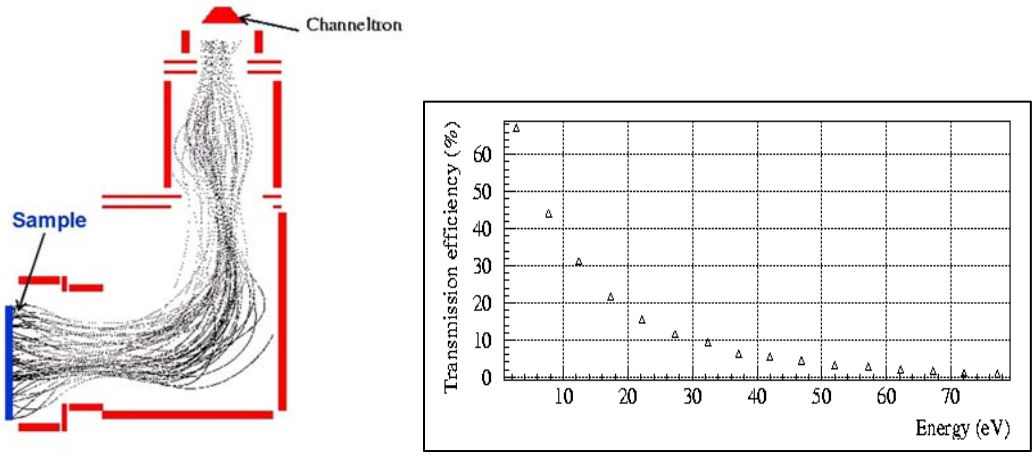


***Figure 1.*** *Left : Detector scheme. Right: Electron transmission curve*

In the right part of Figure 1 the simulated transmission efficiency from the sample position to the channeltron is presented. Since the converted electron energies are very degraded in the sample, this apparatus is very adapted to the $^{235}$U isomer decay measurement. Moreover it minimizes the background due to alpha or beta decays that generate secondary electrons. A grid at the entrance of the electrostatic deviator allows measuring the ingoing electrons spectra by applying different voltages.

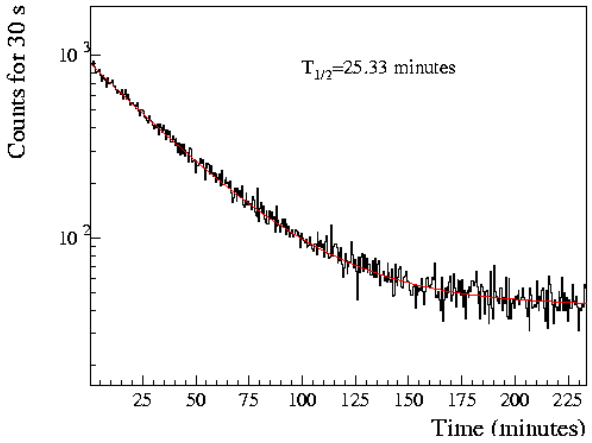


***Figure 2.*** *Example of time spectra showing the $^{235}$U isomer decay.*

In order to minimize the time needed for sample introduction, a vacuum interlock system was used. For the same reason a cryogenic-pump was chosen to have a maximum pump capacity. Only few minutes were needed to introduce the sample and to start the electron counting. The signal from the channeltron was amplified by an Ortec 113 preamplifier and then shaped by a Tennelec TC244 amplifier. The data acquisition system from Fast Comtec is based on the ADC 7074 NIM module, linked by a multiparameter MPA-3 interface to a PC windows computer. This system time-stamps every event, so that time spectra can be constructed. In this experiment bidimensionnal histograms where built from the pulse height amplitude and time parameters. The dwell time for the time spectra was 30s. Figure 2 shows a typical time spectra obtained by counting a $^{235}$U isomer sample.

## Efficiency measurement

In order to characterize the isomer detection efficiency the recoil method has been used to produce $^{235}U^{m}$ samples. A $^{239}$Pu mother sample was used since every alpha decay feed the $^{235}$U isomer. This sample was thin enough (23 Å) to allow the $^{235}U^{m}$ atoms to recoil out of it. These recoiling ions were implanted onto a 1000 Å thick NaCl deposit, which was then dissolved with an electroplating solution. Before making the sample a known amount of $^{235}$U was added to this isomer solution, using a calibrated $^{235}$U solution. The $^{239}$Pu mother sample

activity was $A_{Pu}$=(2.27±0.07).$10^5$ Bq[1]. This mother source was also traced with $^{241}$Pu (2.38±0.98)x$10^6$ Bq in order to measure the collection efficiency. The implanted $^{237}$U activity was measured by γ spectrometry and a collection efficiency of $\varepsilon_c$= 0.31±0.03 was obtained. This value is in accordance with the calculated solid angle of 0.31. For each prepared sample an alpha spectrometry of the final $^{235}$U sample was performed in order to obtain its mass together with the plating efficiency $\varepsilon_p$. Figure 2 shows an example of the time decay measured with the detector for sample prepared by this procedure. The decay was fitted using the function $f(t) = P_1 + P_2 * \exp(-t / T_{1/2} * \ln(2))$. The isomer half-life $T_{1/2}$ was fixed according to the known value obtained from all the measurements made with the same backing. For samples electrodeposited on Ti foils the half life was measured to be 25.33±0.04. For isomers implanted in NaCl it is 28.33±0.04. The amplitude $P_2$ of the isomer decay is then used to calculate the isomer detection efficiency by using the formula:

$$\varepsilon_e = \frac{P_2}{30 \times A_{Pu} \times \varepsilon_p \times \varepsilon_c} \times \frac{\exp\left(t_{cool} / \tau_1\right)}{1 - \exp\left(-t_{coll} / \tau_2\right)}$$

Where $t_{cool}$ and $t_{coll}$ are respectively the cooling and collection durations, $\tau_1$ is the averaged isomer half-life during sample cooling and $\tau_2$ the half-life in sodium chloride.

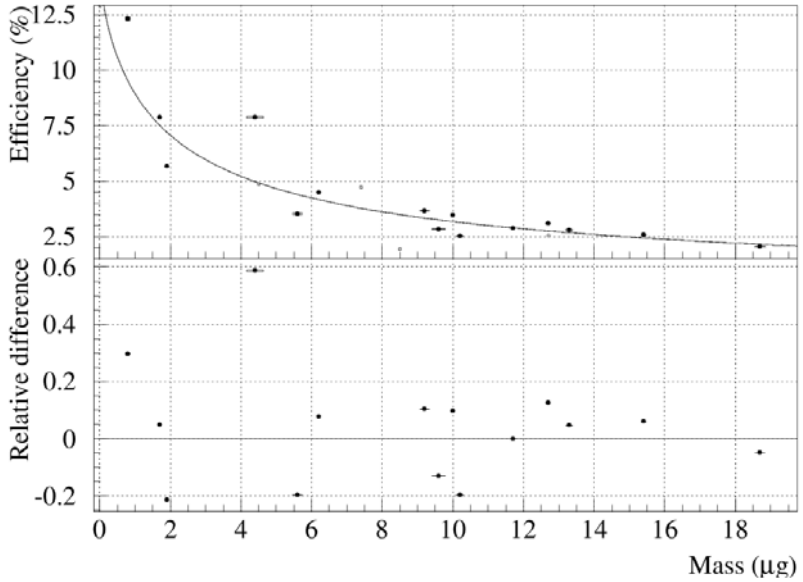


***Figure 3.*** *Isomer detection efficiency against sample mass.*

Figure 3 shows the isomer detection efficiency against mass together with the adjusted curve used for the cross section analysis:

$$\varepsilon_{isomer} = \frac{23.3}{m^{0.761} + 1.61} \qquad \textbf{Eq 1.}$$

One can see that the experimental measurements are very fluctuating. The rms value of the residues between these points and the fitted curve is around 13%. RBS analyses were performed on most of the samples in order to establish a link between these fluctuations and samples parameters (non-uniformities, Pt contaminations). No correlation could be established between these parameters and the efficiency variation. We concluded that these fluctuations were due to surface contaminations.

## Activation measurement

The CALIBAN pulsed reactor located at the CEA Valduc laboratory in France was chosen because it is able to deliver a neutron integrated flux of 3.$10^{14}$ n/cm$^2$ in a fast 60 µs neutronic excursion. Moreover samples could be retrieved from the reactor cave after a cooling time of

[1] Every uncertainty given in this report is a 1σ uncertainty.

only 30 minutes. The neutron spectrum inside the central cavity is a near fission spectrum. Samples could also be irradiated outside the core in a neutron moderated flux by using polyethylene bricks. Such irradiations allowed to study background sources by changing the capture to fission cross sections ratio. In order to infer parasitic activations $^{236}U$, $^{238}U$ and blanks samples were irradiated in fast and/or slow spectra. A $^{238}U$ sample irradiated in a moderated flux showed a very pure $^{239}U$ activation with a measured half life of 23.42±0.44. This value agrees with the $^{239}U$ half life adopted value and prove that no exo-electrons are generated by neutron irradiation. The shots on $^{236}U$ samples showed that the detector was sensitive to secondary electrons generated by fission products. For most shots the neutron flux was measured by activated In foils. For some of the shots the $^{99}Mo$ fission product activity in the irradiated sample was measured by $\gamma$ spectrometry. The temperature rise T of the reactor is monitored by a thermocouple sensor for every shot providing a measurement of the core heating and a third flux measurement. The fluences ratios obtained from these 3 parameters T/In, In/$^{99}Mo$ and T/$^{99}Mo$ have respective rms of 1%, 9% and 9%. Because of low statistics for the $^{99}Mo$ counts the temperature rise measurement was used to measure the neutron flux in the final isomer activation cross section calculation.
Two kinds of shots were performed. The first ones were done with electrodeposited $^{235}U$ samples on thin Ti foils. These samples were then electron-counted. For the second ones stippled $^{235}U$ samples were irradiated before being dissolved again in order to perform a uranium-fission products chemical separation [6]. This last procedure was tested by irradiating $^{236}U$ samples with/without fission product removal. A suppression factor of at least 20 was obtained with this procedure.
For the $^{235}U$ shots the decay spectra was fitted using a two time constant decay in order to take into account the fission products decay. Again the $^{235}U$ isomer half life was fixed to the measured value obtained from the efficiency measurements. Nine shots with chemical separation and 8 shots without fission products removal were done. For every shot a cross section was obtained from the efficiency given by Eq 1, the measured neutron flux, the sample mass and the isomer count in the spectra. Only the $^{235}U$ samples with masses ranging from 5 to 20 µg were retained for the final analysis. Since no correlation was found between the efficiency variation and the thickness homogeneity a weighted averaged cross section was deduced for the 2 series of shots. Samples deposited on Ti foils could be shot several times. For the same sample, fluctuations of the order of the mentioned fluctuation on the detection efficiency were observed. This supports the idea that these fluctuations come from surface contamination, justifying the cross section averaging for measurement done with different masses. For shots with and without fission product removal the respective values of 1.10±0.25 and 1.06±0.27 barns were obtained. These results are preliminary and the sensitivity to the background has to be done.

## Conclusion

The $^{235}U^{m}$ activation cross section has been evaluated in Bruyères le Châtel[7] for neutron energies up to 10 MeV. The corresponding averaged cross section for the CALIBAN flux was calculated to be 0.87 barns. Hence the present measurement is in agreement with this evaluation. Such calculations were also performed at the Los Alamos laboratory[8] by taking two different hypothesis for the $\gamma$ transitions K-hindrances. The calculation allowing some K-mixing gives a much stronger cross section than when assuming no K-mixing. These calculations can not be compared with our measurement yet, since they were done for neutron energies lower than 1.8 MeV.

**References**

[1] V.I. Mostovoi, G.I. Ustroev, Atomnaia Energia 57 (1984) 241 ; W.L. Talbert, Jr. & al., Physical Review C 36(1987)1896 ; A.D'Eer & al. Phys. Rev. C38(1988)1270.
[2] V. Meot & al. CEA Report R-5944.
[3] P.Morel & al. Phys. Rev. A69(2004)06414.
[4] M.Neve de Mevergnies & al. Phys. Lett. B49(1974)428.
[5] Neve de Mevergnies & al. Phys. Rev. Lett. 29(1972)1188 ; V.V.Kol'tsov & al. Izvestiya Akademii Nauk SSSR S. Fiz. 53(1989)2085.
[6] E.Bond & al. J. of Rad. and Nucl. Chem. 276(2008)549.
[7] P.Romain Private communication.
[8] J.E. Lynn *& al.* LA-UR-01-426(2001)45.

# CANDIDE - Coordination Action on Nuclear Data for Industrial Development in Europe

*J. Blomgren[1)], E. Bauge[2)], D. Cano Ott[9)], S. Czifrus[5)], K. Dahlbacka[6)], I. Gonçalves[13)], E. Gonzalez[9)], H. Henriksson[15)], R. Jacqmin[2)], A. Koning[4)], D. Lecarpentier[12)], E. Malambu[8)], A. Mengoni[14)], R. Mills[11)], A. Plompen[3)], G. Rimpault[2)], V. Starý[7)], C. Trakas[10)], P. Vaz[13)], C. Zimmerman[11)]*

1) Department of Physics and Astronomy, Division of Applied Nuclear Physics, Uppsala University, Box 525, S-751 20 Uppsala, Sweden,
2) Commissariat à l'Energie Atomique, France
3) Joint Research Centre - Institute for Reference Materials and Measurements, EU
4) Nuclear Research and consultancy Group, the Netherlands
5) Budapest University of Technology and Economics, Hungary
6) Teollisuuden Voima Oy, Finland
7) Nuclear Research Institute Řež, Czech Republic
8) Studiecentrum voor Kernenergie · Centre d'étude de l'Energie Nucléaire, Belgium
9) Centro de Investigaciones Energéticas, Medioambientales y Tecnológicas, Spain
10) AREVA, France
11) Nexia Solutions, United Kingdom
12) Electricité de France, France
13) Instituto Tecnológico e Nuclear, Portugal
14) International Atomic Energy Agency, UN
15) Nuclear Energy Agency, OECD

Jan.Blomgren@fysast.uu.se

***Abstract:*** A Co-ordinated Action is in progress with the ambition to establish a durable network on nuclear data efforts that are important in the context of minimising the high-level waste stream of nuclear energy. This implies optimal incineration of all actinides that nowadays constitute spent nuclear fuel, in critical and sub-critical reactors. As a consequence, the scope of the project encompasses transmutation in fast critical reactors as well as sub-critical accelerator-driven systems (ADS). The purpose is to identify the needs for improved nuclear data, assess the present status of knowledge, and to estimate what accuracy can be reached with state-of-the-art techniques.

## Introduction

The EC-supported Coordination Action (CA) CANDIDE, Coordination Action on Nuclear Data for Industry Development in Europe, addresses the following two objectives:

- Establishment of better links between academia, research centres and industry end users of nuclear data. This is reflected in the project name.
- Assessment of nuclear data needs for advanced nuclear reactors. The emphasis is on the radioactive waste issue, i.e., either waste transmutation in critical or sub-critical devices or minimizing the production of nuclear waste in future nuclear reactors, as envisaged in some fast critical systems.

For a long time activities concerning all aspects of nuclear data for commercial nuclear power reactors, i.e., nuclear data production, theory, evaluation, validation and industrial use, have been part of a well-organized international community, monitored by large international organizations, like OECD. Recently, a new nuclear data community has been formed around the production of nuclear data for accelerator-driven systems, while the other ingredients of traditional nuclear data work (e.g. evaluation and validation) have to a large degree been

missing up to now. The present project aims at establishing links for this new community to the existing structure of coordinated nuclear data activities in general, and to provide links to industry in particular.
Another recent development in Europe has been the enlargement of the EU, which opens new possibilities in the realm of nuclear data. Integration - both of different research communities and between new and previous member states - is an important objective of the CANDIDE project. Moreover, improved training and integration are essential parts of the CA, exemplified by the development of a European course on nuclear data to be part of the project.
In the public literature, the concept of transmutation is quite often used in a restricted sense, synonymous to accelerator-driven systems for incineration of spent nuclear fuel. CANDIDE has been designed with the intention to consider transmutation in a broader, more general sense, i.e., incineration of spent nuclear fuel by changing the nature of the elements through nuclear reactions. As a consequence, the scope of the proposed CA will encompass transmutation in fast critical reactors as well as sub-critical systems (ADS).
The purpose of CANDIDE is not to produce new experimental data or evaluations, but to review the current modes of nuclear data production, assess the present status of our knowledge, estimate what accuracy can be reached with state-of-the-art numerical simulation techniques, identify the needs for improved nuclear data, and suggest appropriate actions to be taken to meet those needs. A large fraction of the existing data have been obtained far back in time, and it might be beneficial to identify cases where new experiments on already measured reactions could exploit technology improvements. Key input is expected from industrial partners, since they are closely involved in application of nuclear data libraries and their performance.
The final result of the CA will be a report describing the state-of-the-art and giving recommendations to EC outlining how nuclear data research should be organized in FP7 and beyond. Moreover, the organisation of workshops and a training course will lead to broader European involvement in the subject.

## Nuclear data for transmutation of spent nuclear fuel

In the public debate of today, the concept of *transmutation* has often become synonymous with accelerator-driven systems (ADS) for incineration of nuclear waste. This is not surprising, because ADS represents a very innovative option, while the use of critical reactors represent a more conventional alternative. In CANDIDE, however, we will consider transmutation in a very broad sense, not restricted to a particular system or scenario.
Presently, nuclear waste transmutation options are investigated as part of reactor and fuel cycle studies for existing reactor types (PWR, BWR, CANDU), i.e., GEN-III, for evolutionary designs of existing reactors, GEN-III+ (EPR, AP600, etc), for GEN-IV reactors (SFR, GFR, LFR, MSR, SCWR, VHTR) or for dedicated transmutation systems (such as ADS). All these activities generate a significant amount of nuclear data needs either for the feasibility phase of these studies or for the performance phase.
Up to now, there has been a very large research volume spent on data on neutron-induced nuclear reactions up to 20 MeV. This was carried out from around 1950 until today, and was motivated by the needs in the development of civil nuclear power, as well as weapons applications and fusion technology. During the last decade, nuclear data at higher energies have been in the limelight due to the discussions about ADS.
The approaches in these two disciplines differ significantly. This is neither a surprise nor a bad choice, because the underlying physics differs significantly, resulting in different research strategies. Below 20 MeV, a single cross section can be of paramount importance to the entire application. An example is the neutron capture resonance at 6.7 eV in $^{238}$U that provides the Doppler effect so important for the stability of critical reactors. Moreover, some cross sections are fundamentally inaccessible to theory, in particular in the resonance region. As a result, at low energies more or less complete data coverage for major elements is required. Above 20 MeV, the situation is fundamentally different. The cross sections are slowly varying in energy, and the behaviour of the system is always dictated by the sum of a large number of reactions, none of which strongly dominates the performance. Therefore, getting a grip on the overall picture has been a more natural ambition in an initial stage, rather than providing precision data on a single reaction.

Thanks to the nuclear data campaigns for ADS in FP5 and FP6, we have now reached a stage where such an overall picture, although fairly rough in many respects, is appearing. As a consequence, the uncertainty in modelling of various ADS concepts due to nuclear data uncertainties have decreased significantly during the last few years. There is, however, still plenty of room for improvement of ADS-relevant nuclear data, only part of which will be fulfilled by IP-EUROTRANS [1].

Up to now, nuclear data at the energies of critical reactors (less than 10 MeV) and accelerator-driven systems (up to 1 GeV) have not been systematically treated on an equal basis. The importance of this aspect was recently highlighted at the International Workshop on Nuclear Data Needs for Generation IV Nuclear Energy Systems [2], after which a WPEC subgroup was established to investigate the nuclear data needs for advanced reactor systems [3]. We find it important for the further development of nuclear data activities for transmutation, and even for the entire research on transmutation, that the nuclear data from these very different regimes can be compared and used in a consistent manner. This is a major underlying theme of CANDIDE.

In general, the safe, economical, and reliable operation of a nuclear reactor depends on the use of nuclear data to predict several important characteristics of plant operation. In the case of transmutation in general, the major benefit of accurate nuclear data relates specifically to avoiding unnecessary conservatism in design and operation such as shielding requirements, power coefficients for a core loaded with minor actinides, and the related power requirements of the proton accelerator for ADS systems.

Another important difference between a dedicated transmutation system - critical or sub-critical - and a conventional critical power reactor is that for the latter, deficiencies in detailed nuclear data can partly be overcome through normalizing calculations to existing reactor measurements or experience from the operation of prototypes and test rigs. The desire to pursue new designs (Gen-IV as well as ADS concepts) without performing extensive reactor experiments dictates using nuclear data that will support reactor calculations that give dependable results even without experimental re-normalization.

On a (very) broad level, the nuclear data requirements for transmutation of waste fall into two classes: (1) resonance and fast neutron reactions for materials that are specific to transmutation: unconventional structural materials, coolants and (in the case of ADS) targets, and minor actinides, whose abundance in the core is much larger than in a conventional reactor, (2) energy regimes that extend beyond the fast neutron region (up to hundreds of MeV) for the above materials and conventional materials. The first class applies to any transmutation method, i.e., including critical reactors, whereas the second class exclusively applies to ADS. In this project, we will consider both classes.

Although the motivation for the present project arises from waste minimization using novel reactor types, conventional power reactors can still benefit from the outcome of the CA. Indeed, nuclear data needs that apply to a critical power system, in general also apply to transmutation systems, critical as well as sub-critical. For example, the important interplay between $^{238}$U fission, capture and inelastic scattering, is crucial for a precise determination of criticality. Minimizing the uncertainties in these data is also important for transmutation systems. One interest of the CA is to identify needs that are common to various applications.

## Training and networking

CANDIDE is not limited to involvement of existing activities, but will also promote growth for the future. Therefore, an important part of the project has been the development of a dedicated training course on nuclear data for young professionals, the European course on EXperiment, Theory and Evaluation of Nuclear Data (EXTEND), that was held in Budapest in September 2008 (see fig. 1). The target group of this course are young professionals, primarily recently employed staff in industry and at research centres, as well as PhD students in the field. The course has been evaluated by a written questionnaire to the participants, and this revealed that the participants were very pleased with the course. The ambition is to make this a recurring event. This does, however, require sponsor support.

Summer schools in nuclear engineering (e.g., the Eugene Wigner School on Reactor Physics [4] within the ENEN [5] association or the Frédéric Joliot - Otto Hahn summer school [6]) are regularly organized, and there are relatively frequent summer schools on fundamental nuclear physics. Up to now, however, there have been few initiatives to bridge these two communities. EXTEND has been designed to fill this gap.

***Figure 1.*** *The participants in the EXTEND course.*

Besides the development of EXTEND, other activities on training and mobility of young industry professionals and researches, as well as European integration are also foreseen. The most visible example is the extension of the NEMEA workshops series, organized by IRMM, which are included in the CA. The previous NEMEA workshops have been targeting nuclear data research in Eastern Europe, but have now been enlarged to be open to all Europe. Our intention is to make these workshops meeting places for all European scientists in the field, including the nuclear industry, which has previously not been the case. The outcomes of two previous such workshops have been beneficial for the present proposal, in so far that they have promoted valuable links between old and new member states in general, and scientists from these in particular.

## Project strategy

As has been described above, we have identified possibilities to enlarge the nuclear data activities in Europe by integrating the new research communities (ADS research, new member and candidate states) into the already existing structures for nuclear data work, and CANDIDE will address these issues by organizing open workshops intended for bridging gaps between these communities. Moreover, the project itself has been designed to make industry a more visible player in the research-related activities via the top-down approach of CANDIDE. Last but not least, the development of a new course for young professionals is in line with these goals, but it is also intended to foster closer links between nuclear physics and reactor physics.

The project involves a wide range of industry partners. Three reactor construction or manufacturing organizations are represented. AREVA (France) is a leading manufacturer of nuclear reactors in Western Europe, having received widespread attention recently with the two EPRs under construction in Finland and France. The BNFL group (UK) has a wide range of reactors on its repertoire, gas-cooled reactors in the UK as well as light-water reactors (LWR) manufactured by Westinghouse. The Skoda corporation in the Czech Republic is constructing heavy structural parts to nuclear reactors, like reactor vessels, and are represented in the present CA via their technical support organization, NRI Řež.

Two power utilities, TVO (Finland) and EdF (France), participate in the project, representing light water reactor technology. Fuel manufacturing is represented by Nexia/BNFL and AREVA, while reprocessing is represented by Nexia/BNFL.
Design of future ADS-related facilities is represented by SCK•CEN (Belgium) and CIEMAT (Spain).
The validation (CEA Cadarache, NRG Petten) and evaluation (CEA Cadarache, CEA Bruyères-le-Châtel, NRG Petten) teams of the proposed CA represent leading European competence in the field. ITN (Portugal) contributes expertise in nuclear data related to spallation targets. The current-day computer power enables sophisticated nuclear reaction modelling and validation against integral experiments with both deterministic and Monte Carlo software.
On the experimental side, IRMM Geel is the dedicated EU lab for reactor-relevant nuclear data (0-20 MeV), while TSL Uppsala is the primary European facility for neutrons above 20 MeV (up to 200 MeV), which will cover important input for ADS neutronics.
With these partners, we cover the entire chain from industry to experiments, with a top-down approach. The industry partners define the needs from the end-users' perspective, and their participation guarantees that the work is application-oriented. The role of the non-industry partners is to assess the possibilities to provide data of sufficient quality to meet the application needs. As a consequence, the issue of which data is required or need to be improved is primarily an industry concern, while the question of how to reach those goals is mostly dealt with by the non-industry partners. Efficient dissemination is guaranteed by the involvement of the IAEA and OECD/NEA Data Banks.
Improved training, as well as integration of new member states, are important issues for the CA. Improvement of training on nuclear data is undertaken in close collaboration with European Nuclear Education Network (ENEN) [5], and it brings educational resources in old and new member states together. Additional integration is provided by the strong involvement of industry throughout Europe. Close contacts with the EFNUDAT [7] integrated infrastructure initiative have been established.

## Project scientific content

As outlined above, the project concerns the integration of nuclear data efforts for all types of transmutation-relevant nuclear systems, i.e., critical thermal and fast reactors, as well as accelerator-driven systems. Up to now, various nuclear-data projects have concentrated on different sub-sets of the global issue. In the present CA, we attempt to unify important aspects of these activities, with the ambition to provide a consistent basis for comparisons of various waste transmutation options.
A general approach to nuclear data for waste management would imply a very large project. To keep the task limited to a reasonable size, but still with the potential to provide results of relevance to the assessment of various transmutation strategies, the work has to be concentrated to a few issues that are of key importance to both fast critical reactors and ADS.
Up to now, the nuclear data research at classical reactor energies, up to 20 MeV, and the ADS-motivated research above 20 MeV have been conducted with very different approaches. This has made sense, because the pre-conditions have been very different. With the recent development in nuclear data for ADS, resulting from FP5 and FP6 projects, we believe it is now possible to conduct research on what is common to critical reactors and ADS.
A major unifying aspect is the role of neutrons. In both concepts, the major incineration is due to neutron-induced fission. Moreover, other neutron-induced reactions, like capture and scattering, play significant roles in all these techniques. Another common aspect is that the core will contain large amounts of minor actinides, although the composition differs among various systems. Furthermore, the design studies around GEN-IV type systems encompass not only the core but also the full fuel cycle. One important GEN-IV criterion is the reduction of radioactive waste that is competing against other criteria such as sustainability (full use of Uranium or Thorium ores), economics, safety and reliability, proliferation resistance and physical protection.
As a natural consequence of this, a study that could cover only the transmutation aspect of a core would not be complete. We therefore envisage the project to cover all nuclear data that have some relation to the reactors and their associated fuel cycles, whether they are dedicated specifically to transmutation (just like ADS) or if transmutation is only one of their key features.

In the present CA, we intend to assess the data situation for all neutron energies, from thermal and up to the highest available (200 MeV), both experimentally and theoretically. In the first instance, the focus of the CA should be on cores of fast reactors and ADS. Nuclear data are of great relevance also for irradiation effects on materials, radiation protection and a number of other issues. A possible list of data to be studied is given below:

- General purpose files that include (1) cross-sections induced by neutrons, protons and gammas, (2) secondary particle energy distributions, and (3) fission spectra and energy release.
- Gamma production induced by different reaction types.
- Fuel cycle data (fission yields, spallation yields, decay heat).
- Activation files.

Participants from nuclear industry give guidance on the proper parameters to be investigated and optimised. These needs should be translated into data evaluation and measurement requests, to be carried out in FP7 and beyond. Part of the effort in this CA consists of a critical assessment of major and minor actinide data in the latest nuclear data libraries and an assessment of the corresponding uncertainties. This should in a natural way lead to well-focused measurement requests.
As has been emphasized, the industrial needs drive the assessment within the CA. It is worthwhile to point at the close connection of the present collaboration with the OECD-NEA High Priority Request List for nuclear data, where such well-defined requests are collected and reviewed to mobilise the community for their resolution. CANDIDE will serve to identify and propagate the EU interests in this domain and to provide the focus for future EU research on nuclear data. Also in the area of follow up on the formulated requests, CANDIDE is well connected to running EC projects, especially the JEFF project, as mentioned previously.

**Acknowledgements**
This work was financially supported by the European Union, contract 036397.

**References**

[1] EUROTRANS - European Research Programme for the Transmutation of High-Level Nuclear Waste in an Accelerator-Driven System.http://nuklear-server.ka.fzk.de/eurotrans/.
[2] Proceedings of the International Workshop on Nuclear Data Needs for Generation IV Nuclear Energy Systems, ed. P. Rullhusen (Antwerpen, Belgium, 5-7 April 2005). http://www.jrc.cec.eu.int/gen4-workshop/main.html.
[3] M. Salvatores et al., in proceedings of NEMEA-4, Neutron Measurements, Evaluations and Applications, Prague, Czech Republic, October 16-18, 2007, ed. A. Plompen, EU report EUR 23235 EN. See also the Proceedings of International Conference on Nuclear Data for Science and Technology, Nice, France, April 22-27, 2007.
[4] The Eugene Wigner School on Reactor Physics. http://www.reak.bme.hu.
[5] The European Nuclear Education Network. http://www.sckcen.be/ENEN.
[6] The Frédéric Joliot & Otto Hahn Summer School on Nuclear Reactors. http://www-cadarache.cea.fr/fr/cadarache/ecoles/fjohss2007.htm
[7] G. Barreau on behalf of the EFNUDAT consortium, Proceedings of International Conference on Nuclear Data for Science and Technology, Nice, France, April 22-27, 2007. www.efnudat.eu.

# Prospects for nuclear data research at high neutron energies

*J. Blomgren*

Department of Physics and Astronomy, Division of Applied Nuclear Physics, Uppsala University, Box 525, S-751 20 Uppsala, Sweden
Jan.Blomgren@fysast.uu.se

***Abstract:*** Cross section data for neutron-induced nuclear reactions at higher energies than for traditional applications of nuclear physics are required for the further development of sub-critical accelerator-driven systems (ADS) for transmutation of spent nuclear fuel. During the last decade, the situation on microscopic cross sections has improved significantly, to the extent that for the most important reactions, cross section data with uncertainties of about 10 % or less are available for a few key elements at some selected energies. Based on these data, nuclear data libraries up to about 200 MeV have been developed.
In the present publication, the present situation on high-energy neutron data is summarized. Possibilities for future research are outlined, employing existing technology as well as more speculative possible developments. Finally, a recommendation on priorities in future research is given.
The present project is part of the CANDIDE (Coordination Action on Nuclear Data for Industrial Development in Europe) project.

## Introduction

Procedures for measurement, evaluation and validation of nuclear data are since long well established in the classical neutron energy range up to 20 MeV, i.e., the neutron energy range of relevance to critical fission reactors (thermal and fast), as well as fusion applications. With the advent of accelerator-driven systems (ADS), the energy range in which information on neutron-induced nuclear reactions are required for design activities has been significantly increased. In a spallation-driven system, neutrons of energies all the way up to the incident proton energy, i.e., up to GeV energies, are present. Although relatively few neutrons reside at these high energies, their large capability to induce, e.g., materials damage necessitates the nuclear data libraries to be improved significantly above 20 MeV.
The ADS research activities funded by the EU have so far (FP 4, 5 and 6) been dominated by measurements of microscopic cross sections, a fact which has been motivated by the state of knowledge at the time these projects were launched. In particular the HINDAS project [1] in FP5 has resulted in fairly complete data bases on neutron elastic scattering and neutron-induced production of light ions up to about 100 MeV. In addition, fission total cross sections up to 200 MeV on a series of nuclei are now available, to a large extent thanks to ISTC projects. Total cross section data from LANL up to about 600 MeV on a series of nuclei complement the picture [2]. Thus, the most important microscopic cross sections are now available up to at least 100 MeV.
The recent achievements of these projects now motivate an increased attention to integral experiments, especially at ADS-relevant energies, i.e., above 20 MeV, where such experiments are almost absent. Thus, a few existing high-quality integral experiments should be identified. Above 20 MeV some shielding experiments exist, notably the 43 and 68 MeV TIARA transmission measurements for concrete and iron, which is important primarily for structural material studies [3]. Prospects on integral experiments at 175 MeV were presented in the proceedings of the previous NEMEA symposium [4].
In the present publication, the present situation on high-energy nuclear data is summarized. Possibilities for future research are outlined, employing existing technology as well as more speculative possible developments. An extensive review of both the experimental and theoretical state-of-the-art is presented in a forthcoming publication [5]. The present project is part of the CANDIDE (Coordination Action on Nuclear Data for Industrial Development in Europe) project.

## The relation between experiments and theory

Up to now, there has been a very large research volume spent on data on neutron-induced nuclear reactions up to 20 MeV. This was carried out from around 1950 until today, and was motivated by the needs in the development of civil nuclear power, as well as weapons applications and fusion technology. During the last decade, nuclear data at higher energies have been in the limelight due to the discussions about ADS.

The approaches in these two disciplines differ significantly. This is neither a surprise nor a bad choice, because the underlying physics differs significantly, resulting in different research strategies. Below 20 MeV, a single cross section can be of paramount importance to the entire application. An example is the neutron capture resonance at 6.7 eV in $^{238}$U that provides the Doppler effect so important for the stability of critical reactors. Moreover, some cross sections are fundamentally inaccessible to theory, in particular in the resonance region. As a result, at low energies more or less complete data coverage for major elements is required. Above 20 MeV, the situation is fundamentally different. The cross sections are slowly varying in energy, and the behaviour of the system is always dictated by the sum of a large number of reactions, none of which strongly dominates the performance. Therefore, getting a grip on the overall picture has been a more natural ambition in an initial stage, rather than providing precision data on a single reaction.

We have to realize that the task to measure everything that will happen in a future transmutation plant is an insurmountable one. First of all, this is because of practical limitations. At high energies, above 50 MeV or so, *one* cross section for *one* nucleus at *one* energy typically requires about a week of beam time at an international accelerator laboratory. Loosely calculated by industry standards, one week represents a cost of the order of 1 M€. Covering all relevant reactions for all relevant elements at moderate energy intervals would not only present costs approaching national budgets in size, it would also literally take centuries to accomplish with the presently available laboratories.

Furthermore, even if the practical obstacles could be overcome, the situation would still not be satisfactory. In a reactor core, large quantities of short-lived elements can affect the operation, but these isotopes can be impossible to study in experiments.

All these conditions imply that all important data cannot be measured; instead theory has to be used for unmeasured regions. This in turn gives priority to measurements that are decisive for theory development, rather than direct measurements of specific cross sections. Hence, it is possible that reactions not even present in the system, or indirect quantities, should still be measured for theory development reasons.

This also means that at the present stage, when prototype systems still have not been built, there is limited pressure to make measurements covering the full periodic table. Instead, for each of the most important reactions, data on 5-10 nuclei with a reasonable mass coverage is a reasonable goal. It is presently more important that all important reactions are covered with a few good data sets, rather than having data on one of the reactions for many nuclei, if that means a void in the data base on some other key reactions.

If the ADS development progresses to construction and commissioning of a prototype in the scale of 50 MW thermal energy or more, I find it reasonable to raise the ambition level. In that case, I would advocate that about 20 nuclei per major reaction should be studied experimentally. Today, the focus has been on closed-shell nuclei; in such an extended experimental campaign I would like some nuclei in between the closed-shell nuclei as well to get a better grip on mass dependencies. It should also be considered to study the same reaction on a few closely-lying nuclei to verify whether the current models can successfully describe structure differences. Finally, some efforts should be devoted to nuclei of direct technical importance. For instance, today no efforts have been spent on elastic scattering on uranium because it has limited usefulness in model development, but in a prototype system it should be reasonably well known, given the large quantities of uranium present.

In a more distant future, if a full-scale system (of the order or 1 GW thermal energy) were under development, the ambition level should be raised even higher. If we have already 20 nuclei studied at that time, I do not foresee a need to study more nuclei for improved theory, but some more technically motivated nuclei should be studied. In such a situation, I think however that improved accuracy would be more important. That would imply construction of a dedicated laboratory for cross section measurements.

## Present nuclear data status

It is a fairly limited class of reactions that are of major interest for the further development of ADS applications. These are elastic scattering, inelastic neutron emission, light ion production, heavy ion production and fission. In addition, data on total and reaction cross sections are important for model development.

Elastic scattering has been studied on a range of nuclei up to 96 MeV. At present, seven nuclei ranging from $^{1}$H to $^{208}$Pb have been studied [6-8] and an overall uncertainty of about 5 % has been achieved. A novel normalization method has been established that allows elastic scattering data to be normalized absolutely to about 3 % uncertainty [9]. This method, however, works only for elastic scattering. Feasibility studies have shown that the technique as such works up to about 200 MeV, so these studies can be extended up in energy. At present, preparations for a series of elastic neutron cross section measurements at 175 MeV are undertaken, with $^{56}$Fe and $^{209}$Bi as candidates for the first nuclei to be studied.

An experimental programme on inelastic neutron emission, i.e., (n,xn') reactions, is in progress [10]. Data covering a wide energy and angular range have been taken on lead and iron, and the method as such seems to work. It is too early to quote a final uncertainty in the results, but 10 % seems feasible. In parallel, data on carbon, iron, yttrium and lead with a similar quality but a more restricted angular and energy range have recently been extracted by an extended analysis of existing data [11].

Data on light ion production has been acquired on about ten nuclei at 96 MeV, and analysis is in progress. At present, data on five nuclei have been published [12-14]. Normalization has been obtained by simultaneous detection of *np* scattering at an angle where the cross section uncertainty can be estimated to about 5 %, which is the dominating uncertainty in the final light ion production cross sections. These studies are presently being extended to 175 MeV. Data on carbon and iron have been measured, and experiments on lead and uranium are being planned.

Fission cross sections have been studied at many facilities up to about 200 MeV energy. The energy dependencies of the cross sections agree fairly well in shape, but the absolute scale differs by up to 15 % (for a review, see ref. [15]). It is at present not clear what causes this. One possibility is the normalizations used. Another possible cause is that the sensitivity to low-energy neutrons is not under control for some of the experiments. Dedicated experiments to remedy this situation are underway.

In principle, fission cross sections can be measured up to several GeV using white beams with a very high initial proton energy, like at the CERN-nTOF facility [16]. The neutron beam intensity is very low, but the cross sections are large and it is possible to detect a major fraction of the fission fragments, resulting in reasonable statistical precision. A major problem, however, is normalization, since the beam intensity is very difficult to monitor at these very high energies.

There are only a few examples of other fission data than cross sections. This means that important fission parameters, like angular distributions, yields, etc., essentially remain to be investigated at high neutron energies.

Total cross sections have been measured at LAMPF and PSI up to about 600 MeV, with around 1 % uncertainty [2]. The reason for the very good accuracy obtained is that in contrast to the other cross sections discussed, total cross sections can be measured without knowledge of the absolute beam intensity. The dominating uncertainty is knowledge of the target properties, like homogeneity. Therefore, it is difficult to see that major improvements could be expected in total cross section measurements.

Reaction cross sections can be measured with techniques similar to total cross section measurements. The uncertainties can be expected to be slightly larger, because of a slightly more complicated detection and larger corrections. A few reaction cross section measurements were performed about 50 years ago, resulting in uncertainties of about 3 %, but since then, no new data have been published (for a review, see ref. [9]). I estimate that 2 % uncertainties should be attainable in a modern high-quality experiment.

***Table 1.*** *Summary of present status of the most important cross sections on neutron-induced nuclear reactions above 20 MeV (LI: Light ions).*

| Reaction | Status | Uncertainty |
|---|---|---|
| (n,n) | Done up to 100 MeV<br>Underway at 175 MeV | 5 % |
| (n,n'x) | Done up to 100 MeV<br>Underway at 175 MeV | 10 % |
| (n,LI) | Done up to 100 MeV<br>Underway at 175 MeV | 5 % |
| (n,f) | Cross sections up to 200 MeV<br>Possible up to 5 GeV (absolute scale problem)<br>Angular distributions, yields, etc. remaining | 15 %<br>Overall limitation: normalization 5 % |
| (n,tot) | Done up to 600 MeV | 1 % |
| (n,reac) | Done up to 300 MeV, but very old data | 3 % |

## Possibilities with optimization of existing technology

Up to now, no truly dedicated laboratory for high-energy neutron nuclear data studies has been built. All work has been performed at general nuclear physics research machines, at which neutron beam facilities have been installed after the accelerator had been designed. It should be realized, however, that if a dedicated laboratory were designed and built, nuclear data of better quality could be obtained.

There are some technical features of special relevance for high-quality neutron experiments that differ neutron experiments from many (or even most) standard nuclear physics experiments employing charged-particle beams. High beam intensity is indispensable since neutron beams are by definition secondary, with inevitably limited intensities. Short beam pulses with large – and preferably variable – separation in time are other very attractive features. The latter could be obtained with a cyclotron or linear accelerator with a pulse selection system at an early stage in the acceleration.

Such a laboratory could provide conditions allowing all the reactions measured until today to be studied with reduced uncertainties. The limiting factor today is the uncertainty in the *np* scattering cross section, resulting in a 5 % final uncertainty. It is reasonable to presume that with a dedicated neutron laboratory, an uncertainty in the *np* differential cross section of 2 % could be reached, resulting in a final uncertainty of 3 % in experiments measured relative to it. Reducing uncertainties from 5 % to 3 % might not sound like an overwhelming improvement, but for the development of ADS, it could make a significant difference, not at a research stage but when technical large-scale implementation is approaching.

Besides large-scale data production of the already mentioned reaction channels, such a dedicated neutron laboratory could open new areas of research. One scientifically very tempting prospect is multi-ejectile detection. If large pulse separation were available, the target could be surrounded by a high-granularity sphere of neutron detectors, allowing (n,2n), (n,3n), …, etc. reactions to be studied simultaneously. Similarly, the target could be surrounded by detector telescopes for charged-particle detection covering 4π solid angle. With such multi-ejectile detection, correlations could be studied in a way hitherto not even attempted. Last but not least, integral experiments would be greatly facilitated at such a facility.

A limiting factor with present technology is the neutron production. Presently, the $^{7}$Li(p,n) reaction is the most frequently used. The neutron yield is limited by the cooling of the neutron production target, i.e., too intense incident proton beam will result in target melting.

***Table 2.*** *Summary of present uncertainties of the most important cross sections on neutron-induced nuclear reactions above 20 MeV, and estimated uncertainties with optimization of present technology as well as with introduction of high-intensity tagging techniques.*

| Reaction | Present uncertainties | Optimal uncertainties with present technology | Uncertainties with high-intensity tagging |
|---|---|---|---|
| (n,n) | 5 % | 3 % | 1.5 % |
| (n,n'x) | 10 % | 4 % | 2.0 % |
| (n,LI) | 5 % | 3 % | 1.5 % |
| (n,f) | 15 % | 3 % | 1.5 % |
| (n,tot) | 1 % | 1 % | 1.0 % |
| (n,reac) | 3 % | 2 % | 1.5 % |

## Future possibilities

If looking a bit further into the future, we can allow ourselves to be more visionary. To my opinion, the single most important problem to solve if we want a significant development of the field is normalization. At present, we inevitably end up with an uncertainty of about 5 %, because we have to normalize to something, typically *np* scattering, which is known to – at best – 5 %, and it is difficult to see how this can be radically improved upon in a short term with present techniques [17]. As outlined above, reaching a 2 % uncertainty in the *np* scattering cross section should be feasible with a dedicated laboratory using optimized existing technology.

I consider energy resolution to be the second largest problem, with intensity on third place. These two are, however, to a large degree coupled. If you aim for good neutron-beam energy resolution, you have to pay by poor intensity and vice versa. It is presently close to inconceivable to produce neutrons at high energies with a resolution better than 1 MeV with a reasonable intensity. The limited intensity puts severe constraints on the detection, in such a way that the detection often has to be performed with techniques that sacrifice resolution for efficiency, resulting in a final resolution of a few MeV. This means that only in a few rare cases, resolved final states can be studied.

Recently, a way out of the problems above has been proposed. At CERN, planning is ongoing for a beta-beam facility [18]. The background is that neutrino physics has progressed rapidly the last few years, with the discovery of neutrino oscillations as the most visible example. Up to now, essentially all accelerator-produced neutrinos have been muon neutrinos, being the final product of pion decay. Electron neutrinos are much more difficult to produce in large amounts, because they require nuclear beta decay for their creation.

At the proposed CERN beta-beam facility, production of suitable beta-emitting nuclei should be undertaken in an ISOLDE-like facility, and the produced nuclei should be post-accelerated to very high energy by a series of accelerators, the final one being SPS. After acceleration, the ions are directed to a decay ring of race-track shape. At these very high energies, hundreds of GeV per nucleon, there is a very strong Lorentz boost, which means that the neutrino is emitted very close to the beam direction in the laboratory system, in spite of that the emission is isotropic in its moving reference frame. Thereby, intense neutrino beams can be produced. The idea is to build the decay ring so that one straight section points towards a distant neutrino detector to allow studies of electron neutrino oscillations.

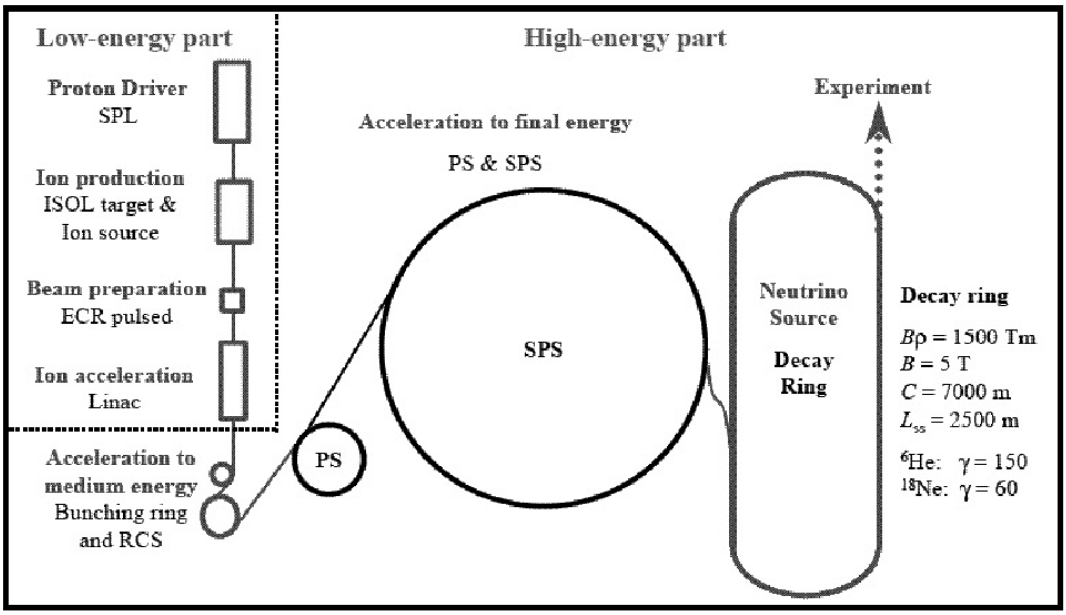


***Figure 1.*** *Overview of the proposed CERN beta-beam facility.*

Intense neutron beams could be a spin-off from that facility. It has been proposed to use two production targets, one for nuclei suited for neutrino emission in the decay ring, and one for beta-delayed neutron emitters. Some unstable neutron-rich nuclei can beta decay to a nucleus that promptly emits a neutron (a process which by the way is of utmost importance to the stability of nuclear power reactors). This neutron has typically an energy of a few hundred keV in its rest frame. By accelerating the beta-delayed neutron emitters up to a few hundred MeV per nucleon, the Lorentz boost is sufficient to focus the beam to reasonable dimensions. All this can be done in parallel with the primary objective, since the accelerators for the neutrino emitters have a long cycle with a low duty factor. Thus, for most of the time there is no injection into the synchrotrons for neutrino emitter acceleration, and then the production targets can be used for beta-delayed neutron emitter production.

The resulting neutron beam has an energy in the 100–500 MeV range with an energy resolution of about 1 MeV, and intensities of about $10^{11}$ n/s are estimated. This should be compared with $10^{6}$ for present-day technology, i.e., an improvement by a factor 100 000 (!). With such intensities, only imagination sets the limit for what can be achieved.

First and foremost, such intensities are not too far from what has been used in proton beam experiments for fundamental nuclear physics. This opens opportunities to study, e.g., the role of isospin in nuclei by conducting a carefully selected set of experiments where information from experiments with neutrons could be combined with previous information from proton-induced reactions. Many types of fundamental physics issues hitherto inaccessible to experiments could be within reach to address. This is such a large field that it deserves its own workshop.

If we now restrict the discussion to nuclear data for ADS applications and turn to my problem list above, it seems feasible that we can address all of them through one experimental trick: tagging. If we use the neutron beam directly for experiments we have essentially only solved the intensity problem, but the other two remain; we end up in a 1 MeV resolution due to the inherent energy spread, and we are still plagued by the normalization problem. Tagging means that we produce a secondary neutron beam of lower, but better known, intensity.

One candidate reaction is to let neutrons scatter from a hydrogen target, and the recoil proton is detected. Since this is a two-body final state, detection of the associated proton means that a neutron must have been scattered to the corresponding direction. Thereby, the normalization problem can be circumvented, since we count the neutrons one by one through the associated particle. If this tagging is performed with high resolution, both in energy and angle, we can also know the neutron energy event by event far better than the initial neutron beam energy resolution. If the tagging is performed with a magnetic spectrometer, the tagger can be made rather insensitive to the ambient background, and a proton energy resolution of better than 100 keV can be obtained, resulting in a comparable neutron energy resolution.

With reasonable estimates on tagger parameters, $10^4$ tagged neutrons with an energy resolution of 100 keV should be possible to reach, given the beam intensity above. This might sound like a poor intensity, but with such a resolution, final states can be well resolved and background becomes much less of a problem, which means that already a small number of events will result in a good accuracy. Moreover, since the intensity can be determined to about 1 % in a typical tagger system, the accuracy is far better than what can be obtained today. In cases when the demands on energy resolution are not as stringent, a thicker tagger target can be used, resulting in increased intensity. This goes faster than linear, because with a worse resolution, the intensity at the tagger is increased, thicker secondary experimental targets can be used, and the detection limitations are less severe. Therefore, even with resolutions that are on the limit to be possible untagged today, we might have tagged beams of intensities exceeding what is presently available in a not too distant future.
A second technique would be to use a similar production as above (1-2 GeV protons on a combined target-ion source) to produce $^6$He, which in turn would be accelerated to hit a target [19]. Roughly, $^6$He can be described as an $\alpha$ particle with two loosely attached neutrons. When hitting a target, the two neutrons are dissociated with a large probability, and continue along the direction of the incident beam with the incident velocity. The charged particles (the remaining $^6$He and residual $^4$He) are bent by a magnet system and a clean neutron beam is produced, with a divergence similar to that of a beta-delayed neutron beam. This latter technique does not have the potential to produce as intense fluxes as the beta-decay in flight, but on the other hand it requires much less advanced accelerators. This technique could possibly be installed at existing CERN facilities after some upgrades. Initial estimates indicate a factor a hundred to a thousand larger neutron fluxes than for present facilities to be within reach.

## Recommendations for future research

In the coming five years, the most important development concerning experiments on nuclear data above 20 MeV for ADS applications is to my opinion an integral experiment at an energy significantly higher than the 68 MeV that presently represents the highest energy studied. At the previous NEMEA symposium, a proposal for such an experiment at 100 and 175 MeV was presented. I believe such an experiment has the highest priority at present.
Next priority would be to complete the (n,n'x) experiments at 100 MeV. So far, two nuclei ($^{56}$Fe and $^{208}$Pb) have been studied where the full neutron emission spectrum has been recorded, but the results remain to be published. I would advocate at least two more nuclei to be studied, for instance $^{12}$C and $^{89}$Y to get at least one light nucleus and one in between iron and lead.
After such an experiment has been carried out, the situation up to 100 MeV would be – for the moment – satisfactory, and I suggest the main attention should be directed towards data on the most important reactions at a higher energy. The only facility in Europe where such experiments at present can be carried out is TSL, which runs 175 MeV as its standard energy. Thus, my third priority is neutron scattering (elastic first priority, with inelastic as second priority) and light-ion production on 5-10 nuclei.
The program outlined above should take about five years to complete with adequate funding. After completion of this program, the possibilities with present technology and existing facilities would essentially be completed. It is of course possible to increase the data base by running more nuclei with existing technology, but if the ambition is to improve the quality, new facilities have to be developed. Even if decided today, it is a ten-year process to commission such a new laboratory. Thus, the list above should serve as a recommendation for research until the construction of a new facility has been decided upon.

**Acknowledgements**
The information from Mats Lindroos is gratefully acknowledged. This work was financially supported by the European Union, contract 036397, Barsebäck Power AB, Forsmark AB, Ringhals AB, the Swedish Nuclear Power Inspectorate, the Swedish Nuclear Fuel and Waste Management, the Swedish Nuclear Safety and Training Centre, the Swedish Defense Research Agency, the Swedish Centre for Nuclear Technology and the Swedish Research Council.

**References**

[1] A. Koning, H. Beijers, J. Benlliure, O. Bersillon, J. Blomgren, J. Cugnon, M. Duijvestijn, Ph. Eudes, D. Filges, F. Haddad, S. Hilaire, C. Lebrun, F.-R. Lecolley, S. Leray, J.-JP . Meulders, R. Michel, R.-D. Neef, R. Nolte, N. Olsson, E. Ostendorf, E. Ramström, K.-H. Schmidt, H. Schuhmacher, I. Slypen, H.-A. Synal, R. Weinreich, J. Nucl. Sci. Tech., Suppl. **2** (2002) 1161.

[2] R.W. Finlay, W.P. Abfalterer, G. Fink, E. Montei, T. Adami, P.W. Lisowski, G.L. Morgan, R.C. Haight, Phys. Rev. C **47** 237 (1993) 237.

[3] H. Nakashima, N. Nakao, S. Tanaka, T. Nakamura, K. Shin, S. Tanaka, H. Takada, S. Meigo, Y. Nakane, Y. Sakamoto, M. Baba, J. Nucl. Sci. Eng. **124** (1996) 243.

[4] J. Blomgren, K. Chtioui. A proposal for an integral neutron data experiment in the 100-200 MeV region, 4th Workshop on Neutron Measurements, Evaluations and Applications - Nuclear data needs for Generation IV and accelerator driven systems, Prague, Czech Republic, October 16-18, 2007. NEMEA-4, EUR Report 23235 EN, Luxembourg: Office for Official Publications of the European Communities, ISBN 978-92-79-08274-0, European Communities, 2008, p. 59.

[5] J. Blomgren, A. Koning, Neutron physics research for the development of accelerator-driven systems, chapter in Nuclear Reactors: Research, Technology and Safety, in press, Nova Publishing (2008).

[6] C. Johansson, J. Blomgren, A. Ataç, B. Bergenwall, S. Dangtip, K. Elmgren, A. Hildebrand, O. Jonsson, J. Klug, P. Mermod, P. Nadel-Turonski, L. Nilsson, N. Olsson, S. Pomp, A.V. Prokofiev, P.-U. Renberg, U. Tippawan, M. Österlund, Phys. Rev. C. **71** (2005) 024002.

[7] P. Mermod, J. Blomgren, C. Johansson, A. Öhrn, M. Österlund, S. Pomp, B. Bergenwall, J. Klug, L. Nilsson, N. Olsson, U. Tippawan, P. Nadel-Turonski, O. Jonsson, A.V. Prokofiev, P.-U. Renberg, Y. Maeda, H. Sakai, A. Tamii, K. Amos, R. Crespo, A. Moro, Phys. Rev. C. **74** (2006) 054002.

[8] A. Öhrn, J. Blomgren, P. Andersson, A. Ataç, C. Gustavsson, J. Klug, P. Mermod, S. Pomp, P. Wolniewicz, M. Österlund, L. Nilsson, B. Bergenwall, K. Elmgren, N. Olsson, U. Tippawan, S. Dangtip, P. Phansuke, P. Nadel-Turonski, O. Jonsson, A.V. Prokofiev, P.-U. Renberg, V. Blideanu, C. Le Brun, J.F. Lecolley, F.R. Lecolley, M. Louvel, N. Marie-Noury, C. Schweitzer, Ph. Eudes, F. Haddad, C. Lebrun, E. Bauge, J.P. Delaroche, M. Girod, X. Ledoux, K. Amos, S. Karataglidis, R. Crespo, W. Haider, Phys. Rev. C. **77** (2008) 024605.

[9] J. Klug, J. Blomgren, A. Ataç, B. Bergenwall, A. Hildebrand, C. Johansson, P. Mermod, L. Nilsson, S. Pomp, U. Tippawan, K. Elmgren, N. Olsson, O. Jonsson, A.V. Prokofiev, P.-U. Renberg, P. Nadel-Turonski, S. Dangtip, P. Phansuke, M. Österlund, C. Le Brun, J.F. Lecolley, F.R. Lecolley, M. Louvel, N. Marie-Noury, C. Schweitzer, Ph. Eudes, F. Haddad, C. Lebrun, A.J. Koning, X. Ledoux, Phys. Rev. C. **68** (2003) 064605.

[10] I. Sagrado Garcia, G. Ban, V. Blideanu, J. Blomgren, P. Eudes, J.M. Fontbonne, Y. Foucher, A. Guertin, F. Haddad, L. Hay, A. Hildebrand, G. Iltis, C. Le Brun, F.R. Lecolley, J.F. Lecolley, J.L. Lecouey, T. Lefort, N. Marie, N. Olsson, S. Pomp, M. Österlund, A. Prokofiev, J.-C. Steckmeyer. International workshop on Fast Neutron Detectors and Applications, Cape Town, South Africa, April 3-6, 2006. Proceedings of Science, PoS (FNDA2006) 009. http://pos.sissa.it.

[11] A. Öhrn, J. Blomgren, A. Ataç, C. Gustavsson, J. Klug, P. Mermod, L. Nilsson, S Pomp, M. Österlund, B. Bergenwall, K. Elmgren, N. Olsson, U. Tippawan, S. Dangtip, P. Phansuke, P. Nadel-Turonski, O. Jonsson, A.V. Prokofiev, P.-U. Renberg, P. Ascher, V. Blideanu, C. Le Brun, J.F. Lecolley, F.R. Lecolley, M. Louvel, N. Marie-Noury, C. Schweitzer, Ph. Eudes, F. Haddad, C. Lebrun, X. Ledoux, M. Blann, S. Chiba, H. Duarte, C. Kalbach, A.J. Koning, Y. Watanabe, to be published.
[12] V. Blideanu, F.R. Lecolley, J.F. Lecolley, T. Lefort, N. Marie, A. Ataç, G. Ban, B. Bergenwall, J. Blomgren, S. Dangtip, K. Elmgren, Ph. Eudes, Y. Foucher, A. Guertin, F. Haddad, A. Hildebrand, C. Johansson, O. Jonsson, M. Kerveno, T. Kirchner, J. Klug, Ch. Le Brun, C. Lebrun, M. Louvel, P. Nadel-Turonski, L. Nilsson, N. Olsson, S. Pomp, A.V. Prokofiev, P.-U. Renberg, G. Rivière, I. Slypen, L. Stuttgé, U. Tippawan, M. Österlund, Phys. Rev. C **70** (2004) 014607.
[13] U. Tippawan, S. Pomp, A. Ataç, B. Bergenwall, J. Blomgren, S. Dangtip, A. Hildebrand, C. Johansson, J. Klug, P. Mermod, L. Nilsson, M. Österlund, N. Olsson, K. Elmgren, O. Jonsson, A.V. Prokofiev, P.-U. Renberg, P. Nadel-Turonski, V. Corcalciuc, Y. Watanabe, A. Koning, Phys. Rev. C **69** (2004) 064609.
[14] U. Tippawan, S. Pomp, A. Atac, B. Bergenwall, J. Blomgren, S. Dangtip, A. Hildebrand, C. Johansson, J. Klug, P. Mermod, L. Nilsson, M. Österlund, N. Olsson, K. Elmgren, O. Jonsson, A.V. Prokofiev, P.-U. Renberg, P. Nadel-Turonski, V. Corcalciuc, A. Koning, Phys. Rev. C. **73** (2006) 034611.
[15] I.V. Ryzhov, G.A. Tutin, A.G. Mitryukhin, S.M. Soloviev, J. Blomgren, P.-U. Renberg, J.-P. Meulders, Y. El Masri, Th. Keutgen, R. Preels, R. Nolte. Nucl. Instr. Meth. **A 562** (2006) 439.
[16] L. Tassan-Got, PoS(FNDA2006)040. http://pos.sissa.it.
[17] Proceedings of Workshop on "Critical Points in the Determination of the Pion-Nucleon Coupling Constant", Uppsala, June 7-8, 1999, ed. J. Blomgren. Phys. Scr. **T87** (2000).
[18] The CERN beta-beam working group, http://cern.ch/beta-beam.
[19] I. Tanihata, T. Nilsson, private communication (2005).

# Improved resonance shape analysis methodology in CONRAD using integral data constraints: case of $^{239}$Pu

*C. De Saint Jean, B. Habert, D. Bernard, G.Noguere, O. Bouland, O. Litaize, O. Serot, C. Suteau, J-M. Ruggieri*

CEA Cadarache, F-13108 Saint Paul lez Durance, France
cyrille.de-saint-jean@cea.fr

***Abstract:*** Recent keff analysis of Pu-fuelled systems with the JEFF-3.1 Evaluated Nuclear Data Files showed the systematic overestimation of the calculated core reactivity.
Sensitivity studies performed on iso-thermal temperature moderator analysis have demonstrated the need for improving the description of the $^{239}$Pu neutron cross sections in the sub-thermal energy range [2]. Knowing the poor accuracy of the EXFOR data below the thermal energy range, integral trends have to be taken into account in the evaluation work. In order to provide reliable results, the generalized least square fitting model implemented in the CONRAD code [9] has been significantly improved (i) to be able to use sensitivity coefficients calculated with the standard perturbation theory (ii) and to provide realistic uncertainties on integral data. The focus of the presentation is to show results obtained on the $^{239}$Pu capture and fission neutron cross sections with an exhaustive integral validation. The user-friendly implementation of such methodology allows an easy generalisation of the present evaluation work to higher neutron energies.

## Introduction

Evaluating uncertainties and correlations in the nuclear data field is of great interest for reactors physicists as it is a major contribution in their own uncertainty propagation evaluation [1]. One major drawback found by reactor physicist is the fact that most of the time the integral (or analytical) experiments were not taken into account sufficiently soon in the evaluation process to remove discrepancies.
In this paper, we are describing a clear mathematical framework to take into account properly the information coming from integral experiment done on reactor mock-up or simple integral experiment (e.g. ICSBEP). In the first part of the paper, the general mathematical description of traditional evaluation process (parameter fitting) will be presented.
Then, the way we can absorb integral experiment results will be described. In addition, a best practise recipe is given to explain how to use the method. In the last chapter, $^{239}$Pu analysis will be presented.

## Traditional parameter estimation

Let $\vec{y} = \{\vec{y}_i\}(i = 1...N_y)$ denote some experimentally measured variables, and let $\vec{x}$ denote the parameters defining the model used to simulate theoretically these variables.

Using Bayes' theorem [3] and especially its generalisation to continuous variables[4], one can settle the following relation between conditional probability density functions (written p(.)) when the analysis of a new data set $\vec{y}$ is performed:

$$p(\vec{x}|\vec{y}, U) = \frac{p(\vec{x}|U)p(\vec{x}|\vec{y}, U)}{\int d\vec{x}p(\vec{x}|U)p(\vec{x}|\vec{y}, U)}$$

where U represents the "background" or "prior" information from which the prior knowledge of $\vec{x}$ is assumed. U is supposed independent of $\vec{y}$. In this framework, the denominator is just normalization constant.

The formal rule [5] used to take into account information coming from new analysed observations is:

$$\text{posterior}\left[(\vec{x}|\vec{y},U)\right] = \text{prior}\left[p(\vec{x}|U)\right]\text{likelihood}\left[p(\vec{x}|\vec{y},U)\right]$$

A fitting procedure can be seen as an estimation of the first two moments of the posterior density probability of a set of parameters $\vec{x}$, knowing a priori information on these parameters and a likelihood which gives the probability density function of observing a data set knowing $\vec{x}$. This is a standard procedure for parameters estimation in the nuclear data field [8,9].

To solve this problem, one has to make some assumptions on the prior probability distribution involved. Given a covariance matrix and mean values, the choice of a multivariate joint normal for the probability density $p(\vec{x}/U)$ is maximizing the entropy [6]. After an additional approximation (so-called Laplace approximation [7]), if the expectation and covariance matrix are $\vec{x}_m$ and $M_x$, the evaluation of posterior expectation and covariance are done by finding the minimum of the following cost function (a generalized least-square):

$$(\vec{x}-\vec{x}_m)^T M_x^{-1}(\vec{x}-\vec{x}_m) + (\vec{y}-\vec{t})^T M_y^{-1}(\vec{y}-\vec{t})$$

## How to take into account Integral experiments?

**Integral experiments ?**
Let us define clearly what we call an integral experiment in this paper.
A possible general (but non-exhaustive) definition:

- international benchmark ICSBEP,
- analytic experiments on reactor mock-up (EOLE, MASURCA,...)
- clear reactor irradiations (PHENIX)

In our case, additional constraints exist: not all experiments are good candidates.
The profile of a good candidate is the following:

- a well described experiment : C/E discrepancies targeted
- experiment must be properly calculated (see Figure.1):
  - bias calculated (C/C')
  - sensitivity coefficients available

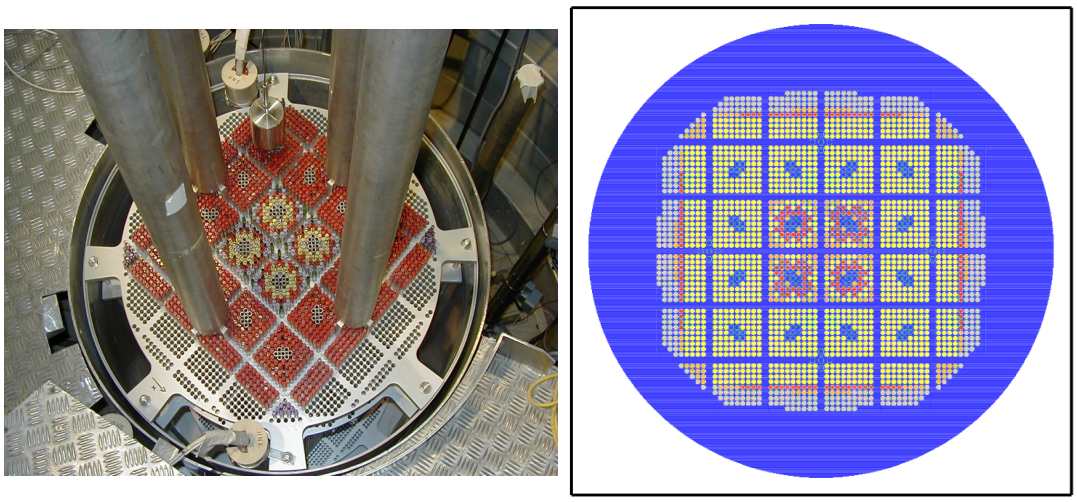

***Figure1.*** *Radial section of EOLE with Tripoli4*

**Information related to integral experiments**

We use the integral experiments in addition to traditional parameter estimation. The "traditional" estimation acts as a prior information close to the "true" value, so slight changes will be done. Given I, a measurement which is related to cross sections ($k_{eff}$ , ...), the first order approximation is valid because of the slight changes. One obtains:

$$I = I_0 + \sum_i \frac{\partial I}{\partial \vec{\sigma}_i}(\partial\vec{\sigma}_i - \vec{\sigma}_i^0)$$

where i represents different kinds of cross-sections (fission, capture, ...). $I_0$ is the calculated value for I and the set of calculated sensitivities is supposed to be constant (when the cross-sections slightly change) :

$$\vec{S}_i = \frac{\partial I}{\partial \vec{\sigma}_i}\frac{\vec{\sigma}_i^0}{I_0}$$

Then, given $I_E$ and $\delta_E$, the measurement and associated standard deviation, one can add to any cost function an additional term which is going to take into account the integral experiment tendencies:

$$(\vec{x} - \vec{x}_m)^T M_x^{-1}(\vec{x} - \vec{x}_m) + ... + ((I_E - I)/\delta_E)^2$$

The participation of the integral experiment in the cost function can be far lower than those of differential experiments. Numerical problems can arise (round off, un-sensitive parameters). Treating both types together could therefore hide the integral effects. Thus, differential and integral experiments are going to be used successively in this paper.

### Integral experiments treatment in CONRAD

To implement previous equations in CONRAD [9] (to take into account integral experiment in the cost function), one has to calculate the gradient of I with respect to the parameter set $\vec{x}_m$:

$$\frac{\partial I}{\partial x_m} = \sum_i \frac{\partial I}{\partial \vec{\sigma}_i}\frac{\partial \vec{\sigma}_i}{\partial \vec{x}_m}$$

$\frac{\partial I}{\partial \vec{\sigma}_i}$ are given by neutronic codes via sensitivity calculations ($\vec{S}_i$) and $\frac{\partial \vec{\sigma}_i}{\partial \vec{x}_m}$ are calculated by CONRAD.

### Best practice to take into account integral experiments

One has to make some assumptions on the level of knowledge associated to the prior evaluation.

**First case**

Suppose that, for a given isotope, in a given energy domain treated by a given model, a proper evaluation of the parameter set $\vec{x}_0$ with its associated covariance matrix $M_x^0$ was performed. This can be considered as your background information U (see previous paragraphs). As a result, there is only one additional term in the cost function:

$$(\vec{x} - \vec{x}_m)^T M_x^{-1}(\vec{x} - \vec{x}_m) + ((I_E - I)/\delta_E)^2$$

In this situation, the parameters covariances represent some most probable intervals of values for the parameters. Using additional information coming from integral measurements will change the parameters in this most probable interval.

**Second case**

You have the knowledge of the parameters but no idea of the associated uncertainties. You must then do a retro-active analysis [8] of the parameters in order to obtain an estimated covariance matrix as follows.
You have to choose a limited set of differential experiments of interest for you energy region. The covariances on the parameters can be estimated with the following equation:

$$M_x^{-1} = \sum_i S_i^T M_y^{-1} S_i$$

where $S_i$ represents the vector of the following derivatives :

$$(S_i)_{jk} = \frac{\partial t_j^i}{\partial x_k}$$

where $t^i$ is the theoretical modelization of $i^{th}$ experiment. Then, the problem becomes of the first type.

## Application to the $^{239}$Pu case

$^{239}$Pu nuclear data accuracy is an important issue for reactor applications. keff analysis of Pu-fuelled systems showed systematic overestimation of the calculated core reactivity.
A first paper was presented to propose modification on cross sections (as well as the modification of the mean number of fission neutrons) [2].
In this paper, we are using the same approach but in a clear mathematical framework.

### Measurements involved for this paper

Measurements of the Isothermal Temperature Coefficient (mainly driven by Moderator Temperature Coefficient: MTC) of 100%-MOx cores were performed in the EOLE facility in cold (20-80 $^{o}$C) and hot operating conditions (150-300 $^{o}$C ).

Experimental validation of the APOLLO2 deterministic code, using both JEF-2.2 and JEFF-3.1 libraries based, demonstrates [10,11]:

- a systematic underestimation of the MTC in cold conditions of (-2.0+/-0.3)pcm/$^{o}$C,
- a well-assessed MTC in hot conditions (+1.0+/-2.0)pcm/$^{o}$C .

The analysis of physical phenomena [11] has shown that the negative error in the low-temperature range is linked to the thermal spectrum shift effect, which is strongly dependant on the sub-thermal and thermal shapes of the plutonium cross sections.
The used integral measurement is thus the MTC measured in EOLE.
We aim at changing the thermal shape, so we focus on the negative resonances and the first positive resonance (at 0.3eV).

### A priori $^{239}$Pu uncertainties estimations

As a priori estimation, we choose the result of [2] which is the JEFF3.1 evaluation with a negative resonance added at -20meV. The covariance matrix on the resonance parameters is missing, so we did a retro-active analysis with CONRAD [9] by using microscopic experiments (second case of previous paragraph). The following experiments were taken into account:

- Weston fission measurements (1993) [12], statistical uncertainties are given on EXFOR and a systematic uncertainties of 0.6% was added as recommended.
- Gwin capture measurements (1971) [13], there is no information about uncertainty on EXFOR, so we have assumed 1% of statistical and 3% of systematic uncertainties.

The retro-active analysis was performed on the [0eV,3eV] energy domain and the parameters of interest (Energy, capture width and fission width) prior covariance matrix was generated. An example of theoretical covariance on the fission cross section is given in Figure 2.

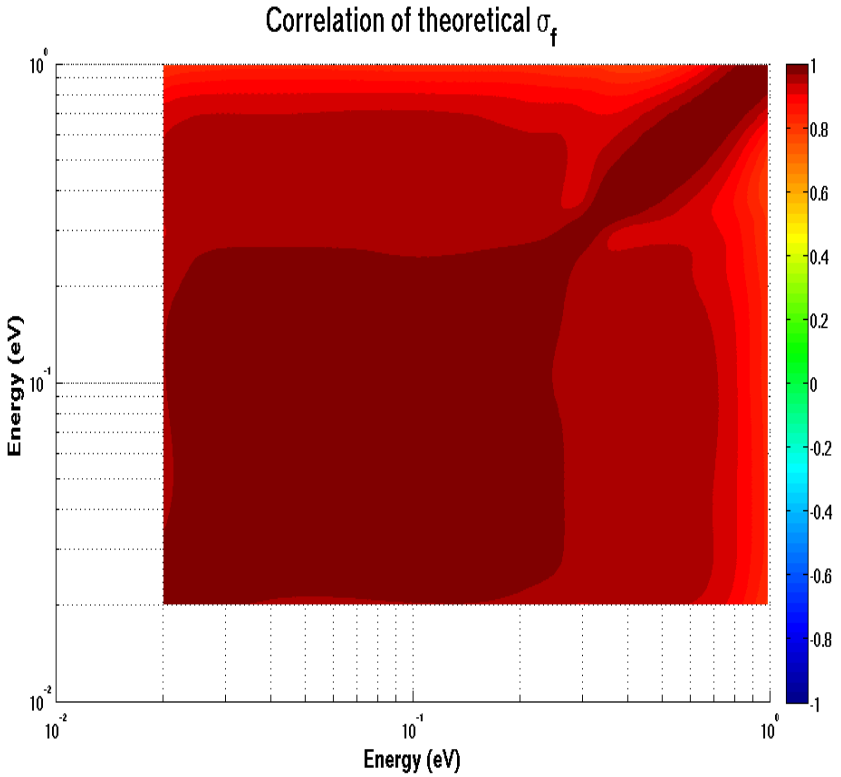


***Figure 2.*** *Fission cross section covariances in the [0eV,1eV] energy range.*

**Selection of parameters for the integral experiment analysis**

Influence of parameters on the MTC was calculated with "Standardized Regression Coefficients":

$$\mathrm{SRC}_x = \left( \frac{\partial \mathrm{MTC}}{\partial x} \frac{\delta_x}{\delta_{\mathrm{MTC}}} \right)^2$$

where the derivatives $\frac{\partial MTC}{\partial x}$ are calculated in conjunction by CONRAD ($\frac{\partial \vec{\sigma}_i}{\partial x}$) and APOLLO2 ($\frac{\partial MTC}{\partial \vec{\sigma}_i}$).

This coefficient give information on parameters which :

- are influential (large $\frac{\partial MTC}{\partial x}$ ),
- and which can give room for variation (not too small $\delta x$ ).

Figure 3. shows SRC values found for the negative resonances and the first positive resonance. A short-list of parameters was found with this SRC analysis.

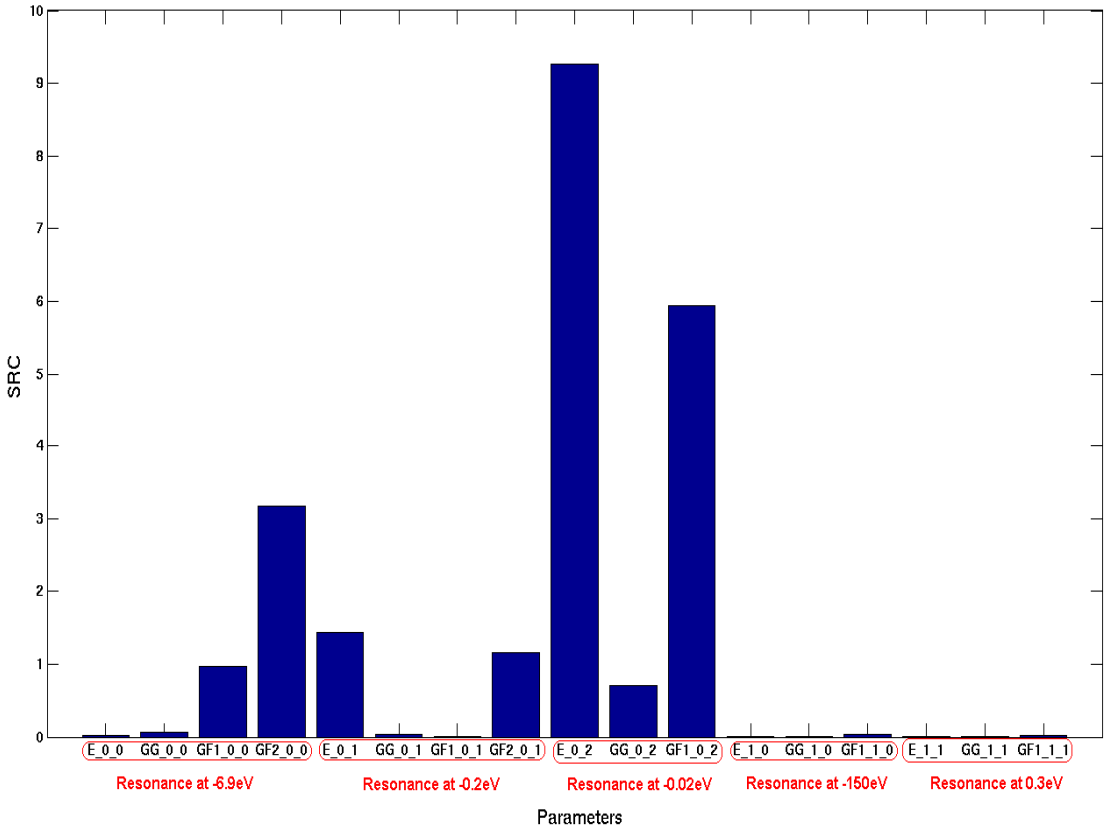


***Figure 3.*** *Standardized Regression Coefficient.*

Because we want to change only the thermal shape, other energy domains must not be affected by parameters variations. Sensitivities of fission and capture cross-sections to these parameters were calculated to check the range of their influence.

The relative sensitivities:

$$\vec{S}_i = \frac{\partial \vec{\sigma}_i}{\partial x} \frac{\vec{x}}{\vec{\sigma}_i}$$

were calculated with CONRAD as well.

For example, the second fission width of the resonance at -6.9eV was dropped out because of his influence on the fission cross section after 0.3eV as can be seen in Figure 4.

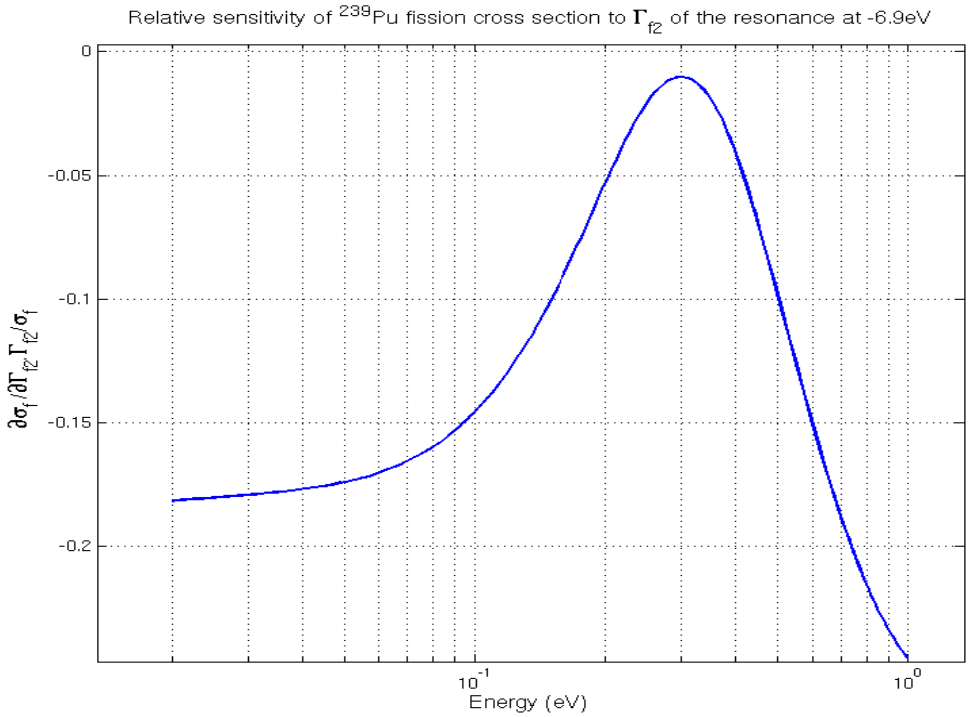


***Figure 4.*** *Relative sensitivity of fission cross section to -6.9eV second fission width.*

Parameters which satisfy above criterion are those of the resonance added by D.Bernard [2]:

$$E = -20 \text{ meV}, \quad \Gamma = 6 \text{ meV}, \quad \Gamma_{f1} = -36 \text{ meV}$$

**Results of the adjustment on integral experiment**

The new estimation of the parameters with CONRAD [9] gives:

$$E = -15.00 \text{ meV}, \quad \Gamma = 6.06 \text{ meV}, \quad \Gamma_{f1} = -31.30 \text{ meV}$$

The new cross-sections have slightly changed, for the thermal values one obtains:

- Fission : 746.74 barns (-0.91 barn with respect to JEFF3.1)
- Capture : 273.18 barns (+2.54 barns with respect to JEFF3.1)
- Total : +1.59 barns with respect to JEFF3.1

The discrepancies on the MTC are summarized in table 1:

***Table 1.*** *MTC discrepancies*

| ***Experiment*** | ***(C-E) pcm/°C*** | | |
|---|---|---|---|
| pcm/°C | JEF 2.2 | JEFF3.1 | This work |
| -15+/-0.3 | -2.0 | -1.87 | -1.54 |

Discrepancy between calculus and experiment on the MTC is still too large. The $^{239}$Pu thermal shape cannot explain the whole problem. Nevertheless, this data assimilation improves slightly the C/E and gives also the covariance matrix on the parameters.

## Conclusion

This paper describes a mathematical framework to add integral experiments information during the evaluation process with the CONRAD code [9].

The integral experiments are seen as feedbacks for an evaluation, so they are used after differential experiments treatment to correct accurately the parameters.

The following conclusions can thus be made:

- use of clear integral experiment can and should be added in the evaluation process;
- best practises should be used and described (non exhaustive presentation here);
- in Cadarache an extensive use of this methodology in conjunction with proper covariances estimations is scheduled with CONRAD;
- the interaction between reactor physicists and nuclear data evaluators should :
  - be imposed ...,
  - append in a clear mathematical framework,
  - be as far as possible automatic,
  - associated with validation benchmarks to avoid non-expected discrepancies.

**References**

[1] G. Aliberti, G. Palmiotti, M. Salvatores, T.K. Kim, T.A. Taiwo, M. Anitescu, I. Kodeli, E. Sartori, J.C. Bosq, J. Tommasi, Nuclear data sensitivity, uncertainty and target accuracy assessment for future nuclear systems, Annals of Nucl. Energy Vol 33, 700-733 (2006).
[2] D. Bernard et al., in Proceedings of the International Conference on Nuclear Data for Science and Technology, Nice, France, 2007, edited by O. Bersillon et al. (EDP Science, 2008).
[3] Bayes, Rev. T., An Essay Toward Solving a Problem in the Doctrine of Chances, Philos. Trans. R. Soc. London 53, pp. 370-418 (1763); reprinted in Biometrika 45, pp. 293-315 (1958).
[4] A. Papoulis and S. U. Pillai, Probability, Random Variables and Stochastic Processes, (McGraw-Hill, 2002).
[5] F. H. Frohner, Nuclear Science and Engineering Vol 126, 1 (1997).
[6] T. M. Cover, J. A. Thomas, Elements of information theory, 2nd Edition. New York: Wiley-Interscience, 2006.
[7] C. P. Robert and G. Casella, Monte Carlo statistical methods, Springer, 2nd edition, 2004.
[8] N. M. Larson, Updated users' guide for SAMMY: multilevel R-matrix fits to neutron data using Bayes' equations, ORNL/TM-9179/7, Oak Ridge National Laboratory, Oak Ridge, TN, USA (2006).
[9] C. De Saint Jean et al., in Proceedings of the International Conference on Nuclear Data for Science and Technology, Nice, France, 2007., edited by O. Bersillon et al. (EDP Science, 2008).
[10] C. Vaglio-Gaudard, A. Santamarina et al., Qualification of APOLLO2 BWR Calculation Scheme on the BASALA Mock-up, Proceedings of the International Conference on Reactor Physics PHYSOR'06, Chicago (USA).
[11] L. Erradi, A. Santamarina and O. Litaize, The Reactivity Temperature Coefficient Analysis in Light Water Moderated UO2 and UO2-PUO2 Lattices, Nuclear Science and Engineering Vol 144, 47 (2003).
[12] L. W. Weston, J. H. Todd and H. Derrien, Normalization and Minimum Values of the 239Pu Fission Cross Section, Nuclear Science and Engineering Vol 115, 164-172 (1993).
[13] R. Gwin, L. W. Weston et al., Simultaneous Measurement of the Neutron Fission an Absorption Cross Sections of Plutonium-239 Over the Energy Region 0.02 eV to 30 keV, Nuclear Science and Engineering Vol 45, 25-36 (1971).

# Activation cross sections for (n, x) reactions on germanium, terbium, lutetium and tantalum isotopes

*N. Dzysiuk, I. Kadenko, R. Yermolenko*

Taras Shevchenko National University of Kyiv, Department of Nuclear Physics
dzysyuk@univ.kiev.ua

***Abstract:*** Neutron cross sections have been measured for Lu, Ge, Ta and Tb isotopes with neutron activation technique. Foils of natural composition were irradiated by fast neutrons produced by neutron generator NG-300/15. Also tantalum samples were irradiated with reactor filtered beams. To ensure results accuracy and precision all the possible sources of uncertainties, including the coincidence summing and self-absorption effects have been taken into account. Calculations of efficiency and correction factors have been performed with Monte Carlo simulations. The cross section results obtained for $^{175}$Lu(n, α)$^{172}$Tm, $^{72}$Ge(n,2n)$^{71}$Ge and $^{181}$Ta(n,γ)$^{182m2}$Ta reactions were reported for the first time. The earlier available cross section upper estimate for nuclear reaction $^{159}$Tb(n,n′α)$^{155}$Eu is reported as one order lower value. Theoretical calculations of excitation functions were conducted with the Talys-1.0 code.

## Introduction

At present the reliable nuclear data is very important for several reasons. Requirements for neutron cross section values with high accuracy depend on gradual enlargement of amount of nuclear data practical applications. The reaction cross sections for incident neutron energies about 14 MeV are very useful in nuclear technology applications and nuclear theory investigations, especially in fusion reactor technology. Due to lack of universal nuclear reaction model such an approach with new and verified nuclear data may be considered as important for testing the applicability of the statistical model for description of (n, 2n) reactions mechanisms on nuclides rather away from the stability line.

But, notwithstanding the fact that there are huge nuclear data bases which involve many neutron activation cross sections data for neutron energy about 14 MeV, some unsolved problems still remain in this energy interval. Except incompleteness of nuclear data bases [1, 2] the discrepancy between existing results has been observed as well, what may lead to errors unrecognized during interpolation of experimental data and to influence the quality of estimated data. Research of radiation capture reactions cross section when a daughter nucleus may be obtained in metastable state is of great importance for nuclear matter structure understanding.

Denoted elements have been selected for investigations due to above described reasons and their utilizations in different areas of human life. $^{181}$Ta as a reactor material is very interesting to study it's interaction with neutrons. Concerning to requests in [2] the most attention was paid to reactions $^{175}$Lu(n, α)$^{172}$Tm and $^{72}$Ge(n,2n)$^{71}$Ge due to lack of such cross-section data in literature at all. Terbium and lutetium are two rear earth elements which are interesting because of their complexity of β-branching and γ-spectra in this mass region. The experimental (n,2n) reaction cross sections values in the rare earth region reported in literature were obtained mostly using poor-resolution counters. Besides that many of the data available has large error bars and often show gross disagreements between one and others. Cross sections of rare reaction as (n,n′α) is important to know what interferences might be present from possible contributions from these rare reactions. Finally, knowledge of cross sections for these reactions is an aid in the proper mass assignment of new activities found in fast neutron studies.

## Experimental method

Determination of all cross sections was performed using neutron-activation technique. The reaction yields have been determined by measurements of induced activity. Samples in the shape of disc foils of natural Tb, Ge, Lu and Ta isotopes have been irradiated with D-T neutrons. Additionally tantalum irradiated by D-D neutrons and reactor filtered beams. The neutron generator NG-300/15, which was designed and built at the Department of Nuclear

Physics, University of Kyiv, has been used as a source of fast neutrons [3]. Experimental research of radiation capture reaction cross section for $^{181}$Ta nucleus has been performed at a research reactor WWR-M of the Institute for Nuclear Research, National Academy of Sciences of Ukraine [4]. The maximum current of deuterium ions beam is 10 mA. To generate neutrons with energy ~ 14 MeV a molecular component of deuteron beam $D_2^+$ has been used. A diaphragm to form a beam with diameter 10 mm has been used to decrease disperse of neutron energy in ion-pipe that allows to use different parts of sample after every irradiated series. Location of deuteron beam axis has been defined from distribution of neutron flux density on the target by method of foil activation. The average neutron energy has been determined experimentally using Zr/Nb ratio method [5]. Stakes of niobium and zirconium foils have been irradiated simultaneously at different angels relative to the incident deuterium beam direction. The indium and cadmium foils were used as additional protection from scattered low energy neutrons.

Several series of experimental measurements have been conducted, gradually irradiated the samples Ge, Tb and then Lu. Samples had a natural composition, before irradiation they have been checked for the presence of impurities. For terbium the angel of the irradiation position with respect to the $d^+$ beam direction was 0 degrees on 75 mm distance from Ti-T target. The lutetium samples were irradiated under 0, 65, 135 degrees and Ge disks at 45, 75, 120 and 150. The average neutron flux density was ~ $1.6 \cdot 10^{10}$ (n/cm$^2$·s) and depended on the specimen position under irradiation. Tantalum disks irradiated by DD-neutrons under 0 degrees with neutron flux ~ $3 \cdot 10^8$ (n/cm$^2$·s) and neutrons flux densities were obtained for used filters: 1.9 keV filter ($^{10}$B, Sc, S, $^{60}$Ni) - $4.81 \cdot 10^6$ (n/cm$^2$·s), 58.7 keV filter ($^{10}$B, Al, S, $^{58}$Ni) - $1.90 \cdot 10^6$ (n/cm$^2$·s), 144.5 keV filter ($^{10}$B, Si, Ti) - $3.87 \cdot 10^6$ (n/cm$^2$·s). For monitoring purpose an absolute value of neutron flux was checked with $^{115}$In(n, γ)$^{116m}$In and $^{93}$Nb(n, 2n)$^{92m}$Nb, $^{27}$Al(n,a)$^{24}$Na reactions. The neutron flux uncertainty was kept as constant within ≤ 5 %. For experiment optimization the neutron spectra were calculated with Monte Carlo approach also [6]. It was taken into account both the real irradiation conditions, sample dimensions and position relative to the Ti-T target. Time of irradiation varied within (5 – 180) min to guarantee maximum reaction yields. Time of measurements varied dependently of reaction product half-lives. The radioactivity of the reaction products was assayed by gamma-ray spectroscopy using a co-axial HPGe detector with sensitive volume ~ 110 cm$^3$, Ge-planar ~ 1 cm$^3$ and low-background anticoincidence spectrometer. Calibration procedure has been performed with a set of standard point sources ($^{133}$Ba, $^{241}$Am, $^{60}$Co, $^{137}$Cs). Cross sections have been determined by relative method and the reactions $^{27}$Al(n, α)$^{24}$Na, $^{93}$Nb(n, 2n)$^{92m}$Nb have been selected as monitor ones. The values of measured cross sections were determined for different gamma energies with subsequent weighted averaging. In the case of $^{71}$Ge due to the absence of suitable gamma-rays KX-ray spectra were acquired and in corresponding formula the fluorescent yields were used. In order to deduce reliable cross-section values, all the sources of biases were thoroughly considered. Because of big thickness (up to 2 mm) and high density of irradiated samples it was necessary to take into account self-absorption effects as well. A modeling approach has been used with Monte Carlo simulations. Correction factor was taken as the ratio of detector efficiency in cases of point and volume radiation sources. The efficiency of point and volume sources (activated foils) was calculated with MCNP 4C code [6], correction factors for coincidence summing have been calculated by Nuclide Master+ code [7]. The input information for these calculations was the parameters about nuclear structure from estimated data base ENSDF and real geometry of measurements.

## Results of measurements

The neutron induced reactions (n, p), (n, α) and (n, 2n) were studied at the average neutron energy of 14.6 MeV for the terbium, germanium and lutetium isotopes. Cross section values for reaction (n,γ) have been determined only for tantalum. Cross section values were measured and presented in Tables 1-3. Each value is based on several independent measurements. The available literature cross section values [1] for incident neutron energies about 14 MeV is given in the same tables for comparison. As a confirmation of accurate using of measurement technique applied it can be considered the fact that for some reactions we gained rather very good agreement with previously measured data.

Theoretical calculations of excitation functions have been performed with code Talys-1.0 [8]. Evaluated data have been taken from ENDF B/VI data base. At neutron energies higher then 8 MeV pre-equilibrium processes do predominate, therefore in calculations of excitation functions two-component exiton model [8] was used. For reaction $^{175}$Lu(n, p)$^{176}$Yb, $^{72}$Ge(n,2n)$^{71}$Ge, $^{175}$Lu(n, α)$^{172}$Tm and $^{176}$Lu(n,α)$^{173}$Tm acceptable agreement observed between results of measurements and calculations (Fig. 1-4).

Considering the fact that at 14 MeV neutron energy the cross section is rather sensitive to pre-equilibrium process, but for alpha-particles an emission is not simple and exiton model only does not work. It is well-known that for nuclear reactions involving alpha-particles, mechanisms like stripping, pick-up, brake-up and knock-out do play an important role and these direct-like reactions are not covered by the exciton model. The cross section of (n, α) reaction near threshold is sensitive to the stripping reaction. In Talys-1.0 [8] for that reason two phenomenological models are developed. The stripping, pick-up, brake-up and knock-out contributions can be adjusted with the Cstrip keyword. Based on them consideration it has been provided an excellent agreement with experiment (Fig.3-4). Calculations also demonstrated that cross sections in specific cases are insensitive for level density parameters (see Fig. 1). This result obtained confirmed again that behavior of nuclear reaction excitation functions for deformed nuclei is not simple and does not belong to one systematic. Fig.2 presents the calculation results with different optical potential. Measured cross section for $^{176}$Lu (n, α)$^{173}$Tm reaction is in well agreement with results provided in [9].

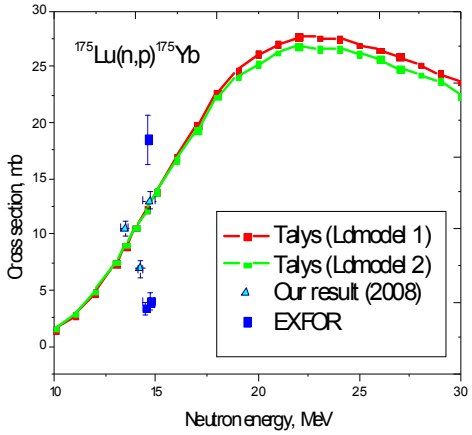


***Figure 1.*** *Comparison of experimental and calculation results for the $^{175}$Lu(n, p)$^{175}$Yb reaction*

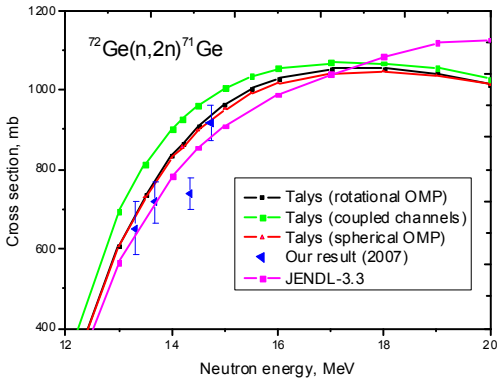


***Figure.2*** *Comparison of experimental and calculation results for the $^{72}$Ge(n, 2n)$^{71}$Ge reaction*

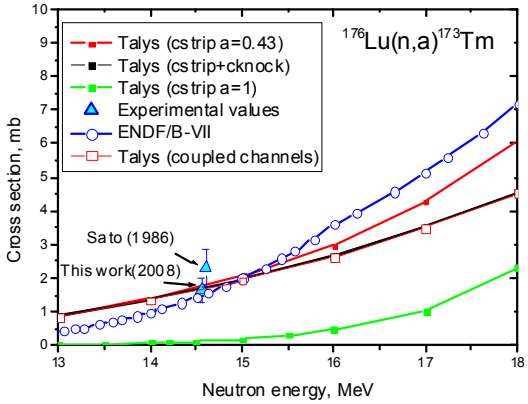


***Figure 3.*** *Comparison of experimental and calculation results for the $^{176}$Lu(n, α)$^{173}$Tm reaction*

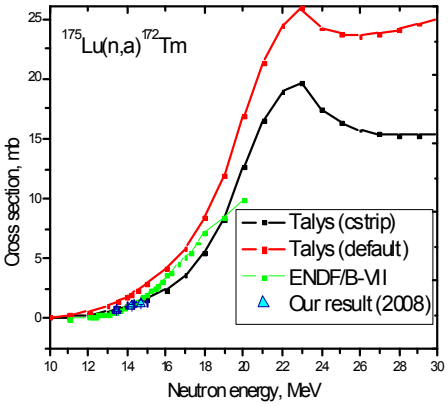


***Figure 4.*** *Comparison of experimental and calculation results for the $^{175}$Lu(n, α)$^{172}$Tm reaction*

***Table 1***. *Measured cross sections for lutetium isotopes.*

| Nuclear reaction | Half-life | Neutron energy, MeV | Cross section, mb | EXFOR [1] |
|---|---|---|---|---|
| $^{175}$Lu(n, 2n)$^{174m}$Lu | 142 d | 13.47 | 480(63) | – |
| | | 14.2 | 382(59) | 515(36) |
| | | 14.56 | 567(60) | 627(52) |
| $^{175}$Lu(n, 2n)$^{174g}$Lu | 3.31 y | 13.47 | 1896(250) | 1890(124) |
| | | 14.2 | 1473(219) | 1670(159) |
| | | 14.6 | 1860(190) | 1900(162) |
| $^{175}$Lu(n, p)$^{175}$Yb | 4.19 d | 13.47 | 10.7(0.7) | – |
| | | 14.2 | 9.8(0.7) | – |
| | | 14.6 | 13.2(0.9) | 18.5(2.2)<br>3.4(0.5) |
| $^{175}$Lu(n, α)$^{172}$Tm | 63.6 h | 13.47 | 0.7(0.1) | – |
| | | 14.2 | 1(0.03) | – |
| | | 14.6 | 1.5(0.2) | – |
| $^{176}$Lu(n, α)$^{173}$Tm | 8.24 h | 14.6 | 1.6(0.3) | 2.3(0.6) |

***Table 2***. *Measured cross sections for terbium at neutron energy 14.56 MeV*.

| Nuclear reaction | Half-live | Cross section, mb | EXFOR [1] |
|---|---|---|---|
| $^{159}$Tb(n, p)$^{159}$Gd | 18,48 h | 4.8(0.5) | 6.6(0.7) |
| $^{159}$Tb(n, α)$^{156}$Eu | 15,19 d | 2.2(0.3) | 2.2(0.5) |
| $^{159}$Tb(n, n′α )$^{155}$Eu | 4,71 y | 0.04(0.02) | <0,30 |
| $^{159}$Tb(n, 2n)$^{158}$Tb | 180 y | 1913(60) | 1909(82) |

***Table 3***. *Measured cross sections for reaction $^{181}$Ta(n,γ)$^{182m2}$Ta.*

| Neutron energy, keV | Δ Neutron energy, keV | Cross section, mb | ΔCross section, mb(%) |
|---|---|---|---|
| 1.9 | 1.5 | 3.7 | 0.3 (8%) |
| 58.7 | 2.7 | 0.8 | 0.2 (18%) |
| 144.5 | 16.8 | 0.7 | 0.1 (13%) |

Theoretical predictions by Talys calculations of reaction yield and experimental measurements have shown that cross section value of reaction $^{159}$Tb(n,n′α)$^{155}$Eu is lower by one order than previous presented data [10].

The cross sections values are measured with less than 10 % uncertainty, though in few cases the error bars are even larger. For many applications such an accuracy may be considered as acceptable and the cross section values themselves as quite reliable since nuclear constants, interfering reactions, contaminations, neutron flux normalization, energy determination, energy spread, energy attenuation in the sample for irradiation to be detected and instrumental factors with necessary corrections have been taken into account.

**Conclusions**

The cross section values obtained can be considered in the process of evaluated data calculation to provide more correct assessment of cross section values for these reactions. The excitation functions for reactions $^{175}$Lu(n,α)$^{172}$Tm and $^{72}$Ge(n,2n)$^{71}$Ge have been measured for the first time at energy range (13.4-14.7) MeV and cross section for $^{181}$Ta(n,γ)$^{182m2}$Ta at energy 2.8, 14.5 MeV and energies of filtered neutron beams (1.9, 58.7 and 144.5 keV) as well. Good correspondence of our results obtained with results of other research groups could be considered as an evidence of the neutron-activation technique correct using. Theoretical calculations indicated that for (n,α) reaction it is very important to take into account special reaction mechanisms. For some reactions we achieved a

considerable improvement in cross section values accuracy. Presented results can be used in estimated data calculation and provide more correct cross section values for testing of nuclear reaction models. One can stress that it is necessary to use an individual approach in theoretical calculations for certain reactions.

**References**

[1] Cross section information storage and retrieval system (EXFOR), National Nuclear Data Center (NNDC), Brookhaven National Laboratory, USA. – http://www.nndc.bnl.gov/index.jsp (online)
[2] Forrest R.A. “Data requirements for neutron activation Part I: Cross section”, Fusion Engineering and Design 81, pp. 2143-2156 (2006).
[3] Primenko G.I., Maidanyuk V.K., Neplyuev V.M. “Generator of 14 MeV neutrons with $5 \cdot 10^{11}$ $s^{-1}$ flux”,/ Devices and technique of experiment – 1989. – № 6. – pp. 39–41 (in Russian)
[4] Gritzay O.O., Kolotyi V.V., Kaltchenko O.I. “Neutron filters at Kyiv Research reactor”, Preprint KINR-01-, (2001)
[5] Agrawal H.M., Pepelnik R. “Determination of the mean neutron energy using the Zr/Nb and the Ni method”, Nuclear Instrum. and Meth. in Physics Research. – 1995. – Vol. A366, pp.349-353.
[6] Briesmeister J.F. MCNP – a general Monte Carlo N-particle transport code. – Los Alamos National Laboratory Report LA-12625-M, 989, (1997).
[7] A. Berlizov, V. Danilenko, A. Kazimirov, S.Solovyova “Statistical modeling of true-coincidence corrections with using of estimated nuclear data in the calculations”, Atomic energy 2006, 100, vol.5, -pp.-382 - 388 (in Russian)
[8] Koning A.J., Duijvestijn M.C. TALYS: Comprehensive nuclear reaction modeling // Proceedings of the International Conference on Nuclear Data for Science and Technology – ND2007, May 22 - 27 – Nice, France (2007).
[9] Sato T., Kanda Y. and Kumabe I. “Activation Cross Sections for (n,p) and (n,$\alpha$) Reactions on Nd, Sm, Yb and Lu at 14.6 MeV”, Journal of Nuclear Science and Technology 12(11), (1975), pp. 681-686
[10] Qaim S.M. “A study of (n,nα) reaction cross sections at 14.7 MeV”, Nuclear Physics A458, pp. 237-245 (1986)

# Fission Research at IRMM

*F.-J. Hambsch [1)], E. Birgersson [1)],I. Fabry [1)], N. Kornilov [1)], A. Oberstedt [2)], S. Oberstedt [1)], S. Zeynalov[1,3)]*

1) European Commission, Joint Research Centre, Institute for Reference Materials and Measurements, Retieseweg 111, 2440 Geel, Belgium
2) Örebro University, School of Science and Technology, 70182 Örebro, Sweden
3) Joint Institute for Nuclear Research, 141980 Dubna, Russia
franz-josef.hambsch@ec.europa.eu

***Abstract:*** New experimental results are presented on the fission characteristics of $^{238}$U(n, f) in the threshold region from $E_n$ = 0.9 to 2.0 MeV and the prompt neutron spectrum from fission of $^{236}$U* induced by neutrons at $E_n$ = 0.5 MeV. Fission properties in the vibrational resonance in the fission cross-section of $^{238}$U at $E_n$ = 0.9 MeV have been investigated for the first time ever. Possible evidence of an angular dependence of the fission neutron spectrum and indications for the observation of scission neutrons are presented. Improved modeling of the neutron emission in spontaneous and neutron-induced fission has resulted in a better description of the experimental data, when scission neutrons are included. Furthermore, IRMM has taken initiative to respond to the NEA data request to improving prompt fission γ-ray emission data.

## Fission modes in $^{238}$U(n,f)

The experiment on $^{238}$U(n,f) has been performed at the Van de Graff accelerator facility of the IRMM. As fission fragment detector a double-sided Frisch-grid ionisation chamber has been used. More details about this detector can be found in Ref. [1].
The highly enriched $^{238}$U (99.9997 %, 132 μg/cm$^2$) target, was prepared at IRMM. The incident neutron energy ranged from 0.9 MeV up to 2 MeV. At the lowest incident neutron energy the fission cross-section was only about 10 mb. The $^7$Li(p,n)$^7$Be and T(p,n)$^3$He reactions were used to produce mono-energetic neutrons. Data analysis has been performed taking into account the Frisch-grid inefficiency, the energy loss in the target as well as in the backing, the pulse-height defect in the counter gas and the momentum transfer of the incoming neutron. After having applied all the mentioned corrections to the raw anode and sum pulse-height signals, a further quality check has been made by comparing the corrected anode signals of both sections of the ionisation chamber. This is shown in Fig. 1. A nearly perfect agreement of the pulse height of both sections is visible. The same is true when the mass distribution is calculated as shown in Fig. 2. Hence, the data analysis has been performed in a proper way.

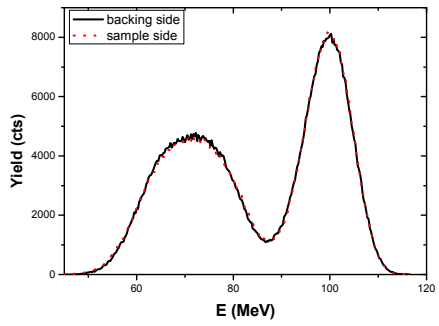


***Figure 1.*** *Comparison of the anode pulse height of the sample side (dashed line) and the backing side (solid line) after applying all corrections.*

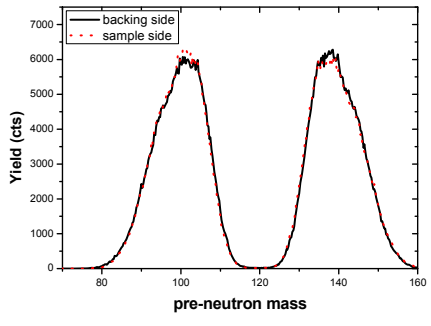


***Figure 2.*** *Comparison between the mass distribution calculated from the backing (solid line) and sample side (dashed line).*

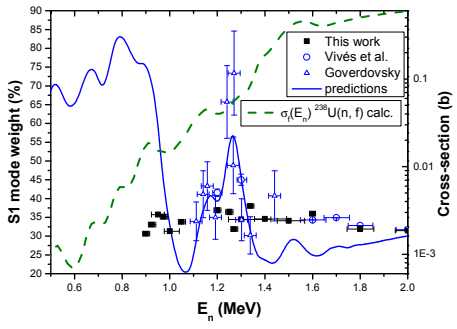


***Figure 3.*** *Weight of the S1 fission mode as a function of incident neutron energy. The full line gives the theoretical prediction [2] and the full points the present results. The open points are from earlier measurements [3, 4] showing strong fluctuations of the fission mode yields.*

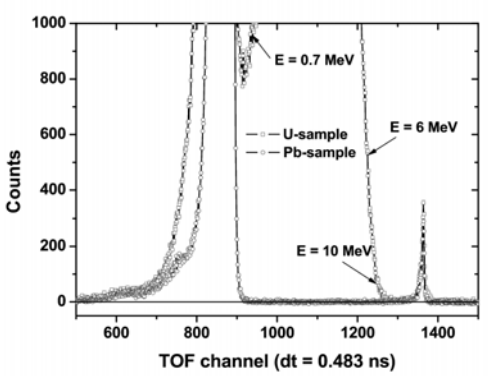


***Figure 4.*** *Time-of-flight spectra for the $^{235}U$ (full symbol) and the Pb- sample (open symbol) at 120 degree. Both spectra were normalized to the elastic neutron scattering peak.*

Unfortunately however, the predictions of the theory for a strong change of the contributions of the different fission modes [2] at the vibrational resonances in $^{238}U(n,f)$ could not be verified as can be seen in Fig. 3. This figure shows the fluctuations of the S1 mode as a function of the incident neutron energy. The full line is the prediction [2], the open symbols are previous measurements [3,4] and the full symbols are results of the present work [5].

## The prompt fission neutron spectrum

The present measurements were also carried out at IRMM, using the fast neutron time-of-flight technique. A pulsed proton beam of about 1.3 ns FWHM at 1.25 MHz repetition rate and 0.5 μA average current was used. Mono-energetic neutrons of 0.52 MeV average energy were produced using the $^{7}Li(p,n)$ reaction. A metallic $^{235}U$ sample (93.15 % enrichment, 161.28 g) and a similar sized lead sample were applied for foreground and background measurements, respectively. Figure 4 shows the time-of-flight spectra for the uranium and lead runs. Both spectra were normalized to the elastic neutron scattering peak. No time dependent peculiarities were found in the lead-sample background run in the secondary neutron energy range of interest from 0.7 MeV to 12 MeV.

Up to three NE213-equivalent liquid scintillation detectors of 10.2 cm diameter and 5.1 cm length were used in the measurement. At first two of them at 90 degree (flight path 2.73 m) and at 120 degree (flight path 2.40 m). The neutron production target to sample distance was ~5 cm. The results of this experiment have been presented at ND2007 [6].

In a second experiment three identical neutron detectors were used at a flight path of 2.24 ± 0.01 m placed at 90, 150 and 120 degrees. The distance from the neutron production target to the sample was ~8 cm.

A third experiment was done with different sample positions relative to the neutron target to check the possible influence on the polarization of the incident neutron beam. In all experiments, the detectors were shielded against direct and room-scattered neutrons. Pulse-shape analysis was used to reduce the γ-ray background. The detector efficiencies were measured relative to the $^{252}Cf$ standard spectrum using a specially designed fast ionization chamber [7]. The energy spectra were corrected for detector efficiency, for neutron multiple scattering in the sample, and for time resolution. A detailed description of the experimental procedure will be published elsewhere [8].

The experimental prompt fission neutron spectra (PFNS) were normalized to unity and the average neutron energy was calculated. A Maxwellian spectrum was fitted in the energy range of 0.7-1.5 MeV and 9-11 MeV to the measured spectrum and an extrapolation to zero and to 20 MeV was done. The average energies measured in both runs are given in Table 1.

***Table 1.*** *Average energy of the PFNS for all angles and runs*

| Angle, degree | <E>, MeV Run 1 | <E>, MeV Run 2 | <E>, MeV Run 3 |
|---|---|---|---|
| R90 | 2.004 | 2.002 | 2.021 |
| L90 | | | 2.007 |
| L120 | 2.076 | 2.050 | |
| R150 | | 2.026 | 1.975 |

The PFNS at all investigated angles and for all runs are shown in Fig. 5 as a ratio to a Maxwellian distribution with the same average energy.

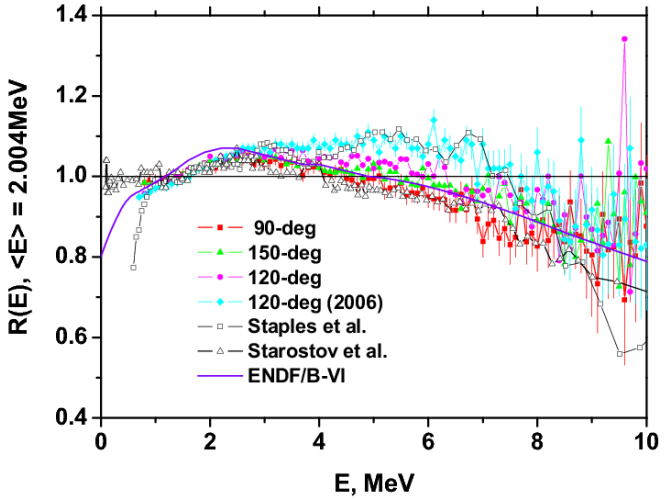


***Figure 5.*** *Comparison between the present results at several angles (full symbols) with data of Ref. [10] (open squares) and Ref. [9] (open triangles). Also ENDF/B-VI is given as full line.*

A very good agreement of our data at 90 degree is observed with the data of Ref. [9] over the whole prompt fission neutron energy range. For some of the other newly measured data a data set in literature can be found which agrees also very well. The ENDF/B-VI data do deviate mainly at low secondary neutron energies smaller 2 MeV.

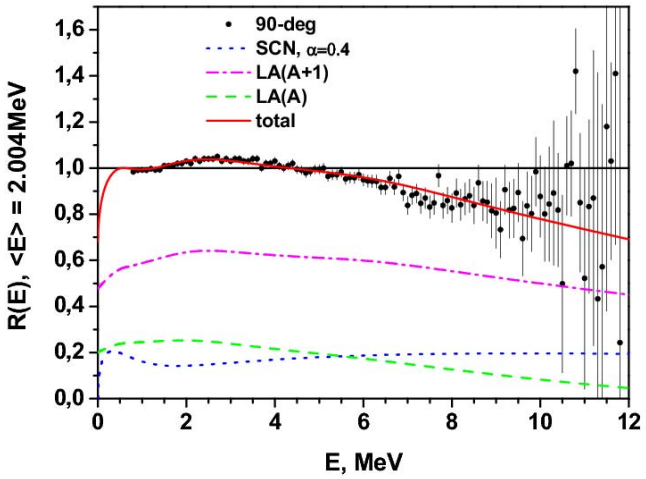


***Figure 6.*** *Modeling of the PFNS using three sources of neutron emission (broken lines).*

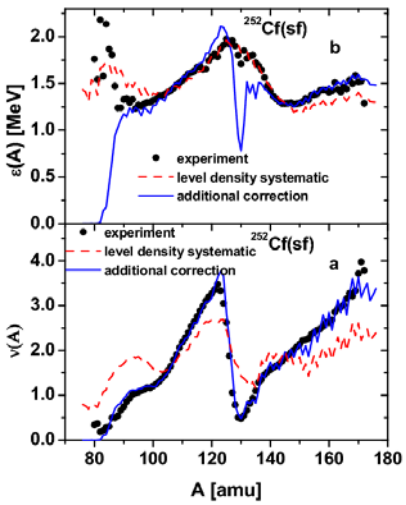


***Figure 7.*** *a. Experimental neutron multiplicity for $^{252}$Cf [15] (full symbols) compared to the model calculations. The dashed line is based on the level density systematic of Ignatjuk [16] and the full line on the additional correction (see text).*
*b. Experimental average neutron energy [15] (full symbols) compared to model calculations. The dashed line is based on Ref. [16] and the full line on the additional correction.*

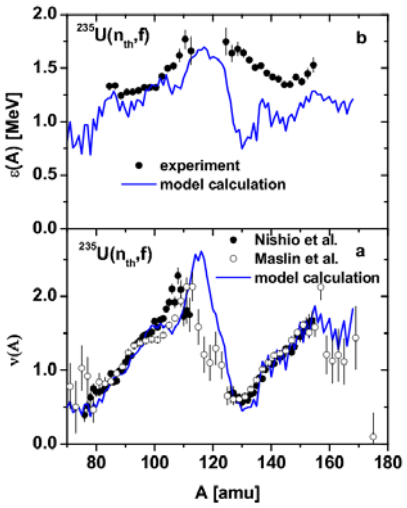


***Figure 8.*** *a. Experimental neutron multiplicity for $^{235}$U($n_{th}$,f) of Ref. [17] (full symbols) and Ref. [18] (open symbols) compared to our model calculations (full line).*
*b. The experimental average neutron energy of Ref. [17] (full symbols) compared to our model calculation (full line).*

Altogether, the present results point to the presence of an angular anisotropy in prompt neutron emission which was already discussed e.g. in Ref. [10]. The PFNS was, however, never analyzed with an angular dependence in mind and the deviation may have been masked by statistical uncertainties.

The observed difference for the data obtained at 120 degree between run 1 and 2 still needs some clarification. The only difference between the two experiments was the sample to source distance. The present results obviously show a tendency of an angular dependence of the PFNS, although unexpected and physically not understood. The observed angular anisotropy of the PFNS cannot be explained with the fission-fragment angular anisotropy in the laboratory system. For a fission-fragment angular anisotropy A = W(0°)/W(90°) – 1 = 0.06 [11] the spectrum ratio at 90 degree to the 120 degree is much closer to unity and does not correlate with the energy dependence of the present results. Hence, the presently observed anisotropic neutron emission can only be connected with neutron emission before scission of the compound nucleus, the so-called scission neutrons. In this case fission neutrons should be emitted from three sources. This is shown in Fig. 6 leading to a perfect agreement with the experimental data at 90 degree emission angle from 0.7 MeV to 10 MeV of prompt neutron energy.

The description of the experimental data is much better than with the so-called Los Alamos (LA) model [12]. However, the spectrum measured in our experiment at 90 degree emission angle, which is in perfect agreement with Ref. [9], can not explain the integral experimental data. The average ratio of the calculated to the experimental cross sections is <R> = C/E = 0.956 ± 0.008. At the same time, this ratio calculated with the 120-degree spectrum (<E> = 2.036MeV) is <R> = 0.994 ± 0.007. These results are based on our model calculation extrapolated to thermal incident neutron energy.

In conclusion, an angular-dependence of the PFNS was measured for the first time using detectors at 90, 120 and 150 degree. None of the obligatory corrections (detector efficiency, multiple scattering in the sample, uncertainties of sample and neutron beam position, time resolution, time independent background) did reveal any systematic errors that may have

produced the measured anisotropy. We may describe this effect by changing the contribution of the low energy component of the scission neutron spectrum only, but we have presently no scientific explanation of this approach. In addition, we have no idea how to explain the discrepancy between available microscopic and macroscopic data.

### Neutron multiplicity and average energy versus fission fragment mass split

For the calculation of the neutron multiplicity versus fragment mass and total kinetic energy (TKE), the two-dimensional distribution Y(A,TKE) has been calculated in the framework of the multi-modal random-neck rupture fission model [13] using the same ideas as developed in Ref. [14]. Model parameters were adjusted iteratively by comparing the calculated with the experimental one-dimensional Y(A) and TKE(A) distributions. Four fission modes were assumed – one symmetric mode and three asymmetric modes.

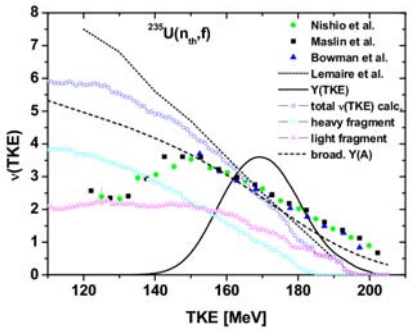


***Figure 9.*** *Experimental neutron multiplicity versus TKE data for $^{235}$U(nth,f) (closed symbols) compared to the model calculation (open symbols). The dashed line shows the calculation taking into account a broadening of the experimental data, the dotted line represents the results of Ref. [21]. The experimental data are from Refs. [17, 18, 22].*

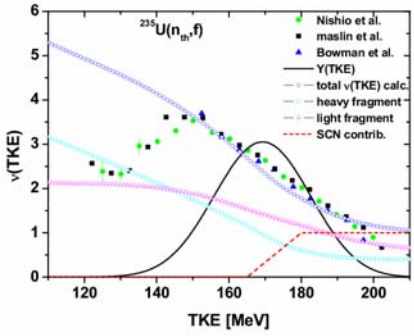


***Figure 10.*** *The same as in Fig. 11, but now the contribution of the scission neutrons is taken into account and is given by the dashed line.*
*The experimental data are from Refs. [17, 18, 22].*

Neutron emission has been calculated based on the total excitation energy (TXE) by assuming an unchanged charge distribution. The TXE is shared between light and heavy fragments assuming thermo-dynamic equilibrium.
For each target nuclei $^{235}$U(n$_{th}$,f), $^{244,248}$Cm(sf) and $^{252}$Cf(sf) the dependence of neutron multiplicity and neutron energy on the fission fragment mass, $\nu$(A) and $\varepsilon$(A) was calculated. The $^{252}$Cf results together with the experimental data of Ref. [15] are given in Fig. 7. A description of the $\nu_{exp(A)}$-data of Ref. [15] is not possible using the level density systematic of Ignatyuk [16] under the assumption of thermo-dynamic equilibrium (see dashed line in Fig. 7a). However, the "bell like" dependence for $\varepsilon$(A) can be reproduced reasonably well (see dashed line in Fig. 7b). A correction factor on the share of the excitation energy of the fragments of 0.40 < cor(A) < 1.25 needs to be applied to reproduce the $\nu_{exp(A)}$-data in Fig. 7a (full line) .
For $^{235}$U(n$_{th}$,f) the Nishio et al. [17] and Maslin et al. [18] experimental data for $\nu$exp(A) were rather well described with cor(A) = 0.9 in the framework of our model (full line in Fig. 8a). However, the model failed again to predict $\varepsilon$(A) (full line in Fig. 8b).
It is obvious from Figs. 9, 10 that $\nu$(TKE) is overestimated for low TKE and the positive slope d$\nu$/dE observed cannot be reproduced. Actually, this is a very difficult energy region to assess in experiments based on the double energy (2E) method. An event from the range of maximum yield with moderate excitation and $\nu$ ~ 3-4, if false identified, will most probably be registered in either the symmetric or very asymmetric mass range [19]. This would effectively lead to a reduction of $\nu$ at low TKE. Hence, a low $\nu$(TKE) in conjunction with a positive slope d$\nu$/dE may point to systematic errors in the experiment.

A good agreement in slope and absolute value is found at higher TKE (see Fig. 9). However, at still higher TKE a constant difference between theoretical and experimental data becomes evident. This cannot be explained due to experimental problems. Introducing scission neutron emission [20] at higher TKE made the agreement between experiment and model calculation much better (see Fig. 10).

## Prompt fission γ-ray studies

The γ-ray energy released in fission accounts for about 10% of the total energy release in the core of a standard nuclear reactor. Although the characteristics of γ-ray emission, e. g. multiplicity, total energy and spectrum, is fairly well known for neutron capture and inelastic neutron scattering, fission γ-rays are the major source of uncertainty in the modelling of γ-heating in nuclear energy applications. One particular challenge in modelling new generation reactor neutron kinetics is to calculate the γ-heat deposition e. g. in steel and ceramics reflectors without $UO_2$ blankets. According to Ref. [23] those modern designs requires γ-heating to be known with an uncertainty as low as 7.5% (1σ). The comparison of various benchmark experiments with calculated γ-heating data shows a systematic underestimation ranging from 10 to 28% for the main fuel isotopes $^{235}U$ and $^{239}Pu$. This is attributed to deficiencies in γ-ray production data in evaluated nuclear data files [24]. Data found in modern nuclear-data libraries all date back to experiments performed in the early 1970's [25,26,27]. In those experiments NaI scintillation detectors were used as γ-ray spectrometer with an ionisation chamber as fission trigger.

Therefore, requests for new measurements on prompt γ-ray emission in the reactions $^{239}Pu$ (n,f) and $^{235}U$(n,f) have been formulated and included in the Nuclear Data High Priority Request List of the NEA (Req. ID: H3, H4) [28]. IRMM has the possibility to investigate the feasibility of measuring those characteristic quantities as the γ-ray spectrum, multiplicity and the correlation with fission-fragment mass and excitation energy with the requested accuracy to describe γ-heating within 7.5%.

The measurement of prompt fission γ-rays emitted from highly excited fission fragments directly after scission is very difficult, because γ-ray emission is accompanied by prompt neutron emission. Those neutrons do induce signals as well in the γ-ray detector via inelastic scattering at or neutron capture in the detector itself.

In the past large NaI crystal scintillation detectors have been used to measure fission γ-rays. Iodine has a non-negligible cross-section for neutron reactions and, therefore, the time-of-flight technique has been employed to separate neutrons from γ-rays. The separation capability highly depends on the time-resolution of the experimental set-up, which is determined by the resolution of the fission-chamber and/or the pulse-width of the accelerator and the γ-ray detector itself. In case of NaI detectors a timing resolution of around 5 ns may be achieved. All presently existing experimental data date back to the early 1970's and both reactor scientists and evaluators of nuclear data have severe doubts on their reliability.

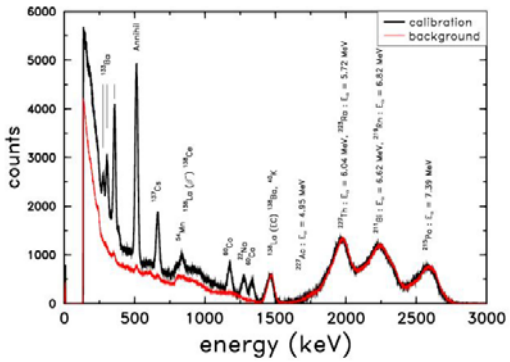


***Figure 11.*** *Calibration spectrum taken with a 1.5"x1.5" $LaCl_3$:Ce scintillation detector. The background due to the intrinsic detector activity is shown as the lower (red) line.*

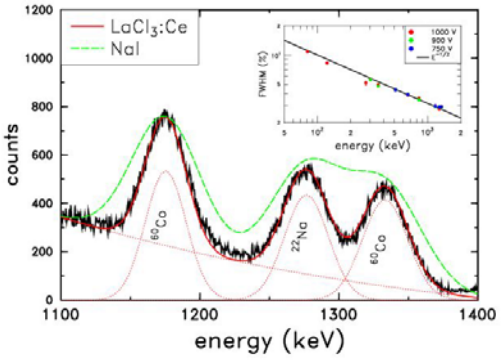


***Figure 12.*** *Energy resolution of a 1.5"x1.5" $LaCl_3$:Ce detector at $^{22}$Na and $^{60}$Co $\gamma$-decay energies compared to a characteristic spectrum of a NaI scintillation detector (see text).*

The goal of our recently started study is the investigation of a novel type of crystal scintillation detectors, produced from cerium-doped lanthanum halides, with a timing resolution almost one order of magnitude better than for traditional NaI detectors allowing for a better n/$\gamma$ separation by means of time-of-flight, and with a superior energy resolution. In Figs. 11 and 12 first characteristic single spectra are shown demonstrating the superior energy resolution of $LaCl_3$:Ce compared to a NaI detector. The background originating from the intrinsic $\alpha$- and $\beta$-activity due to the radioactive $^{138}$La and $^{223}$Ac will be suppressed when measuring $\gamma$-rays in coincidence with the corresponding fission fragment or relative to the neutron beam pulse. The inlet in Fig. 12 shows the detector resolution as a function of the $\gamma$-ray energy, which nicely follows the expected dependence ~ $1/E^{1/2}$.

**References**

[1] C. Budtz-Jorgensen et al., Nucl. Instr. Meth. A285 (1987) 209.
[2] F.-J. Hambsch et al., Ann. Nucl. Energy 32 (2005) 1297.
[3] F. Vives et al., Nucl. Phys. A 662 (2000) 63.
[4] A. Goverdovsky et al., in Proc. 8th Int. Seminar on Interaction of Neutrons with Nuclei, Dubna, May 17-20, 2000, E3-2000-192, p. 298.
[5] E. Birgersson et al., submitted to Nucl. Phys. A.
[6] N.V. Kornilov et al., in Proc. of the Int. Conf for Nucl. Data for Sci. and Tech., ND2007, Nice, France, Apr 2007, to be published.
[7] N.V. Kornilov et al., JRC-IRMM, Neutron Physics Unit, Scientific report 2005, p. 67.
[8] N.V. Kornilov et al., An experimental study of prompt neutrons from 235U fission, Internal report GE/NP/01/2007/02/14, submitted to Nucl. Phys. A.
[9] B.I. Starostov et al., in Proc. 6th Conf. for Neutron Physics, Kiev, 1983, Obninsk 1984, pp. 285, EXFOR 40871, 40872, 40873.
[10] M.M. Islam, H.-H. Knitter, Nucl. Sci. Eng. 50 (1973) 108.
[11] F.-J. Hambsch, Nuclear data standards for nuclear measurements, NEADC -311 "U", INDC(SEC)-101, 1992, p. 59.
[12] D.G.Madland, J.R.Nix, Nucl. Sci. Eng. 81, 213 (1982).
[13] U. Brosa, S. Grossmann, A. Müller, Physics Reports 197 (1990) 167.
[14] N.V. Kornilov, A.B. Kagalenko, in Proc. of 11th Int. Seminar on Neutron Interaction with Nuclei (ISINN-11), Dubna 2003, 144.
[15] C. Budtz-Jørgensen, H.-H. Knitter, Nucl. Phys. A490 (1988) 307.
[16] V. Ignatyuk, K. Istekov, G.N. Smirenkin, Sov. J. Nucl. Phys. 29 (1979) 450.
[17] K. Nishio et al., Nucl. Phys A632 (1998) 540.
[18] E.E. Maslin, A.L. Rodgers, W.G.F. Core, Phys. Rev. 164 (1967) 1520.
[19] F.-J. Hambsch, S. Oberstedt, Nucl. Phys. A617 (1997) 347.
[20] N.V.Kornilov et al., Nuclear Physics A789 (2007) 55.
[21] S. Lemaire et al., Phys. Rev. C72 (2005) 024601.
[22] J .W. Boldeman, A.R. Musgrove, R.L. Walsh, Aust. J. Phys. 24 (1971) 821.

[23] G. Rimpault, Proc. Workshop on Nuclear Data Needs for Generation IV, April 2005 (Editor: P. Rullhusen) Antwerp, Belgium, World Scientific, ISBN 981-256-830-1 (2006) 46.
[24] G. Rimpault, A. Courcelle, and D. Blanchet, Nuclear Data High Priority Request List of the NEA (Req. ID: H3, H4; explanatory note).
[25] R. W. Peelle and F. C. Maienschein, Phys. Rev. C3 (1971) 373.
[26] F. Pleasonton, R. L. Ferguson, and H. W. Schmitt, Phys. Rev. C6 (1972) 1023.
[27] V. V. Verbinski, H. Weber, and R. E. Sund, Phys. Rev. C7 (1973) 1173.
[28] Nuclear Data High Priority Request List of the NEA (Req. ID: H3, H4).

# Experimental techniques for nuclear data: State of the art and future prospects

*H. Harada*

Japan Atomic Energy Agency, Nuclear Science and Engineering Directorate, Tokai-mura, Naka-gun, Ibaraki, 319-1195 Japan
harada.hideo@jaea.go.jp

***Abstract:*** Recent advancements in experimental techniques mainly used for the determination of the neutron capture cross sections are reviewed, related to advanced reactor systems, accelerator driven systems, and advanced fuel cycles. Here, experimental techniques include intense neutron sources, advanced detectors, and methodologies. The technique using laser Compton scattering gamma-rays is included as one of the new methodologies. These experimental techniques have been utilized for obtaining new nuclear data and also reducing uncertainties of nuclear data. The recent new results and the achieved uncertainties using these techniques are discussed using some examples. We conclude with some speculations on the future prospects achieved by the improved experimental techniques.

## Introduction

The need and rule of nuclear data for advanced nuclear systems and future energy supply have been reviewed in ref. [1], and the impact of reducing nuclear data uncertainties was stressed on the assessment of new concepts, on safety features and economics.
The uncertainties of nuclear data, although they are limited, have been evaluated. ***Table 1*** shows the comparison between the evaluations and the experiment on the neutron capture cross section of $^{107}$Pd for thermal neutrons. There was no direct measurement before ref. [2] at 2007. The values [3, 4] evaluated before the measurement are about 4 times smaller than the measured value. The discrepancy is much larger than ten times of the evaluated uncertainty in ref. [3]. This example shows the difficulty of the evaluations of nuclear data and its uncertainty in the case that there is no direct measurement.
***Table 2*** shows the comparison between the two different evaluations [4, 5] on the uncertainties of the fission cross section of $^{244}$Cm and the neutron capture cross section of $^{237}$Np for neutron energy range 0.5-1.35 MeV. The uncertainties by Aliberti *et al*. [5] are about 5 times larger than those in JENDL-3.3 [4, 6] in the both case. To deduce the accurate nuclear data and appropriate uncertainty, origins of uncertainties in measurements need to be clarified.

***Table 1.*** *The comparison of experimental data with evaluated data: The case of the neutron capture cross section of $^{107}$Pd for thermal neutrons*

| References | $^{107}$Pd(n, γ) |
|---|---|
| J, Nucl. Sci. Technol., 44, 103 (2007) [2] | 9.16 ± 0.27 b |
| Atlas of Neutron Resonances (2006) [3] | 2.54 ± 0.20 b |
| JENDL-3.3 (2002) [4] | 2.007 b |

***Table 2.*** *The comparison of different evaluated data: The case of the fission cross section of $^{244}$Cm and the neutron capture cross section of $^{237}$Np for fast neutrons*

| References | $^{244}$Cm(n, f) 0.5-1.35 MeV | $^{237}$Np(n, γ) 0.5-1.35 MeV |
|---|---|---|
| J. NSE, 146, 13 (2004) [5] | 40 % | 15 % |
| JENDL-3.3 (2002) [4] | 7.7 % | 3.4 % |

The different measurements sometimes give inconsistent results: the reported uncertainties are too small to account for the discrepancy. To account for this discrepancy, there should be other uncertainties, which have not been recognized by the experimentalists. This situation is shown in Fig. 1.

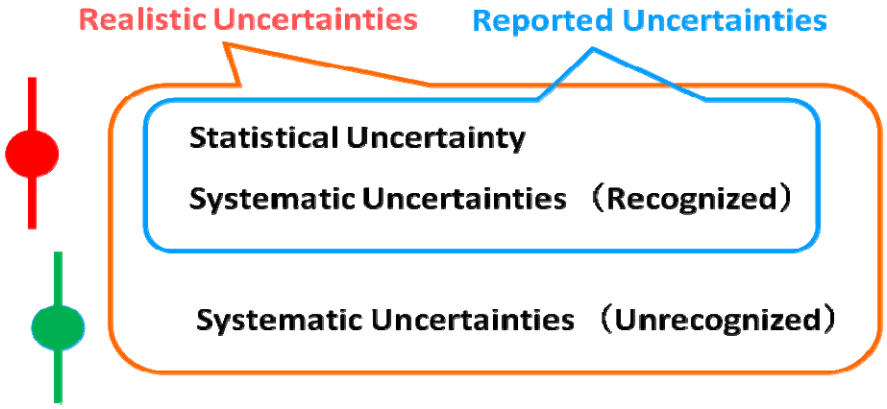


***Figure 1.*** *Uncertainties in experiments*

Experimental efforts have been concentrated in reducing these experimental uncertainties, and in developing required techniques. In the next section, recent experimental efforts are reviewed including development of devices, methodologies, together with some results. The future prospects are discussed in the last section.

## Experimental techniques

The importance of accurate nuclear data of radioactive nuclei, such as minor actinides and long-lived fission products, has been recognized, and experimental efforts have been done in the world. However, there are some difficulties in the measurements of radioactive samples, since the sample itself emits strong radiations and disturbs measurements, and also the preparation of the sample satisfying the requirement is difficult in many cases. To overcome these difficulties, high intensity neutron sources and high efficiency detectors have been developed. The traditional methods have also been applied in some cases. The state of the art techniques mainly in the measurements of neutron capture reactions are reviewed.

***Table 3.*** *Pulsed neutron facilities, arbitrary selected, which are currently used for the purpose of nuclear data measurements. Parameters in the table show a typical parameter recently reported. Variable ranges of these parameters are not shown here.*

| Facility<br>Reference | Beam<br>energy | Beam power<br>n Intensity | Beam pulse width<br>Pulse per sec | Flux<br>Flight path |
|---|---|---|---|---|
| IRMM, GELINA<br>ND2007, p.563 | Electron<br>100 MeV | 6 kW | 1 ns<br>800 Hz | <br>@ 12 m |
| ORNL, ORELA<br>ND2007, p.441 | Electron<br>180 MeV | 5 kW<br>$10^{13}$ n/s | 8 ns<br>525 Hz | <br>@ 40 m |
| Kyoto, e Linac<br>ND2007, p.591 | Electron<br>30 MeV | 1 kW | 100 ns<br>100 Hz | <br>@ 10 m |
| CERN, n-TOF<br>ND2007, p.537 | Proton<br>20 GeV | 9 kW<br>$10^{15}$ n/s | 6 ns<br>0.4 Hz | $4\times10^{5}$ n/cm$^2$/s<br>@ 185 m |
| LANL, Lujan<br>ND2007, p.415 | Proton<br>0.8 GeV | 80 kW | 135 ns<br>20 Hz | <br>@ 20 m |
| J-PARC, MLF<br>(Expected) | Proton<br>3 GeV | 1 MW<br>~ $10^{17}$ n/s | ~ 100 ns<br>25 Hz | ~ $10^{9}$ n/cm$^2$/s<br>@ 22 m |

**Neutron sources**

Pulsed neutron facilities, arbitrary selected, are summarized in Table 3, which are currently used for the purpose of nuclear data measurements. The neutrons produced by electron accelerators have been used for nuclear data measurements for a long period as was summarized in ref. [7]. Proton spallation reaction can produce neutrons more efficiently compared to electron induced (γ, n) reaction. The nuclear data instruments have been developed in the three facilities having spallation neutron sources, n-TOF at CERN, LANCE at LANL, and Material and Life science Facility MLF at J-PARC. The beam line 4, named as neutron-nucleus reaction instrument NNRI, in the MLF has been developed, and received first neutrons at May 30, 2008. The beam power is going to be increased up to 1 MW. The measurement of nuclear data will be started at 2009. Figure 2 shows the specifications of the NNRI and nuclear data measurement plans in near future [8].

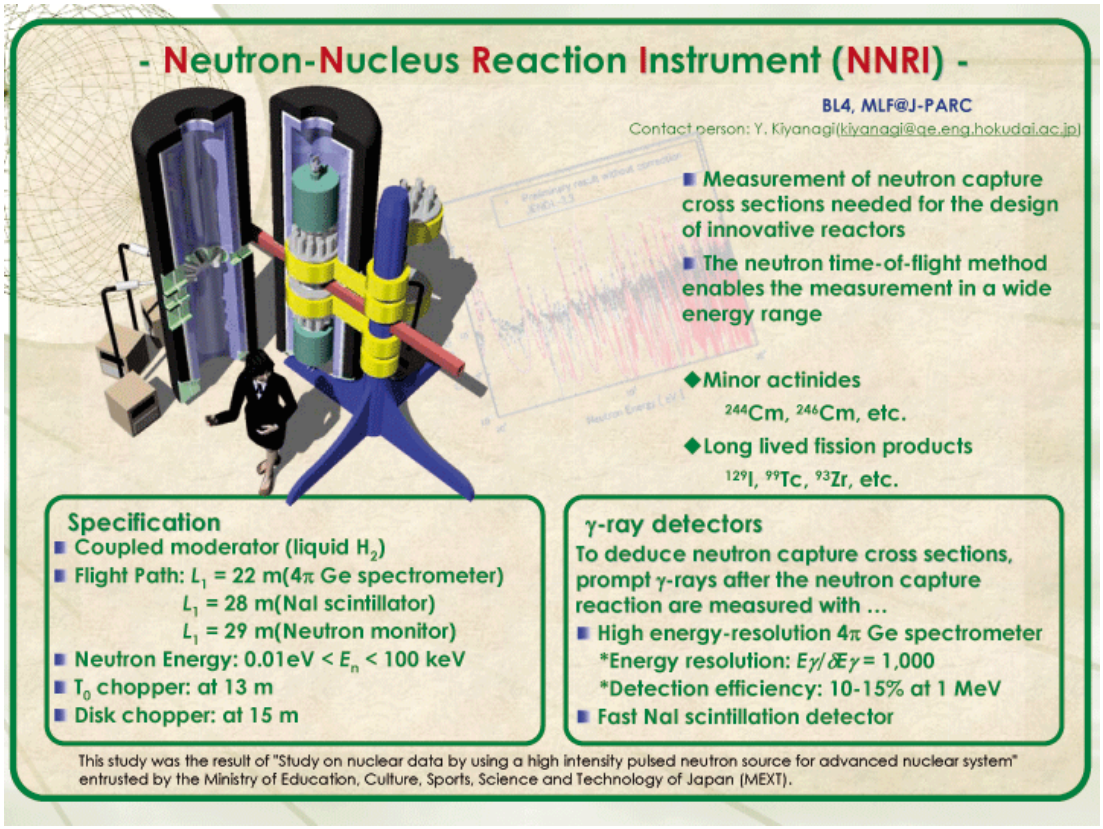


***Figure 2.*** *The specifications of the neutron-nucleus reaction instrument NNRI constructed in the* Material and Life science Facility MLF at J-PARC

The lead slowing-down spectrometers driven by these pulsed neutrons have also been used to measure the cross sections of radioactive samples [9, 10].

Although the intense pulsed neutrons become available, neutrons generated in nuclear reactors are still important for the measurements of nuclear data because their strong intensities of neutron fluxes enable unique techniques. For an example, the utilization of a double neutron capture reaction enables the neutron cross section measurement for very shot-lived nucleus. It was successfully demonstrated in the case of the measurement of the $^{238}$Np(n, γ) cross section for thermal neutrons [11], whose half-life is as short as 2 days.

Not only the activation method as used in the case of $^{238}$Np but also the prompt γ spectroscopic methods have been successfully used to determine the neutron capture cross sections using the neutron guide instrument *et al.* This method enables the measurement even in the case that the activation method could not be applied due to a capture product not emitting any observable radiation. The neutron capture cross sections of $^{99}$Tc [12], $^{107}$Pd [2] and $^{93}$Zr [13] have been determined by the prompt γ spectroscopic method. Those of $^{99}$Tc [14] and $^{129}$I [15] have also been measured by the prompt γ spectroscopic methods at

Budapest. Those of $^{99}$Tc and $^{129}$I could be measured by an activation method, and therefore, cross checks of the data determined by utilizing independent methods are possible.

**Detectors and data aquisition**

For neutron capture cross section measurements, the $C_6D_6$ detectors have been used in many facilities because of its low sensitivity to neutrons scattered from a sample. The pulse height weighting technique is used to deduce the capture cross sections. Tain *et al.* [16, 17] and Borella *et al.* [18] independently examined the accuracy achieved using this technique. It should be noted that the NaI detector has also been successfully used in combination with the pulse height weighting technique [19].

The 4π type gamma-ray spectrometers have been developed and used for the nuclear data measurements. The BGO scintillators [20], $BaF_2$ scintillators [21, 22], and Ge solid state detectors [23] have been used. The highly segmented design enabled the measurement using a small amount of sample [22]. It is anticipated that the achieved accuracy using these new types of spectrometers are carefully studied.

On the data acquisition, the systems with flash-ADCs have been developed and successfully utilized for the measurements together with these advanced detectors. Recent progresses have been reported in ref. [24-26].

The recently developed $LaBr_3$(Ce) and $LaCl_3$(Ce) scintillators have superior characteristics compared to other scintillators. The energy resolutions of these scintillators are superior to that of a NaI detector. Figure 3 shows the pulse-height spectra measured by the 3" times 3" $LaBr_3$(Ce) detector for $^{60}$Co and $^{152}$Eu gamma-ray sources, where the backgrounds originating from the β and γ rays of $^{138}$La (the half-life is about $10^{11}$ years) in the detector were subtracted. These scintillators are expected to be used in the next generation nuclear data measurement instruments because of their superior characteristics.

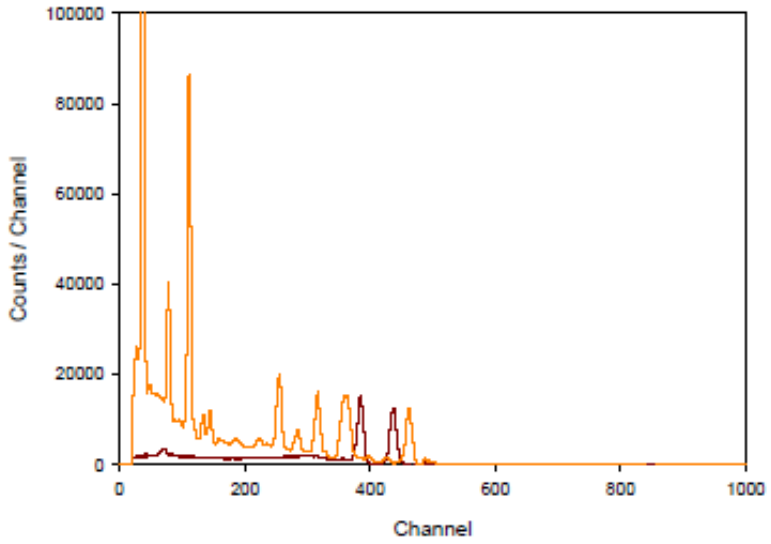


***Figure 3.*** *The pulse-height spectrum measured by the 3" times 3" $LaBr_3$(Ce) detector for $^{60}$Co (brown solid lines) and $^{152}$Eu (orange solid lines).*

**New techniques**

The Surrogate reaction method using a transfer reaction has been developed aiming at determining the cross section that is difficult to be measured directly [27]. For an example, the $^{236}$U(n, f) cross section was obtained from a Weisskopf-Ewing analysis of Surrogate $^{238}$U($^3$He, α) measurements.

Recently, the inverse reaction method using the (γ, n) reaction has been studied to deduce the (n, γ) cross sections [28]. The laser Compton back-scattering photons have been used for the measurements together with the high-resolution high-energy photon spectrometer (HHS) [29] and the 4π $^3$He neutron detector. The developments of these innovative measurement techniques are important and challengeable, especially when the method enables to measure the important or requested nuclear data for the first time.

## Future prospects

The highest-precision frontier research in nuclear data measurements should be a key to satisfy the target accuracies on the nuclear data requested for realizing the innovative nuclear reactors and fuel cycles. The efforts reducing statistical and systematic (recognized) uncertainties will be main important tasks in near future. After that, the comparison of the independent high-quality measurements will help to identify the origin of the unrecognized systematic uncertainty. By combining these efforts, the realistic uncertainties of nuclear data are expected to be much reduced.

**Acknowledgements**
The work on the $LaBr_3$(Ce) detector was supported by Grant-in-Aid for Scientific Research (B) (19360431).

**References**

[1] J. Bouchard, “Nuclear data for innovative fission reactors and fuel cycles”, Proc. Int. Conf. on Nuclear Data for Science and Technology - ND2007, April 2007, Nice, France, p.1 (2007).
[2] S. Nakamura et al., “Thermal-Neutron Capture Cross Section of Palladium-107”, J. Nucl. Sci. Technol., 44, 103 (2007).
[3] S.F. Mughabghab, Atlas of Neutron Resonances, Elsevier 2006.
[4] K. Shibata, et al., “Japanese evaluated nuclear data library Version 3 Revision-3: JENDL-3.3,” J. Nucl. Sci. Technol., 39, 1125 (2002).
[5] G. Aliberti et al., “Impact of nuclear data uncertainties on transmutation of actinides in accelerator-driven assemblies”, Nucl. Sci. Eng., 146, 13 (2004).
[6] G. Chiba, ERRORJ-Covariance Processing Code Version2.2, JNC TN9520 2004-003 (2004).
[7] J.A. Harvey ed., Experimental Neutron Resonance Spectroscopy, Academic Press, New York and London (1970).
[8] http://j-parc.jp/MatLife/en/instrumentation/bl04/BL04.html.
[9] K. Kobayashi et al., “Measurement of Neutron Capture Cross Section of $^{237}$Np by Linac Time-of-Flight Method and with Linac-driven Lead Slowing-down Spectrometer”, J. Nucl. Sci. Technol. 39, 111 (2002).
[10] D. Rochman et al., ”Cross-section measurements for $^{239}$Pu(n,f) and $^{6}$Li(n,α) with a lead slowing-down spectrometer”, Nucl. Instrum. Methods, A564, 400 (2006).
[11] H. Harada et al., “Measurement of Effective Capture Cross Section of $^{238}$Np for Thermal Neutrons”, J. Nucl. Sci. Technol. 41, 1 (2004).
[12] K. Furutaka et al., “Prompt gamma rays emitted in thermal-neutron capture reaction by 99Tc and its reaction cross section”, J. Nucl. Sci. Technol. 41, 1033 (2004).
[13] S. Nakamura et al., “Thermal-Neutron Capture Cross Sections of Zirconium-91 and Zirconium-93 by Prompt □-ray Spectroscopy”, J. Nucl. Sci. Technol., 44, 21 (2007).
[14] J.L. Weil et al., “The 99Tc(n, □)100Tc cross section, $^{99}$Tc(d, p)$^{100}$Tc and the $^{99}$Tc decay scheme and neutron binding energy”, Proc. Int. Conf. on Nuclear Data for Science and Technology - ND2007, April 2007, Nice, France, p.611 (2007).
[15] T. Belgya et al., “The thermal neutron capture cross section of $^{129}$I”, Proc. Int. Conf. on Nuclear Data for Science and Technology - ND2007, April 2007, Nice, France, p.631 (2007).
[16] J.L. Tain et al., “Accuracy of the pulse height weighting technique for capture cross section measurements”, J. Nucl. Sci. Technol., Sup.2, p.689 (2002).
[17] U. Abbondanno et al., “New experimental validation of the pulse height weighting technique for capture cross-section measurements”, Nucl. Instrum. Methods, A521, 454 (2004).
[18] A. Borella et al., ”The use of C6D6 detectors for neutron induced capture cross-section measurements in the resonance region”, Nucl. Instrum. Methods, A577, 626 (2007).
[19] J. Nishiyama et al., “Measurements of keV-neutron capture cross sections and capture gamma-ray spectra for Sn and Gd isotopes”, Proc. Int. Conf. on Nuclear Data for Science and Technology - ND2007, April 2007, Nice, France, p.615 (2007).
[20] O. Shcherbakov et al., ” Measurement of neutron capture cross section of 237Np from 0.02 to 100eV”, J. Nucl. Sci. Technol., 42, 135 (2007).
[21] E.-I. Esch, et al.., “Measurement of the $^{237}$Np(n, γ) cross section from 20 meV to 500 keV with a high efficiency, highly segmented 4π BaF2 detector”, Phys. Rev., C77, 034309

(2008).
[22] C. Guerrero et al., “The neutron capture cross sections of $^{237}$Np(n, $\gamma$) and $^{240}$Pu(n, $\gamma$) and its relevance in the transmutation of nuclear waste”, Proc. Int. Conf. on Nuclear Data for Science and Technology - ND2007, April 2007, Nice, France, p.627 (2007).
[23] M. Mizumoto, et al., “Neutron capture cross section measurements on 237Np with a 4$\pi$ Ge spectrometer”, Proc. Int. Conf. on Nuclear Data for Science and Technology - ND2007, April 2007, Nice, France, p.603 (2007).
[24] U. Abbondanno et al., “The data acquisition system of the neutron time-of-flight facility n_TOF at CERN”, Nucl. Instrum. Methods, A538, 692 (2005).
[25] A. Kimura, et al., “Performance of a data acquisition system for a large germanium detector array”, Proc. Int. Conf. on Nuclear Data for Science and Technology - ND2007, April 2007, Nice, France, p.587 (2007).
[26] A. Laptev et al., “High-speed data acquisition system for the neutron time-of-flight experiments”, Nucl. Instrum. Methods, A557, 621 (2006).
[27] J. Escher et al., “Surrogate reactions: the Weiskopf-Ewing approximation and its limitations”, Proc. Int. Conf. on Nuclear Data for Science and Technology - ND2007, April 2007, Nice, France, p.325 (2007).
[28] K.Y. Hara et al., ”Measurement of the $^{152}$Sm($\gamma$, n) Cross Section with Laser-Compton Scattering $\gamma$ Rays and the Photon Difference Method”, J. Nucl. Sci. Technol., 44, 938 (2007).
[29] H. Harada et al., ”Response of a high-resolution high-energy photon spectrometer (HHS) to monochromatic high-energy gamma rays”, Nucl. Instrum. Methods, A554, 306 (2005).

# Activation cross-sections measurement of Bi-209 using quasi-monoenergetic neutrons below 35 MeV.

*M. Honusek[1)], P. Bém [1)], V. Burjan [1)], U. Fischer [2)], M. Götz [1)], V. Kroha [1)], J. Novák [1)], S.P. Simakov [2)] and E. Šimečková [1)]*

1) Nuclear Physics Institute, CZ - 250 68 Řež, Czech Republic
2) Forschungszentrum Karlsruhe, DE -76021 Karlsruhe, Germany
honusek@ujf.cas.cz

***Abstract:*** In the framework of continuing the experimental tests of neutron activation cross-section data the activation of $^{209}$Bi isotope was investigated using fast quasi-monoenergetic neutrons from the NPI cyclotron-based neutron source. The $^{209}$Bi nuclide is the only one stable isotope of Bi and hence it constitutes an important possibility to study the reactions (n,3n), (n,4n) and (n,5n) at higher neutron energy region.
Sample foils were irradiated by neutrons with quasi-monoenergetic spectrum peaked at 19.0, 24.1, 29.5 and 34.5 MeV. Neutrons were generated in the source reaction p-$^{7}$Li by protons at energies of 22.1 27.1, 32.1 and 36.5 MeV, respectively. After sample irradiation the induced gamma activities were measured at various cooling times using HPGe detectors and employing the gamma spectrometry method.
The analysis of resulting specific activities of reaction products was carried out in terms of C/E ratio (E - measured reaction rate, C - the corresponding value calculated by means of the evaluated cross section from EAF-2007 library and the applied neutron spectrum as well). The neutron flux and spectra at sample positions were predicted using double-differential cross-section data of the source reaction $^{7}$Li(p,n) measured by other authors.
The Au foils serving as monitors were irradiated together with Bi foils.
The cross-section data of the $^{209}$Bi(n,3n)$^{207}$Bi, (n,4n)$^{206}$Bi, (n,5n)$^{205}$Bi reactions are derived on the basis of C/E values and compared with other experimental data from the literature.

## Introduction

The neutron cross-section data of reactions at incident energies $E_n$ > 20 MeV are needed to improve the accuracy of neutronic calculations incorporated with various fission and fusion technologies like Fluoride-Molten-Salt-Reactor systems, IFMIF (International Fusion Material Irradiation Facility) and for the tests of nuclear reaction models as well.
The previous experimental data for (n,xn) reaction on $^{209}$Bi are summarized in [1] . Data concerning (n,3n) reaction for neutron energy region $E_n \geq 20$ MeV were published in [2,3,4]. The reactions (n,4n) and (n,5n) were experimentally studied in [4] only, where the region up to the higher neutron energies was covered. The comparison of experimental data and values calculated using EAF version 2007 database are summarized in [5].
In the following sections we briefly describe the quasi-monoenergetic p-$^{7}$Li neutron source, the activation experiment on Bi foils and the method of data evaluation. The resulting radioactive isotopes were studied by means of gamma spectroscopy methods.
The preliminary analysis in terms of C/E results was carried out using the cross-section data from EAF version 2007 library and neutron spectra from Ref. [6]. The corrections of spectral flux at sample position due to geometry effects were discussed. The cross-sections for some reactions were obtained.

## Experimental equipment and neutron spectrum

The target station of quasi-monoenergetic neutron source based on $^{7}$Li(p,n) reaction was presented in previous work [7]. The proton beam from Rez isochronous cyclotron U120M strikes the Li foil at variable energies from 11 to 38 MeV. The carbon backing serves as a beam stopper.
The stack of irradiated foils (Bi + Au) was activated simultaneously at two distances (48 and 88 mm) from the Li foil to test the effect of the flux-density gradient in the vicinity of neutron source. The weights of foils (14 and 15 mm in diameter) were approximately of 0.14 g and 0.7 g for Au and Bi, respectively. The time profile of the neutron source strength during the irradiation was monitored by the proton beam current on the neutron-source target,

recorded by a calibrated current-to-frequency converter on PC. The typical proton beam current was about 3 μA. Irradiated samples were investigated by means of gamma-spectroscopy method. Two calibrated HPGe detectors of 23 and 50 % efficiency and FWHM of 1.8 keV at 1.3 MeV were used. Activated isotopes were identified on the basis of $T_{1/2}$, γ-ray energies and intensities. Cooling times of gamma measurement ranged from minutes to approx. 100 day. (Each foil was measured at approx. 8 cooling times).
To evaluate the neutron spectral flux at sample positions the spectral yield of source reaction p+$^{7}$Li(C backing) were taken from the Ref. [6], where TOF method of neutron spectra measurement at long distances was used. The spectra consist of quasi-monoenergetic part corresponding to the reactions to g.s. and 0.429 MeV states in $^{7}$Be, and of the low-energy tail generated a) by other reactions on $^{7}$Li and b) by reactions of protons on carbon stopper.
Neutrons were generated in the source reaction p-$^{7}$Li by protons at energies of 22.1 27.1, 32.1 and 36.5 MeV, respectively. Corresponding neutron energies at maximum of quasi-monoenergetic peak are 19.0, 24.1, 29.5 and 34.5 MeV.
The neutron spectra [6] were measured at different set of energies compared to present experiment. To obtain the spectra corresponding to present proton beam energies the interpolation procedure was used [7].

## Comparison of experimental and calculated cross section data for Bi isotopes

In Table 1 the observed reactions on Bi are shown for which experimental specific isotope activities were obtained.

***Table 1.*** *Isotopes observed from irradiations of Bi foil.*

| Isotope | $T_{1/2}$ | reaction | Threshold (MeV) |
|---|---|---|---|
| Bi205 | 15.31 d | Bi209(n,5n) | 29.625 |
| Bi206 | 6.243 d | Bi209(n,4n) | 22.444 |
| Bi207 | 31.55 y | Bi209(n,3n) | 14.416 |

***Table 2.*** *C/E values for reactions on Bi209 target.*

| Ep(MeV) | C/E 48 mm | error(%) | P/T(%) |
|---|---|---|---|
| | C/E 88 mm | | |
| | | | |
| **Bi209(n,3n)Bi207** | | | |
| 36.5 | 0.878 | 3 | 42.99 |
| | 0.817 | 4 | |
| 32.1 | 0.890 | 4 | 71.33 |
| | 0.725 | 4 | |
| 27.1 | 1.118 | 3 | 92.79 |
| | 0.926 | 3 | |
| 22.1 | 1.052 | 3 | 99.29 |
| | 0.944 | 3 | |
| | | | |
| **Bi209(n,4n)Bi206** | | | |
| 36.5 | 0.935 | 4 | 94.99 |
| | 0.801 | 3 | |
| 32.1 | 1.443 | 4 | 99.38 |
| | 1.197 | 3 | |
| 27.1 | 14.01*) | 5 | 100 |
| | 11.43*) | 3 | |
| | | | |
| **Bi209(n,5n)Bi205** | | | |
| 36.5 | 6.952*) | 6 | 99.97 |
| | 5.395*) | 3 | |

*) Very sensitive to the front of the cross-section

The comparison between measured and calculated data is based on the usual C/E ratio, where C and E correspond to the calculated and experimental activity, respectively. In the calculations, the cross section data were taken from EAF-2007.
The obtained C/E values for Au isotopes which serve as the monitor are close to the values ≈1 in ref.[7] (and references cited herein). The detailed study of reactions on Au is under progress.
The C/E values are given in Table 2 for both distances (48 and 88 mm) of Bi foils from Li foils. Ep means the proton beam energy. In the calculations, the simple $1/r^2$ – dependence was accepted to calculate the spectral flux at sample positions using data from ref. 4. In the next section, the observed deviation from $1/r^2$ – law caused by the space- and energy dependent effect of no point-like geometry of experimental arrangement is partly discussed. The P/T values are obtained from the convolution of neutron spectra and cross-section data (here, P and T correspond to the convolution values over the area of the quasi-monoenergetic peak and total area, respectively). It helps us to select the data where the effects of the quasi-monoenergetic peaks are dominated. The errors given in Table 2 correspond to the determination of experimental specific activities only.

## Effect of neutron angular distribution of source reaction

The ratios of C/E values for 48 and 88 mm calculated for cases where quasi-monoenergetic peak dominates (P/T > 90 %) systematically deviate from unity (1.18, err. 2%). We try to understand this deviation as resulting from the effect of angular distribution of neutron source reaction. Taking data from the Fig.4 in Ref. 6, the correction factor of 1.09 could be estimated choosing “ad hoc” a parabolic approach to spectral yield data [4] for angels <10 deg. We must stress the fact, that our conclusion is only preliminary and is based on the Fig.4 in Ref. [6], where the description of distribution at small angels is not clear enough. Further effects such as the finite size of proton beam spot and/or the suppressed contribution of fast neutrons from parasite sources were omitted in the calculations. Of course, the numerical data on the p-7Li cross section data are needed. As a preliminary approach, we used the C/E ratios at 88 mm for the next analysis. The 10 % systematical errors were added to the errors of measured activities (Table 2). These errors come mainly from uncertainty of spectral yield data claimed in Ref. [6].

## Cross-section calculation

We can preliminary estimate cross-section values in some cases for high P/T values, where quasi-monoenergetic neutron peak dominates. The corresponding experimental cross-section $CS_e(En) = \langle CS_c \rangle/(C/E)$ (Ref.[10]) for energy $E_n$ at maximum of quasi-monoenergetic peak. The $\langle CS_c \rangle$ value is EAF-2007 library cross-section averaged in neutron spectrum of the peak. The results are summarized in Table 3, the systematic error of CS is included. The errors of $E_n$ correspond to the half thickness of quasi-monoenergetic peak and uncertainty of 1% of proton energy.

***Table 3.*** *Experimental cross-sections in the reactions Bi209(n,xn) for the neutron energy En.*

| $E_n$ (MeV) | $E_n$ error (MeV) | C/E accepted | $CS_e$(En) (b) | CS error (%) |
|---|---|---|---|---|
| | | | | |
| **Bi209(n,3n)Bi207** | | | | |
| 24.1 | 0.9 | 0.926 | 1.793 | 10 |
| 19.0 | 1.2 | 0.944 | 1.020 | 10 |
| | | | | |
| **Bi209(n,4n)Bi206** | | | | |
| 34.5 | 0.9 | 0.801 | 1.475 | 10 |
| 29.5 | 1.0 | 1.197 | 0.699 | 10 |
| 24.1 | 0.9 | 11.43 | 1.731 E-3 | 10 |
| | | | | |
| **Bi209(n,5n)Bi205** | | | | |
| 34.5 | 0.8 | 5.395 | 2.30 E-2 | 10 |

The cross-section results together with other results [1] are shown in Fig.1. Only the regions of interest are shown. In the case of "sensitive" values (Table 2), the small shift of neutron spectrum in energy may cause bring down values C/E, but in the same time $<CS_c>$ values are lowered without substantial effect on cross-section values.

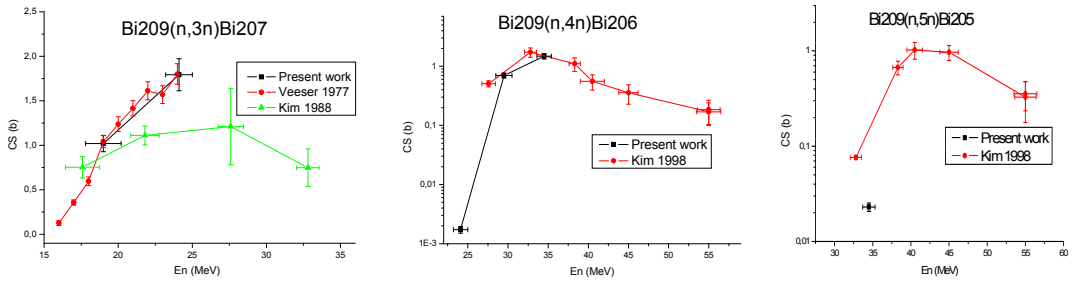


***Figure 1.*** *Cross-sections of the reactions $^{209}$Bi(n,xn).*

Within present preliminary approach, the cross-section of reaction (n,3n) at the neutron energy 24.1 MeV corresponds better to behavior of the data published by Vesser 1977 [2] rather than those given by Kim 1998 [4]. The cross-section at the energy 19.0 MeV is in overall agreement with previously published data.
The cross-sections of (n,4n) reaction are not in disagreement with previously published data [4]. The data of (n,5n) reaction are in strong disagreement with [4].

## Conclusions

The isotope activities produced in Bi foils by neutrons with energies below 35 MeV were measured using the quasi-monoenergetic p-7Li neutron source. The spectral yield data for $^{7}$Li(p,n) from Ref. [6] and cross-sections from EAF-2007 were used to the analysis of measured data.
The C/E ratios for four neutron energies were obtained. They are not far from the unity, excluding cases where strong dependence of data on neutron energies exists. The effect of neutron angular distribution was discussed. In some cases, the cross-section values were obtained and compared with previous data.

**Acknowledgements**
This work was performed with partial support of EFDA Technology Program, the Ministry of Education and the Ministry of Trade and Industry of CR.

**References**

[1] EXFOR database, http://www-nds.iaea.org/exfor, status July 2008
[2] L.A.Veeser, E.D.Arthur, P.G.Young, Phys.Rev. C16 (1977) 1792
[3] G.A.Prokopets, Yadernaya Fizika 32, 37, 198007
[4] E.Kim et al., Nuclear Science and Engineering 129 (1998) 209
[5] R. A. Forrest, J. Kopecky, M. Pillon, A. Klix, J-Ch Sublet, S. P. Simakov, P. Bém, M. Honusek and E. Šimečková, UKAEA Report, UKAEA FUS 547, 2008
[6] Y.Uwamino et al., NIM A389 (1997) 463
[7] M.Honusek, P.Bém, V.Burjan, U.Fischer, M.Götz, V.Kroha, J.Novák, S.P.Simakov, E.Šimečková, NEMEA 4, Prague 2007, Proceedings p.39
[8] T.S.Soewarsono, JAERI-M-92-027, 354, 9203 (1992)
[9] Y.Uwamino et al., Nuclear Science and Engineering 111 (1992) 391
[10] R.A.Forrest, NEMEA 4, Prague 2007, presentation.

# Neutron cross-section covariances for tungsten isotopes at energies up to 150 MeV

*A.Yu.Konobeyev, U.Fischer, P.E.Pereslavtsev*

Institut für Reaktorsicherheit, Forschungszentrum Karlsruhe GmbH, 76021 Karlsruhe, Germany
konobeev@irs.fzk.de

***Abstract:*** New versions of evaluated nuclear data files for tungsten isotopes with atomic mass numbers 182, 183, 184, and 186 including covariances are discussed. The covariances were obtained on the basis of novel computational approach implemented in the set of computer programs BEKED. BEKED performs the treatment of experimental data, provides the run of codes used for cross-section and covariance calculations, and performs the global evaluation of nuclear data.
The data evaluation for tungsten isotopes has been performed with BEKED using available experimental data and results of nuclear model calculations.

## Introduction

The evaluation of cross-section covariances and the evaluation of nuclear data using the covariance information increase the quality and reliability of those data and creates the principal basis for the further correct application of evaluated data.
The present work discusses the new version of evaluated nuclear data files for tungsten isotopes prepared in Forschungszentrum Karlsruhe (FZK) including the information about cross-section covariances. The evaluation covers the energy range of primary neutrons from $10^{-11}$ to 150 MeV.
The evaluation of cross-sections and covariances was performed using the prepared set of computer programs BEKED[1]. The method of the evaluation and the results obtained are discussed below.

## Method of the data evaluation

The evaluation procedure includes the selection and analysis of experimental data, cross-section calculations using nuclear models, the computation of covariance matrices resulting from model calculations, the estimation of cross-sections and covariances using available experimental information and calculated cross-sections and covariance matrices.
Various approaches [1,2] can be used in the BEKED code system to produce evaluated cross-sections and the covariance information.

### Unresolved resonance and fast energy region

#### Nuclear model calculations

Covariance matrices for cross-sections predicted by nuclear models are obtained using the Monte Carlo method described in Ref.[3]. The generation of covariances implies: i) the definition of the “best” set of parameters for the “best” nuclear models used for the cross-section calculation, ii) the definition of uncertainties of model parameters, iii) the Monte Carlo sampling of N number of input data sets for the code implementing selected “best” models, iv) the execution of calculations for obtained input data files, and v) the calculation of covariance matrices for particular reactions

$$V_{ij} = N^{-1} \sum_{k=1}^{N} (\sigma_{ik} - \sigma_{i0})(\sigma_{jk} - \sigma_{j0}),$$

where $\sigma_{ik}$ is the cross-section corresponding to the “i”-th primary neutron energy in the “k”-th Monte Carlo history, $\sigma_{i0}$ is the cross-section obtained using the “best“ set of model parameters as described below.
The corresponding correlation matrix is equal to

[1] Die BEwertung der KErnDaten (Evaluation of nuclear data)

$$C_{ij} = V_{ij}(V_{ii} \times V_{jj})^{-1/2}$$

Various models for the calculation of the nuclear level density showing the minimal deviations in the comparison of calculated and measured neutron and proton reaction cross-sections at primary energies up to 150 MeV [4] were used to get $\sigma_{i0}$ values for various reaction channels. The Fermi gas model from Ref.[5] combined with the constant temperature model [6], the back-shifted Fermi gas model [6], and the generalized superfluid model [6,7] implemented in the TALYS code [6] were applied for calculations for tungsten isotopes. The value of $\sigma_{i0}$ was calculated as follows

$$\sigma_{i0} = \sum_{m=1}^{M} w_{(m)}\, \sigma_{i,(m)} ,$$

where $\sigma_{i,(m)}$ is the cross-section calculated for the "i"-th primary neutron energy using the "best" set of parameters of the level density model "m", $w_{(m)}$ is the statistical weight of the "m" model obtained from the comparison of the cross-sections calculated using this model and experimental data [4], M is the number of all considered models for the nuclear level density calculation.

The generation of input data sets by Monte Carlo is performed for adopted models for the calculation of nuclear level density taking into account their weights $w_{(m)}$. The procedure includes also the variation of parameters of the optical model and the pre-equilibrium model.

Figure 1 shows the example of correlation matrices for the (n,2n) and (n,p) reaction cross-sections obtained using nuclear model calculations.

Using BEKED the computation of covariances can be performed with the help of the TALYS code [6], ALICE/ASH [8] code, and the ECIS code [9].

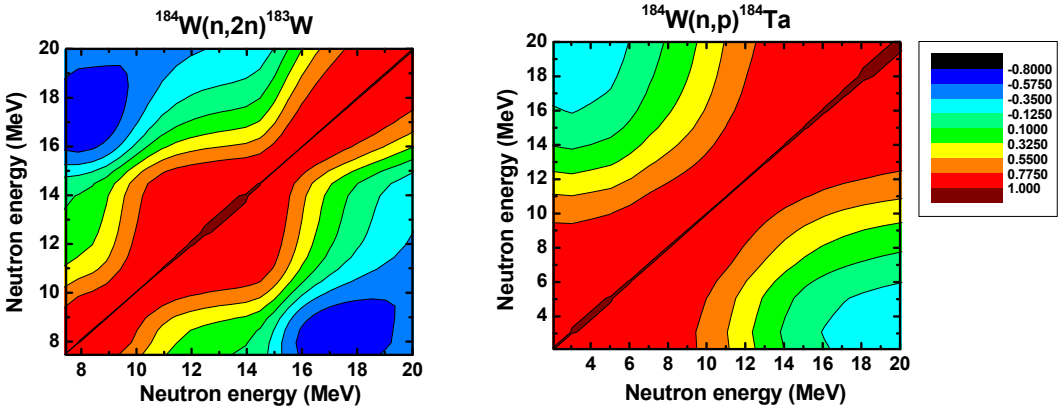


***Figure 1.*** *Correlation matrix for $^{184}W(n,2n)^{183}W$ and $^{184}W(n,p)^{184}Ta$ reaction cross-sections obtained using nuclear models.*

**Use of experimental data**

Depending on the user's choice the evaluation of cross-sections and covariances with BEKED can be performed using the unified Monte Carlo approach [1] or the generalized least-squares method [2]

**Unified Monte Carlo approach**

According to Ref.[1] the evaluation is performed using the following expressions

$$\sigma_i^{eva} = \sum_{k=1}^{N} \sigma_{ik} p(\sigma_k) \left( \sum_{k=1}^{N} p(\sigma_k) \right)^{-1} ,$$

$$V_{ij} = \sum_{k=1}^{N} \sigma_{ik}\sigma_{jk} p(\sigma_k) \left( \sum_{k=1}^{N} p(\sigma_k) \right)^{-1} - \sum_{k=1}^{N} \sigma_{ik} p(\sigma_k) \sum_{k=1}^{N} \sigma_{jk} p(\sigma_k) \left( \sum_{k=1}^{N} p(\sigma_k) \right)^{-2} ,$$

where "k" index refers to the k-th Monte Carlo history, $\sigma_{ik}$ is selected randomly using the uniform probability distribution

$$\sigma_{ik} = \sigma_i(\min) + \xi(\sigma_i(\max) - \sigma_i(\min)) ,$$

here $\xi$ is the random number from the (0,1) interval and

$$p(\sigma) \propto \exp\left(-0.5\left[(\sigma-\sigma_{exp})^T \times V_{exp}^{-1} \times (\sigma-\sigma_{exp}) + (\sigma-\sigma_{calc})^T \times V_{calc}^{-1} \times (\sigma-\sigma_{calc})\right]\right),$$

where V is the covariance matrix, index "exp" corresponds to experimental data and "calc" to results of model calculations.

**Generalized least-squares method**

Calculations are performed using the GLSMOD code [2]. The code has been modified to provide the interaction between various modules of BEKED.

Figure 2 shows an example for uncertainties of cross-sections obtained from nuclear model calculations before the fit to experimental data and uncertainties of the final evaluation obtained after the use of experimental data. Figure 3 illustrates evaluated data for the (n,n') and (n,2n) reaction cross-section for $^{186}$W.

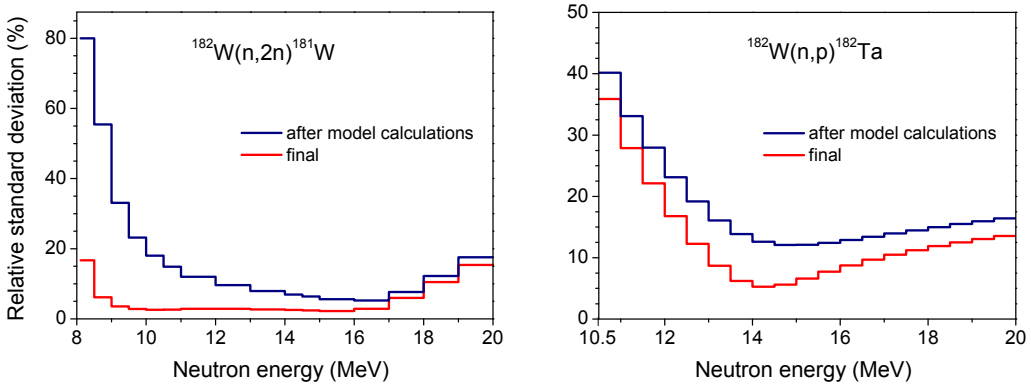


***Figure 2.*** *Uncertainties for $^{182}$W(n,2n)$^{182}$W and $^{182}$W(n,p)$^{182}$Ta reaction cross-sections corresponding to calculations using nuclear models (blue line) and obtained from the evaluation taking into account available experimental data (red line)*

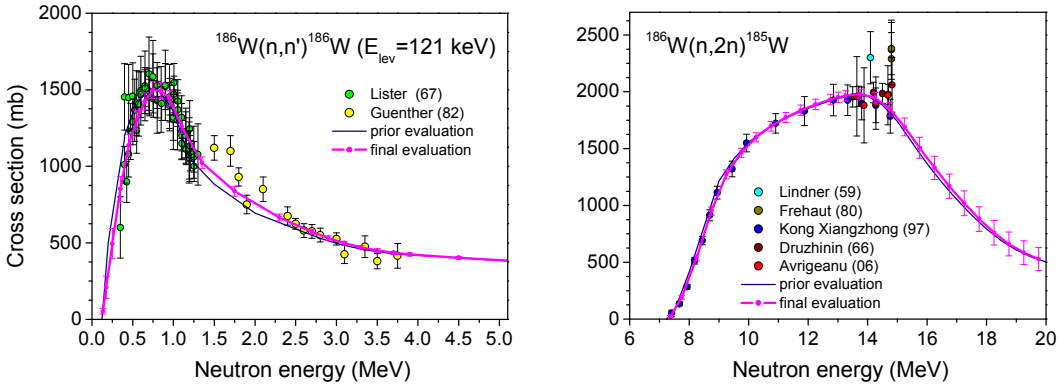


***Figure 3.*** *Example of evaluated cross-sections for $^{186}$W(n,n')$^{186}$W ($E_{lev}$=0.121 MeV) and $^{186}$W(n,2n)$^{185}$W reactions.*

**Resolved resonance energy region**

The uncertainty of cross-sections and covariances are calculated using the available information about the uncertainty of resonance parameters. The information is taken from Ref.[10] and from EXFOR. The special module of BEKED is used to read EXFOR data and get evaluated values of neutron and radiative widths and their uncertainties.

The evaluation of cross-section covariances is performed using the Monte Carlo method. The technique is close to the one described above.

Using the information about neutron resonance parameters and their uncertainties several thousand files in ENDF/B-6 format with different MF=2, MT=151 sections are generated by Monte Carlo. The files obtained are processed using NJOY modules RECONR and

GROUPR. Covariances are calculated using the information from output data files after the NJOY processing.

## Results of evaluation

Available experimental data and data evaluated at FZK [11] were used to get new evaluated data for tungsten isotopes. The evaluation of cross-sections and covariances has been performed for $^{182}$W, $^{183}$W, $^{184}$W, and $^{186}$W.
Uncertainties and covariances for total and elastic scattering cross-sections were obtained at neutron energies up to 150 MeV using the TALYS [6], ECIS [9] codes and experimental data. The TALYS code was applied in the neutron energy range where the contribution of compound processes in the elastic scattering dominates. At higher energies calculations were carried out using the ECIS code.
The evaluation for separate reaction channels were performed up to the neutron energy 20 MeV. The limitation is caused only by the adopted structure of the evaluated data file written in ENDF/B-6 format using the MF=3/MF=6 representation.
The evaluation was performed for all important reaction channels, including (n,γ), (n,2n), (n,3n), (n,p), inelastic scattering and others.
Data for covariances were written in the MF=33 file according to the ENDF/B format.
Figure 4 shows as an example of uncertainties obtained for total and radiative capture cross-sections for $^{183}$W and $^{186}$W.

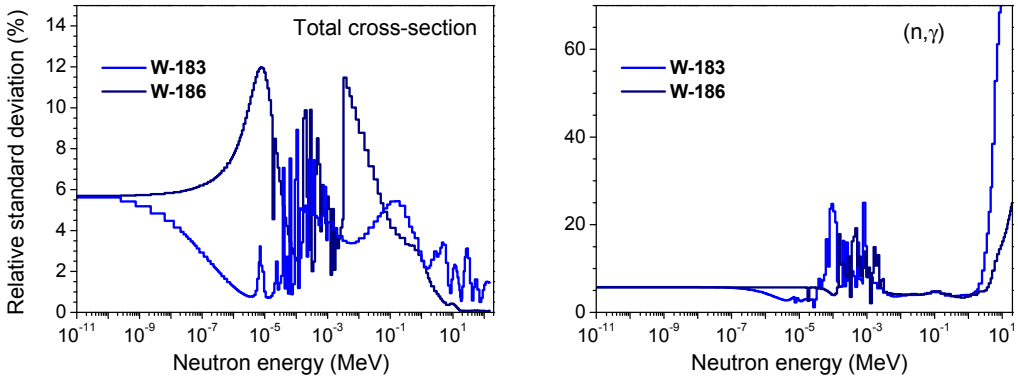


***Figure 4.*** *Relative standard deviation for the total cross-section and the radiative capture cross-section for $^{183}$W and $^{186}$W.*

**References**

[1] D.L. Smith, “A Unified Monte Carlo Approach to Fast Neutron Cross Section Data Evaluation”, ANL/NDM-166 (2008).
[2] D.L. Smith, “A Least-Squares Computational Tool Kit”, ANL/NDM-128 (1993).
[3] D.L. Smith, “Covariance Matrices for Nuclear Cross Sections Derived from Nuclear Model Calculations”, ANL/NDM-159 (2004).
[4] A.Yu. Konobeyev, U. Fischer, “Global comparison of TALYS and ALICE code calculations with measured neutron and proton induced reaction cross-sections at energies up to 150 MeV”, this Workshop.
[5] A.V.Ignatyuk, G.N.Smirenkin, A.S. Tishin, Sov. J. Nucl. Phys. 21, 255 (1975).
[6] A.J. Koning, S. Hilairey, M. Duijvestijn, “TALYS-1.0” (2007) http://www.talys.eu/
[7] A.V. Ignatyuk, R. Capote, Nuclear Level Densities, IAEA-TECDOC-1506 (2006) p.85, http://www-nds.iaea.org/RIPL-2/handbook.html
[8] C.H.M. Broeders, A.Yu. Konobeyev, Yu.A. Korovin, V.P. Lunev, M. Blann, Forschungszentrum Karlsruhe Report FZKA 7183, 2006; http://bibliothek.fzk.de/zb/berichte/FZKA7183.pdf
[9] J. Raynal, “ECIS96”, Proc. Spec. Meeting on the Nucleon Nucleus Opt. Model up to 200 MeV, Bruyères-le-Chatel, France, (1996), http://www.nea.fr/html/science/om200/raynal.pdf
[10] S. Mughabghab, “Atlas of Neutron Resonances. Resonance Parameters and Thermal Cross Sections. Z=1-100”, Fifth Edition, Elsevier (2006).
[11] P. Pereslavtsev, U. Fischer, “Validation analysis of FZK evaluated data files for W isotopes”, EFFDOC-1051 (2008), http://www.nea.fr/html/dbdata/projects/effdoc.html

# Global comparison of TALYS and ALICE code calculations with measured neutron and proton induced reaction cross-sections at energies up to 150 MeV

*A.Yu.Konobeyev, U.Fischer*

Institut für Reaktorsicherheit, Forschungszentrum Karlsruhe GmbH, 76021 Karlsruhe, Germany
konobeev@irs.fzk.de

***Abstract:*** Neutron and proton induced reaction cross-sections for target nuclei with atomic number from 12 to 83 and incident energies from 0.1 to 150 MeV have been calculated using TALYS, ALICE/ASH, and HMS ALICE codes using different models for the description of the nuclear level density. More than thirty thousand experimental points from EXFOR have been used for the comparison with calculations. The obtained results give hints about the best approach for the cross-section calculation for nuclei with different masses.

## Introduction

The goal of the work is the study of uncertainties in the calculation of cross-sections for neutron and proton induced reactions using popular approaches and codes. The calculations were performed with the TALYS code [1], ALICE/ASH code [2], and HMS ALICE [3]. Results of calculations were compared with experimental cross-sections from EXFOR for target nuclei with the atomic number from 12 to 83. Obtained deviation factors show appropriate models for the calculation of nuclear reaction cross-sections for different ranges of target nuclei.
Following deviation factors [4-7] were used for the comparison of results of calculations with experimental data

$$H = \left( \frac{1}{N} \sum_{i=1}^{N} \left( \frac{\sigma_i^{exp} - \sigma_i^{calc}}{\Delta\sigma_i^{exp}} \right)^2 \right)^{0.5}, \quad D = \frac{1}{N} \sum_{i=1}^{N} \left| \frac{\sigma_i^{exp} - \sigma_i^{calc}}{\sigma_i^{exp}} \right|, \quad R = \frac{1}{N} \sum_{i=1}^{N} \frac{\sigma_i^{calc}}{\sigma_i^{exp}},$$

$$F = 10^{\left( \frac{1}{N} \sum_{i=1}^{N} \left[ \log(\sigma_i^{exp}) - \log(\sigma_i^{calc}) \right]^2 \right)^{0.5}}, \quad L = \left[ \sum_{i=1}^{N} \left( \frac{\sigma_i^{calc}}{\Delta\sigma_i^{exp}} \right)^2 \left( \frac{\sigma_i^{calc} - \sigma_i^{exp}}{\sigma_i^{calc}} \right)^2 \Bigg/ \sum_{i=1}^{N} \left( \frac{\sigma_i^{calc}}{\Delta\sigma_i^{exp}} \right)^2 \right]^{0.5},$$

$P_x = N_x/N$,

where $\sigma_i^{exp}$ and $\Delta\sigma_i^{exp}$ are the measured cross-section and its uncertainty; $\sigma_i^{calc}$ is the calculated cross-section; N is the total number of experimental points used to the comparison with calculations; $N_x$ is the number of experimental points with the ratio $1/x < \sigma_i^{calc} / \sigma_i^{exp} < x$.

## Experimental data

Experimental data used for the comparison with calculations and evaluated data were taken from EXFOR. Measured non-cumulative yields of radionuclides for (p,x) and (n,x) reactions including the radiative capture were selected for the comparison. Details are given in Table 1 and Refs.[6,7].

***Table 1.*** *Experimental data selected for the comparison with calculations*

| projectile | range of projectile energy (E) | range of target nuclei (Z) | total number of experimental points (Z,A,E) | number of points (Z,A,E) at energies above 20 MeV |
|---|---|---|---|---|
| protons | 0 – 150 MeV | 12 – 83 | 19691 | 10321 |
| neutrons | 0.1 – 64.4 MeV | 13 – 83 | 17937 | 615 |

## Results

Tables 2-4 shows deviation factors H, D, R, F, L, $P_{1.3}$, $P_{2.0}$, and $P_{10.0}$ obtained using (p,x) reaction cross-sections calculated with the TALYS-1.0 code. Data in Table 2 correspond to the whole energy range of projectiles under consideration and two ranges of target nuclei with the atomic number below and above 40. Table 3 and 4 present deviation factors for the proton energy range from 5 to 50 MeV and from 50 to 150 MeV, respectively. The comparison of data in Tables 2-4 shows that the worse agreement between calculations and experimental data is observed at the proton energies from 0 to 5 MeV.
Deviation factors calculated using TALYS-1.0 for neutron induced reaction cross-sections are given in Table 5. Table 6 present the comparison of results obtained using TALYS-1.0, ALICE/ASH, and HMS ALICE.
The comparison with experimental data shows that calculations with TALYS-1.0 provide the best overall description of measured cross-sections for the range of target nuclei considered in the present work. All considered models for the calculation of the nuclear level density have close values of deviation factors for (p,x) reactions and target nuclei with Z < 40. The best results for nuclei with Z < 40 are obtained using the IST(-) and MG models (see details in Table 2). The range with Z > 40 shows more scatter in predictions of various models. The IST(-) model has here the largest values of the H and L- factors at the range of projectiles up to 50 MeV.
The HMS ALICE code has the minimal value of the H, R, and L-factors for target nuclei with Z > 40. The minimal values of other important factors correspond to TALYS-1.0 calculations.

***Table 2.*** *Values of various deviation factors for (p,x) reactions obtained by the TALYS-1.0 code using different models for the calculation of the nuclear level density: the Fermi gas model with the energy dependent nuclear level density parameter (IST) (ldmodel=1), the "back-shifted" Fermi gas model (BSF) (ldmodel=2), the generalized superfluid model (SF) (ldmodel=3), the microscopic level density according to Goriely's (MG) (ldmodel=4), the level density according to Hilaire's (MH) (ldmodel=5). Calculations using first three models were performed without ("–") and with ("+") the explicit description of the collective enhancement of the level density. Data correspond to the incident proton energy from 0 to 150 MeV. The best value and other results, which are different from the best one within 2 % are underlined.*

| Factors | IST (–) | IST (+) | BSF (–) | BSF (+) | SF (–) | SF (+) | MG | MH |
|---|---|---|---|---|---|---|---|---|
| Targets with atomic number (Z) from 12 to 39 | | | | | | | | |
| H | 144. | 144. | 144. | 145. | 144. | 144. | 144. | 145. |
| D | 1.18 | 1.23 | 1.21 | 1.30 | 1.28 | 1.33 | 1.19 | 1.22 |
| R | 1.88 | 1.93 | 1.92 | 1.99 | 1.96 | 1.98 | 1.91 | 1.91 |
| F | 2.17 | 2.24 | 2.19 | 2.37 | 2.28 | 2.42 | 2.20 | 2.28 |
| L | 0.951 | 0.943 | 0.947 | 0.939 | 0.952 | 0.944 | 0.948 | 0.945 |
| $P_{1.3}$ | 0.427 | 0.415 | 0.425 | 0.400 | 0.419 | 0.395 | 0.436 | 0.423 |
| $P_{2.0}$ | 0.802 | 0.784 | 0.801 | 0.755 | 0.786 | 0.740 | 0.795 | 0.775 |
| $P_{10.0}$ | 0.980 | 0.977 | 0.979 | 0.973 | 0.976 | 0.973 | 0.979 | 0.976 |
| N | 13685 | 13681 | 13689 | 13679 | 13693 | 13680 | 13694 | 13674 |
| Targets with atomic number from 40 to 83 | | | | | | | | |
| H | 25.0 | 25.1 | 23.1 | 25.4 | 23.3 | 31.9 | 23.9 | 21.0 |
| D | 0.608 | 0.728 | 0.634 | 0.799 | 0.611 | 0.866 | 0.674 | 0.684 |
| R | 1.35 | 1.42 | 1.37 | 1.47 | 1.35 | 1.53 | 1.40 | 1.38 |
| F | 2.21 | 3.20 | 2.25 | 3.76 | 2.15 | 3.74 | 2.72 | 2.81 |
| L | 0.863 | 0.857 | 0.840 | 0.853 | 0.847 | 0.898 | 0.839 | 0.820 |
| $P_{1.3}$ | 0.510 | 0.447 | 0.489 | 0.431 | 0.516 | 0.453 | 0.470 | 0.451 |
| $P_{2.0}$ | 0.842 | 0.764 | 0.829 | 0.733 | 0.837 | 0.745 | 0.799 | 0.769 |
| $P_{10.0}$ | 0.979 | 0.952 | 0.980 | 0.940 | 0.980 | 0.942 | 0.971 | 0.968 |
| N | 5336 | 5331 | 5343 | 5324 | 5341 | 5320 | 5346 | 5345 |

***Table 3.*** *The same as in Table 2, but for the incident proton energy from 5 to 50 MeV.*

| Factors | IST (–) | IST (+) | BSF (–) | BSF (+) | SF (–) | SF (+) | MG | MH |
|---|---|---|---|---|---|---|---|---|
| Targets with atomic number (Z) from 12 to 39 | | | | | | | | |
| H | 22.1 | 24.9 | 22.8 | 26.6 | 24.0 | 24.7 | 22.1 | 25.5 |
| D | 0.597 | 0.592 | 0.574 | 0.597 | 0.651 | 0.628 | 0.583 | 0.604 |
| R | 1.29 | 1.29 | 1.27 | 1.28 | 1.31 | 1.24 | 1.31 | 1.30 |
| F | 1.95 | 1.98 | 1.95 | 2.09 | 2.01 | 2.15 | 2.01 | 2.03 |
| L | 0.386 | 0.399 | 0.384 | 0.413 | 0.427 | 0.409 | 0.377 | 0.410 |
| $P_{1.3}$ | 0.471 | 0.471 | 0.474 | 0.454 | 0.465 | 0.434 | 0.484 | 0.473 |
| $P_{2.0}$ | 0.848 | 0.843 | 0.853 | 0.812 | 0.837 | 0.788 | 0.838 | 0.827 |
| $P_{10.0}$ | 0.984 | 0.983 | 0.984 | 0.981 | 0.981 | 0.979 | 0.983 | 0.981 |
| N | 8656 | 8655 | 8652 | 8654 | 8652 | 8650 | 8656 | 8650 |
| Targets with atomic number from 40 to 83 | | | | | | | | |
| H | 24.1 | 20.9 | 19.9 | 18.2 | 21.3 | 20.1 | 22.7 | 17.7 |
| D | 0.527 | 0.572 | 0.531 | 0.592 | 0.506 | 0.564 | 0.585 | 0.570 |
| R | 1.31 | 1.34 | 1.31 | 1.34 | 1.28 | 1.30 | 1.36 | 1.31 |
| F | 2.10 | 2.36 | 2.15 | 2.46 | 2.06 | 2.46 | 2.33 | 2.37 |
| L | 0.842 | 0.800 | 0.792 | 0.758 | 0.817 | 0.796 | 0.814 | 0.766 |
| $P_{1.3}$ | 0.546 | 0.497 | 0.529 | 0.480 | 0.554 | 0.505 | 0.495 | 0.496 |
| $P_{2.0}$ | 0.853 | 0.804 | 0.843 | 0.779 | 0.857 | 0.795 | 0.806 | 0.797 |
| $P_{10.0}$ | 0.982 | 0.974 | 0.981 | 0.971 | 0.982 | 0.971 | 0.980 | 0.974 |
| N | 3728 | 3725 | 3728 | 3724 | 3730 | 3721 | 3725 | 3723 |

***Table 4.*** *The same as in Table 2, but for the incident proton energy from 50 to 150 MeV.*

| Factors | IST (–) | IST (+) | BSF (–) | BSF (+) | SF (–) | SF (+) | MG | MH |
|---|---|---|---|---|---|---|---|---|
| Targets with atomic number (Z) from 12 to 39 | | | | | | | | |
| H | 8.6 | 11.0 | 10.6 | 14.4 | 10.0 | 15.3 | 11.5 | 14.9 |
| D | 0.543 | 0.581 | 0.543 | 0.617 | 0.619 | 0.591 | 0.575 | 0.630 |
| R | 1.05 | 1.10 | 1.09 | 1.15 | 1.14 | 1.13 | 1.11 | 1.11 |
| F | 2.60 | 2.72 | 2.51 | 2.76 | 2.74 | 2.74 | 2.56 | 2.81 |
| L | 0.595 | 0.659 | 0.682 | 0.743 | 0.649 | 0.785 | 0.731 | 0.783 |
| $P_{1.3}$ | 0.398 | 0.384 | 0.419 | 0.391 | 0.399 | 0.430 | 0.422 | 0.373 |
| $P_{2.0}$ | 0.732 | 0.719 | 0.768 | 0.710 | 0.736 | 0.722 | 0.744 | 0.681 |
| $P_{10.0}$ | 0.964 | 0.956 | 0.963 | 0.954 | 0.960 | 0.958 | 0.964 | 0.955 |
| N | 2632 | 2628 | 2639 | 2627 | 2643 | 2632 | 2641 | 2627 |
| Targets with atomic number from 40 to 83 | | | | | | | | |
| H | 20.8 | 29.0 | 23.5 | 33.9 | 21.0 | 48.3 | 19.6 | 19.3 |
| D | 0.762 | 1.080 | 0.807 | 1.261 | 0.783 | 1.525 | 0.844 | 0.842 |
| R | 1.38 | 1.53 | 1.43 | 1.68 | 1.39 | 1.95 | 1.45 | 1.37 |
| F | 2.57 | 6.07 | 2.56 | 8.64 | 2.43 | 8.42 | 3.99 | 4.15 |
| L | 0.906 | 0.946 | 0.919 | 0.953 | 0.909 | 0.974 | 0.880 | 0.893 |
| $P_{1.3}$ | 0.419 | 0.324 | 0.415 | 0.308 | 0.445 | 0.339 | 0.404 | 0.349 |
| $P_{2.0}$ | 0.824 | 0.661 | 0.813 | 0.622 | 0.812 | 0.635 | 0.773 | 0.717 |
| $P_{10.0}$ | 0.971 | 0.882 | 0.975 | 0.841 | 0.972 | 0.852 | 0.943 | 0.949 |
| N | 1343 | 1338 | 1343 | 1326 | 1343 | 1325 | 1347 | 1348 |

***Table 5.*** *The same as in Table 2, but for neutron induced reactions (n,x) at incident neutron energies from 0.1 to 64.4 MeV for target nuclei with atomic number from 13 to 83*

| Factors | IST (–) | IST (+) | BSF (–) | BSF (+) | SF (–) | SF (+) | MG | MH |
|---|---|---|---|---|---|---|---|---|
| H | 9.9 | 9.7 | 10.6 | 10.5 | 11.3 | 11.3 | 10.5 | 10.8 |
| D | 0.582 | 0.570 | 0.598 | 0.596 | 0.615 | 0.620 | 0.600 | 0.615 |
| R | 1.34 | 1.33 | 1.32 | 1.32 | 1.31 | 1.30 | 1.36 | 1.33 |
| F | 2.11 | 2.07 | 2.14 | 2.11 | 2.14 | 2.13 | 2.12 | 2.14 |
| L | 0.370 | 0.369 | 0.419 | 0.416 | 0.450 | 0.459 | 0.387 | 0.410 |
| $P_{1.3}$ | 0.539 | 0.553 | 0.499 | 0.509 | 0.463 | 0.455 | 0.527 | 0.493 |
| $P_{2.0}$ | 0.852 | 0.854 | 0.835 | 0.841 | 0.834 | 0.825 | 0.844 | 0.826 |
| $P_{10.0}$ | 0.983 | 0.983 | 0.982 | 0.982 | 0.983 | 0.982 | 0.983 | 0.982 |
| N | 17875 | 17876 | 17875 | 17876 | 17870 | 17870 | 17875 | 17869 |

***Table 6.*** Values of deviation factors for (p,x) reaction cross-sections obtained by TALYS-1.0, ALICE/ASH, and HMS ALICE codes using the generalized superfluid model for the calculation of the nuclear level density. Data correspond to the incident proton energy from 5 to 150 MeV. Only the points, where all three types of calculations give non-zero cross-sections, are used for comparison. See captions to Table 2

| Factor | TALYS-1, SF(–) | TALYS-1, SF (+) | ALICE/ASH | HMS ALICE |
|---|---|---|---|---|
| Targets with atomic number (Z) from 12 to 39, N= 10988 | | | | |
| H | 21.7 | 23.0 | 30.6 | 48.0 |
| D | 0.637 | 0.612 | 0.789 | 0.824 |
| R | 1.29 | 1.22 | 1.30 | 1.20 |
| F | 1.97 | 2.10 | 3.82 | 4.04 |
| L | 0.431 | 0.424 | 0.583 | 0.773 |
| $P_{1.3}$ | 0.458 | 0.441 | 0.343 | 0.270 |
| $P_{2.0}$ | 0.827 | 0.784 | 0.692 | 0.630 |
| $P_{10.0}$ | 0.984 | 0.980 | 0.939 | 0.905 |
| Targets with atomic number from 40 to 83, N=4881 | | | | |
| H | 18.6 | 18.1 | 15.7 | 14.6 |
| D | 0.467 | 0.601 | 0.544 | 0.538 |
| R | 1.21 | 1.26 | 1.22 | 1.15 |
| F | 1.87 | 3.30 | 2.31 | 2.28 |
| L | 0.803 | 0.788 | 0.765 | 0.769 |
| $P_{1.3}$ | 0.535 | 0.469 | 0.480 | 0.474 |
| $P_{2.0}$ | 0.859 | 0.762 | 0.784 | 0.803 |
| $P_{10.0}$ | 0.989 | 0.947 | 0.975 | 0.973 |

**References**


[1] A.J. Koning, S. Hilairey, M. Duijvestijn, “TALYS-1.0” (2007) http://www.talys.eu/

[2] C.H.M. Broeders, A.Yu. Konobeyev, Yu.A. Korovin, V.P. Lunev, M. Blann, “ALICE/ASH”, Report FZKA 7183, 2006; http://bibliothek.fzk.de/zb/ berichte/FZKA7183.pdf

[3] M.Blann, A.Yu.Konobeyev, W.B.Wilson, S.G.Mashnik, “Code Alice”, Ver.July 2008.

[4] R. Michel, R. Bodemann, H. Busemann, R. Daunke, M. Gloris, H. -J. Lange, B. Klug, A. Krins, I. Leya, M. Lüpke, S. Neumann, H. Reinhardt, M. Schnatz-Büttgen, U. Herpers, Th. Schiekel, F. Sudbrock, B. Holmqvist, H. Condé, P. Malmborg, M. Suter, B. Dittrich-Hannen, P. -W. Kubik, H. -A. Synal, D. Filges, Nucl. Instr. Meth. B129, 153 (1997).

[5] H.Leeb, M.T.Pigni, I.Raskinyte, Proc. Int. Conf. on Nuclear Data for Science and Technology, Santa Fe, USA, Sep. 26 – Oct. 1, 2004, p.161

[6] C.H.M. Broeders, A.Yu. Konobeyev, L. Mercatali, Kerntechnik 71, 174 (2006) 174.

[7] A.Yu. Konobeyev, C.H.M. Broeders, U.Fischer, L.Mercatali, Kerntechnik 73, 49 (2008).

# Towards consistent uncertainty information in nuclear data files

*H. Leeb*

Atominstitut der Österreichischen Universitäten, Technische Universität Wien,
Wiedner Hauptstraße 8-10, 1040 Vienna, Austria
leeb@kph.tuwien.ac.at

***Abstract:*** The status of the development of a consistent method for the determination of reliable covariance matrices from nuclear model calculations is presented. The method relies on Bayesian statistics and gives emphasis on the proper choice of the prior. Apart from the previously developed contributions stemming from parameter uncertainties a new formulation of covariance matrices associated with model defects is given. The method defines the model defects via the ability of the chosen nuclear models to describe reaction observables of nuclei of a reference group. Combining the covariance matrices due to parameter uncertainties and due to model defects provides a complete prior. A first application of the method to generate prior covariance matrices for oxygen is shown. In addition the concept of nuclear data evaluation is revisited. In particular the importance of a proper treatment of the correlations between different experiments is pointed out. Although the energy range beyond 20 MeV was the primary focus, the developed formalism can also be applied at lower energies.

## Introduction

The knowledge of all relevant nuclear data and their uncertainties is an important prerequisite for the design and construction of nuclear facilities, the radiation safety as well as for the development of novel nuclear technologies. The presently available nuclear data libraries provide consistent sets of cross sections and spectra for most isotopes in the energy range up to 20 MeV and have been generated to satisfy the needs of conventional nuclear technology. Except for selected isotopes these nuclear data files do not contain covariance matrices for cross section uncertainties which are required for the optimization of designs and the estimate of safety margins.

At present there is a worldwide effort to update the nuclear data libraries for neutron-induced reactions with regard to two aspects: (i) to extend the energy range up to about 200 MeV in order to satisfy the needs of current fusion research to identify the best suited materials (studies envisaged at IFMIF) and to estimate the safety margins of novel reactor technologies (GenIV and ADS); (ii) to provide consistent covariance matrices of cross section uncertainties for all isotopes. The extension of the energy range is not trivial because of the increasing number of energetically open channels and the limited sets of available experimental data. The latter implies that evaluated nuclear data file beyond 20 MeV rely substantially on nuclear model calculations. This fact is important with regard to the inclusion of uncertainty information for which no established method is available at present. It was pointed out in ref. [1] that in such evaluations three sources of uncertainties occur: (i) uncertainties of the nuclear model parameters, (ii) numerical errors and (iii) model defects. While the former two can be obtained within the nuclear models, the estimate of the model defects is still an open question and requires recourse to experimental information.

Recently, motivated by the demand of the user community, there have been several attempts to generate covariance matrices associated with modelling, especially for cross section uncertainties. Most of these approaches assume variations of the model parameters to reproduce best the available experimental data, but also to provide associated covariance matrices of the cross section uncertainties. Along this line extended Monte Carlo simulations have been performed by Koning [2] and Koning and Rochmann [3] for almost all fissionable nuclei. More sophisticated methods based on Bayesian statistics are the *Unified Monte Carlo Approach* [4], the *Generalized Least Square Method* and the *Kalman Filter Technique* [5] which accounts for a-priori knowledge. All these methods refer to the evaluated experimental data assuming that they can be reproduced by nuclear models. Thus they provide covariance matrices associated with parameter uncertainties. Apart from ref. [1] model defects are not considered and only recently Mercatali et al. [6] presented a comparison of various criteria for the quality of a nuclear model.

In this contribution we present a method for the determination of covariance matrices from model calculations starting from the basics of Bayesian statistics. In section 2 we consider the generation of the prior. In particular we briefly revisit the theory for the determination of covariance matrices due to parameter uncertainties. Emphasis is given to the model defects, for which two formulations are presented. In sect. 3 the concept of nuclear data evaluation and some specific problems are discussed. Concluding remarks are given in the final section.

## Prior determination

It is well established that a consistent evaluation of nuclear data has to be performed within the framework of Bayesian statistics [7]. Thus the evaluation process is governed by Bayes theorem,

$$p(\underline{x} \mid \underline{\sigma}, M) = \frac{p(\underline{\sigma} \mid \underline{x}, M)}{p(\underline{\sigma} \mid M)} p(\underline{x} \mid M) , \tag{1}$$

where $p(\underline{x}|\underline{\sigma},M)$ is the conditioned probability distribution that the proposition $\underline{x}$ is true under the conditions of $\underline{\sigma}$ and of the model $M$. Here we use the propositions relevant in nuclear data evaluation, i.e. $\underline{x}$ refers to the parameters of the model, $\underline{\sigma}$ to the set of experimental data and $M$ denotes the nuclear model. The bars below $x$ and $\sigma$ indicate that both quantities are vectors. Via Bayes theorem (1) there is a well-defined modification of the probability distribution due to the inclusion of experimental data and consequently of the mean values of the parameters and the associated covariance matrices. The use of the proper prior distribution $p(\underline{x}|M)$ is a key point in any application of Bayes theorem, especially for nuclear data evaluations which suffer from a scarcity of experimental data. In the following subsections we will consider the main contributions to the covariance matrices for the prior.

### Parameter uncertainties

One obvious source of uncertainty is the limited knowledge of the values of the best model parameters. Applying the concepts of maximum information entropy and invariant measures by Jaynes [8] to nuclear data evaluation, we could determine unique a-priori distribution of the model parameters [9,10] by the use of additional physics constraints. In principle on maximizes the information entropy taking into account the a-priori knowledge via constraints. This requires the solution of

$$\delta\left\{-\int dx_1 \cdots \int dx_n \, p(\underline{x}) \ln \frac{p(\underline{x})}{m(\underline{x})} + \sum_{k=1}^{K} \lambda_k G_k\left[p(\underline{x})\right] - \lambda_0 \left[\int dx_1 \cdots \int dx_n \, p(\underline{x}) - 1\right]\right\} = 0 , \tag{2}$$

where $m(\underline{x})$ is an invariant measure ensuring the form invariance under change of variables. The a-priori knowledge, e.g. mean values and correlations of the parameters, enters via the constraints expressed by the functional $G_k$ and determine also the corresponding Lagrange parameters $\lambda_k$, $k=1,2, \ldots K$. We did not solve the full variation problem, but transform to a set of uncorrelated eigenparameters $\underline{y}$ for which the probability is of product form and

$$m(\underline{y}) = \prod_{\kappa=1}^{K} 1/\, y_\kappa . \tag{3}$$

Assuming that only the mean values of $y_k$ are known, the a-priori distribution is then given by

$$p(\underline{y} \mid M) = \prod_{\kappa=1}^{K} \frac{1}{Z(\lambda_\kappa)} \frac{1}{y_\kappa} \exp(-\lambda_\kappa y_\kappa) \tag{4}$$

with the partition function

$$Z(\underline{\lambda}) = \prod_{\kappa=1}^{K} Z(\lambda_\kappa) = \prod_{\kappa=1}^{K} \frac{1}{y_\kappa} \exp(-\lambda_\kappa y_\kappa). \tag{5}$$

The method has been applied to neutron-oxygen cross sections using the reaction code TALYS with default parameters and an adapted optical potential for neutron-oxygen scattering. In Fig. 1 the correlation matrix for the total cross section uncertainties are shown in the energy range between 10 and 60 MeV. The variance of the total cross section varies between 15% at 10 MeV and 25% at 60 MeV.

### Model defects

The description of nuclear reactions represents a complex many-nucleon problem, for which no ab-initio calculations are possible at present. Therefore one must take recourse to nuclear

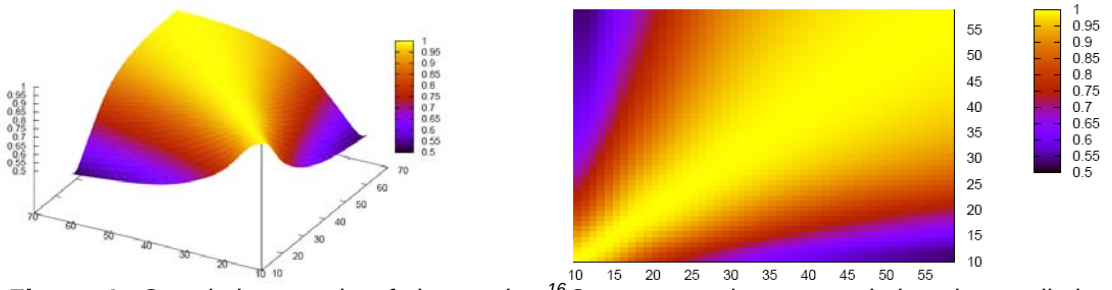

***Figure 1.*** *Correlation matrix of the total n-$^{16}$O cross section uncertainties due to limited knowledge of the parameters.*

models with effective parameters to describe specific features of the reactions. Obviously such a model cannot account for all peculiarities of the reaction process and it may happen that there exists no set of model parameters which reproduces the actual values of the observables of interest. This so-called *model defect* must be taken into account in a prior for nuclear data evaluations based on modelling. In the past only phenomenological ad hoc assumptions for covariance matrices were used [1]. The main problem is the lack of an appropriate framework because neither statistical arguments nor the theory underlying the various models are applicable. Hence, there exists no unique formulation of model defects and the only guideline is its compatibility with the concepts of statistics in order to include model defects into the prior for nuclear data evaluation. Reference to experimental data is required to quantify model defects, but at the same time one must avoid double counting. Therefore we propose to use experimental data for a group of reference nuclei (e.g. neighbouring nuclei) in the same energy range, assuming that the predictive power of the model for this group is approximately equivalent to those nuclei subject of the evaluation. Along this line we have worked out two formulations: (a) a *scaling procedure* which defines for the nucleus of interest an energy-independent scaling factor for each reaction channel and (b) a *remodelling procedure* which defines an energy-dependent scaling factor for each reaction channel. The latter is denoted as remodelling because the energy-dependent scaling factor changes the inherent features of the nuclear model.

The mathematical formulation is based on a common framework. We assume that $N$ isotopes build up the group of reference nuclei and choose an energy grid with $M$ bins with energy $E_m$, $m=1, \ldots, M$ at the centre of the $m$-th bin. It is important that for the nuclei of the reference group there are sufficient experimental data available for the reaction channel $c$ of interest. Furthermore we introduce an index set $S^{(c)}(m,n)$ to classify the experimental data for the reaction channel $c$ for the $n$-th isotope of the reference group in the $m$-th energy bin. Thus we can determine the bin-quantities

$$\left\langle D_n^{(c)}\left(E_m\right)\right\rangle = \sum_{j\in S^{(c)}(m,n)} w_j^{(c,m,n)} \frac{\sigma_{ex}^{(c)}\left(E_j\right)}{\sigma_{th}^{(c)}\left(E_j\right)}, \qquad \left\langle \left(D_n^{(c)}\left(E_m\right)\right)^2\right\rangle = \sum_{j\in S^{(c)}(m,n)} w_j^{(c,m,n)} \left(\frac{\sigma_{ex}^{(c)}\left(E_j\right)}{\sigma_{th}^{(c)}\left(E_j\right)}\right)^2 \quad (6)$$

with the weights

$$w_j^{(c,m,n)} = \frac{\sigma_{th}^{(c)}\left(E_j\right)}{\sum_{j'\in S^{(c)}(m,n)} \sigma_{th}^{(c)}\left(E_{j'}\right)} \quad . \quad (7)$$

Here $E_j$ is the energy of the $j$-th experimental point and 'ex' and 'th' refer to experimental and model cross section, respectively.

<u>*Scaling Procedure for Model Defects*</u>: Main idea is the definition of an overall energy-independent scaling factor $D^{(c)}$ obtained by averaging over all energies and isotopes of the reference group

$$D^{(c)} = \frac{1}{N}\sum_{n=1}^{N}\left\langle D_n^{(c)}\right\rangle \qquad \text{with} \qquad \left\langle D_n^{(c)}\right\rangle = \sum_{m=1}^{M} w_m^{(c,n)}\left\langle D_n^{(c)}\left(E_m\right)\right\rangle . \quad (8)$$

For consistency the weights $w_m^{(c,n)}$ should be in accordance with (7). The covariance matrix of the cross section uncertainties of the considered isotope is then introduced via

$$\left\langle \Delta\sigma^{(c)}(E_m)\Delta\sigma^{(c')}(E_{m'})\right\rangle = \sigma_{th}^{(c)}(E_m)\sigma_{th}^{(c')}(E_{m'}) \tag{9}$$
$$\times\frac{1}{N}\sum_{n=1}^{N}\left[\left(\left\langle D_n^{(c)}(E_m)\right\rangle - D^{(c)}\right)\left(\left\langle D_n^{(c')}(E_{m'})\right\rangle - D^{(c')}\right)+\delta_{cc'}\delta_{mm'}\left(\left\langle\left(D_n^{(c)}(E_m)\right)^2\right\rangle - \left(\left\langle D_n^{(c)}(E_m)\right\rangle\right)^2\right)\right].$$

The first term of Eq. (9) is due to the defect of the model, while the second reflects the uncertainty of the scaling factor. However, it must be remarked that this covariance matrix is not fully of statistical nature.

*Remodelling Procedure for Model Defects*: In this formulation we define an energy-dependent scaling factor from the nuclei of the reference group

$$D^{(c)}(E_m) = \frac{1}{N}\sum_{n=1}^{N}\left\langle D_n^{(c)}(E_m)\right\rangle. \tag{10}$$

Defining the energy dependent difference of the scaling parameter for each isotope of the reference group,

$$\Delta D_n^{(c)}(E_m) = \left\langle D_n^{(c)}(E_m)\right\rangle - D^{(c)}(E_m)\ , \tag{11}$$

allows the definition of the covariance matrix for remodelling

$$\left\langle \Delta\sigma^{(c)}(E_m)\Delta\sigma^{(c')}(E_{m'})\right\rangle = \sigma_{th}^{(c)}(E_m)\sigma_{th}^{(c')}(E_{m'})$$
$$\times\frac{1}{N}\sum_{n=1}^{N}\left[\Delta D_n^{(c)}(E_m)\Delta D_n^{(c')}(E_{m'})+\delta_{cc'}\delta_{mm'}\left(\left\langle\left(D_n^{(c)}(E_m)\right)^2\right\rangle - \left(\left\langle D_n^{(c)}(E_m)\right\rangle\right)^2\right)\right]. \tag{12}$$

This definition associated with remodelling satisfies some basic rules of statistics.

*Model defects for oxygen:* These formulations of the model defects have been applied to neutron-induced reaction cross sections of oxygen. For the reference group we chose the neighbouring nuclei $^{12}$C, $^{14}$N, $^{19}$F, $^{20}$Ne, $^{23}$Na and $^{24}$Mg and extracted the corresponding experimental data from the EXFOR library for $\sigma_{tot}$, $\sigma_{elastic}$, $\sigma_{nonelastic}$, $\sigma$(n,γ), $\sigma$(n,n'), $\sigma$(n,p), $\sigma$(n,d), $\sigma$(n,t), $\sigma$(n,$^3$He) and $\sigma$(n,α). Using again TALYS with default values and an optical potential adapted to neutron-oxygen scattering we determined the scaling factors for all reaction channels for both procedures. Because of length limitations only the correlations obtained by the scaling procedure for the total cross section are shown in Fig. 2. The corresponding variance of the model defect is about 15% at 10 MeV and increases up to 35%

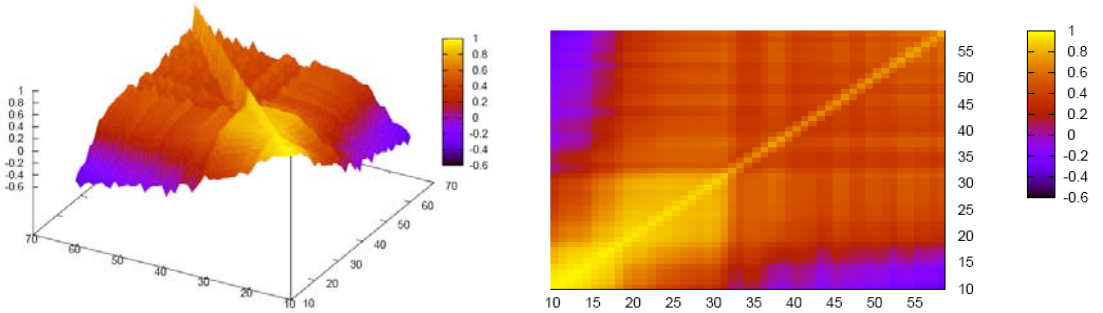


***Figure 2.*** *Correlation of the model defects of the total neutron-$^{16}$O cross section obtained with the energy-independent scaling procedure.*

at 60 MeV. These large uncertainties reflect the limitations of the model to describe quantitatively the reaction cross sections of the reference group. Calculations of the correlations via the procedure of remodelling leads apart from a slightly smaller variance to similar correlation pattern.

**Covariance matrices of complete prior**

Combining the covariance matrices stemming from parameter uncertainties and the model defects yields the covariance matrices of the complete prior. At a first glance we are most interested in the cross sections and their error bands associated with the complete prior. The corresponding results for both procedures are shown in Fig. 3 for the total cross section. It is not a surprise that the obtained error bands are rather wide because the applied nuclear

models are not optimized for light nuclei. Nevertheless these results are very promising because the error bands for different formulations of the model defects overlap. Furthermore,

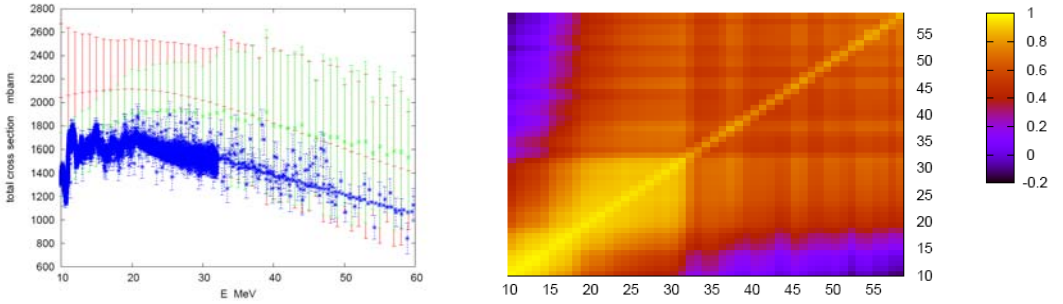


***Figure 3.*** *Left: A-priori value of the total neutron-$^{16}$O cross section and the corresponding error bands which account for parameter uncertainties and model defects. The results for the scaling procedure are denoted in red, those for remodelling by green. Right: Correlation matrix of the prior for the total neutron-$^{16}$O cross section obtained by the scaling procedure.*

despite the limitations of the model, the available experimental data (not used in the determination of the prior) lie in the intersection of the error bands, thus confirming the reliability of the approach.

In order to perform a consistent evaluation of nuclear data a reliable covariance matrix is required. In Fig. 3 we also show the correlation matrix of the prior for the total neutron-$^{16}$O cross section for the scaling method. The matrix show strong correlations between the cross sections at different energies. However, a more careful consideration reveals that the correlations of the full prior are less stiff than those stemming from parameter uncertainties. On the other hand the correlations are more stiff than those used in phenomenological ad hoc priors, e.g. by Vonach and Tagesen [11]. This can directly be seen in Fig. 4 which shows the covariance matrices at fixed *E+E'*. This behaviour is very promising because on the one hand it allows the necessary flexibility beyond the model, but at the other hand it ensures an increased stiffness with regard to single data points. Thus one expects a smooth behaviour of the evaluated cross sections avoiding unphysical fluctuations of the mean values.

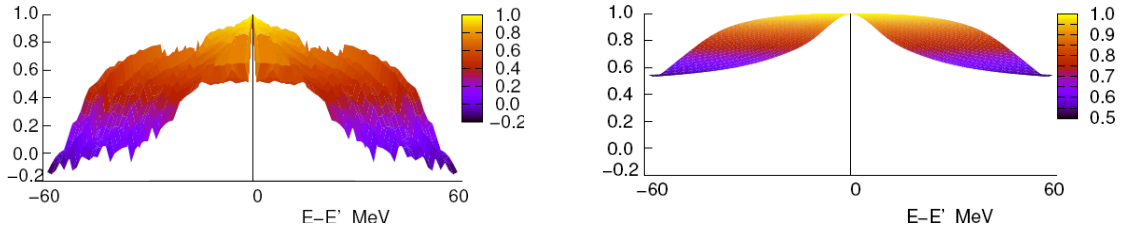


***Figure 4.*** *Comparison of correlations of total cross section uncertainties of the complete prior (left) and of the parameter uncertainties (right). The three-dimensional surface is seen along the diagonal, thus the dependence perpendicular to the diagonal is seen (E+E'=const).*

## Evaluation process

The evaluation process combines via Bayesian statistics the experimental data with the a-priori knowledge in order to determine consistent values and uncertainties for the corresponding observables. In principle Bayes theorem (1) can easily be implemented via Monte Carlo techniques. However, most applications in nuclear data evaluation make use of a linearized version of Bayes theorem, which assumes normal distributions for the prior. The implementation of the linearized version of Bayes theorem becomes particularly simple if the dimension of the covariance matrix associated with experimental data is small. Therefore it is used to perform a sequential process and to include one experiment after the other. Thus the a-posterior mean values and covariance matrices are used as a prior for the inclusion of the next data set and so on. This linearized update procedure is widely applied in nuclear data evaluations. It is implemented in the program GLUCS by Vonach and Tagesen [11] and is

also used in the SAMMY code. In principle also the Kalman filter technique [5] corresponds to such a linearized Bayesian update procedure.
The Bayesian update procedure led to reasonable results in nuclear data evaluations exclusively based on experimental data [11]. However, there are some recent evaluations with strong involvement of nuclear models, which led to unphysically small uncertainties of the evaluated cross sections. This outcome has raised some questions about the evaluation process based on Bayesian statistics. Recently, it was pointed out in a schematic example [12] that the underestimation of uncertainties in the Bayesian update procedure is due to the neglect of correlations between experiments. It is obvious that this phenomenon becomes more evident in evaluations relying on modelling because nuclear models generate strong correlations between different observables. In order to account for correlations between experiments the Correlated Bayesian Update Approach (CBUA) [12] has been proposed recently. It approximates the effect of correlations between different experiments in the Bayesian procedure, keeping all the advantages of the update algorithm. The CBUA is rather simple, but is only a crude approximation. A careful treatment requires the inclusion of all correlated experimental data in one step. This procedure implies the inversion of matrices with large dimension and may generate numerical errors. Therefore, a careful analysis of the experimental covariance matrix will be important to find blocks of negligible correlations, thus reducing the effective dimensions of the involved matrices. This procedure is rather involved and time consuming.

## Summary

We have outlined a consistent procedure for nuclear data evaluation which is completely based on Bayesian statistics. The procedure makes use of a well defined prior which accounts for parameter uncertainties as well as model defects. The prior due to model parameter uncertainties is uniquely obtained via the method of maximum information entropy, the concept of invariant measures and basic physics constraints. To account for model defects two consistent formulations have been worked out and implemented, which use experimental data from a reference group not subject to the evaluation.
The method was applied to neutron-induced reactions on oxygen and a complete prior was provided. An important outcome of these calculations is the fact that the covariance matrices associated with the complete prior is less stiff than those usually obtained from parameter uncertainties. However, the correlations of the prior are stronger than phenomenological ad hoc priors used in some experimental data evaluations, thus avoiding strongly fluctuating mean values in the evaluation.
In summary, the available procedure for the determination of the prior represents an important step towards reliable uncertainty information in nuclear data files based on modelling. Finally we remark on the problem of the Bayesian update procedure, which inherently ignores correlations between experiments. Ideas to overcome this difficulty are discussed and their implementations is in progress.

**Acknowledgements**
The work, supported by the European Commission under the contract between EURATOM and the Austrian Academy of Sciences, was carried out within the framework of the European Fusion Development Agreement (EFDA). The views and opinions expressed herein do not reflect necessarily those of the European Commission.

**References**
[1] M.T. Pigni, H. Leeb, Uncertainty estimates of evaluated 56Fe cross sections based on extensive modelling at energies beyond 20 MeV, in Proc. Int. Workshop on Nuclear Data for Transmutation of Nuclear Waste, GSI, 2003, (A. Kelic, K.-H. Schmidt, eds.) (GSI Darmstadt, ISBN 3-00-012276-1, 2004) p. PO21.
[2] A. Koning, New working methods for nuclear data evaluation: how to make a nuclear data library, in Proc. Int. Conf. On Nulcear Data for Science and Technology, (O. Bersillon, F Gunsing, E. Bauge, R. Jacqmin, S. Lerey, eds.) EDP Sciences, 2008, DOI: 10:105/ndata:07683 (in print), April 22-27, 2007, Nice, France.
[3] A. Koning, D. Rochman, TALYS-based Evaluated Nuclear Data Library, http://www.talys.eu/tendl-2008.

[4] R. Capote, D.L. Smith, Performance of Unified Monte Carlo Method of Data Evaluation, in Proc. of the Int. Workshop on Neutron Cross Section Covariances, Port Jefferson, June 24-27, 2008; Nuclear Data Sheets 109 (2008) (in print).
[5] P. Talou, T. Kawano, P.G. Young, Covariance matrices for ENDF/B-VII 235,238U and 239Pu evaluated files in the fast energy region, in Proc. Int. Conf. On Nulcear Data for Science and Technology, (O. Bersillon, F. Gunsing, E. Bauge, R. Jacqmin, S. Lerey, eds.) EDP Sciences, 2008, DOI: 10:105/ndata:07679 (in print), April 22-27, 2007, Nice, France.
[6] L. Mercatali, A.Yu. Konobeyev, C.H.M. Broeders, On the uncertainty in the nuclear model calculation of neutron and proton induced reaction cross sections, in Proc. Int. Conf. On Nulcear Data for Science and Technology, (O. Bersillon, F. Gunsing, E. Bauge, R. Jacqmin, S. Lerey, eds.) EDP Sciences, 2008, DOI: 10:105/ndata:07342 (in print), April 22-27, 2007, Nice, France.
[7] Th. Bayes Rev., An essay Toward Solving a Problem in the Doctrine of Chances, Phil. Trans. Roy. Soc. 370 (1763); Reprint with biographical note by G.A. Barnard in Biometrika 45 (1958) 293.
[8] E.T. Jaynes, Phys. Rev. 106 (1957) 620; 108 (1957) 171.
[9] H. Leeb, M.T. Pigni, Basic statistics and consistent covariances for nuclear data files, in Proc. Workshop on perspectives of nuclear data in the next decade, (E. Bauge, ed.), Bruyeres-le-Chatel, 2005, (NEA/OECD, Paris, 2006) Vol. 6121, p. 233.
[10] M.T. Pigni, Reliability of optical potentials for nuclear data evaluation, PhD thesis, TU Wien (2006).
[11] H. Vonach et al., Physics Data 13 (1992) 7; S. Tagesen, H. Vonach, A. Wallner, J. Nucl. Sci. And Technology 2 (2002) 140.
[12] H. Leeb, D. Neudecker, Th. Srdinko, Consistent procedure for nuclear data evaluation based on modelling, in Proc. of the Int. Workshop on Neutron Cross Section Covariances, Port Jefferson, June 24-27, 2008, Nuclear Data Sheets 109 (2008) 2762.

# ADS experiments in the JINR Dubna

*M. Majerle*[1,2]
*for the "Energy Plus Transmutation" collaboration*

1) Nuclear Physics Institute of ASCR PRI, 250 68 Řež near Prague, The Czech Republic
2) FNSPE of CTU, 115 19 Prague, The Czech Republic
majerle@ujf.cas.cz

***Abstract:***: Rich tradition of experiments connected with Accelerator Driven Systems (ADS) exists in the Joint Institute for Nuclear Research (JINR) in Dubna, Russia. The focus is on experiments where relativistic protons and deuterons (<2 GeV) are directed to thick, lead targets (in some experiments surrounded by uranium blanket or graphite moderator). The produced spectra of secondary particles are measured with several types of detectors: activation detectors, solid state nuclear track detectors, nuclear emulsions, $^{3}$He counters and others. The data from these experiments are useful in the design of further experimental and real ADS, as well as for benchmark tests of Monte Carlo codes. To improve the accuracy of the codes, extensive sets of cross-section data are needed. Most of these cross-sections are not experimentally measured and evaluated data are used in simulations. Some necessary measurements were already started by our group, but more detailed and independent data are needed.

## Introduction

Accelerator-driven systems (ADS) are considered to be a promising option for future nuclear energy production and nuclear waste incineration. In ADS spallation neutrons (produced via interactions of high energy ions with heavy nuclide targets – lead, tungsten …) are added to subcricital reactor core to sustain the fission chain reaction. ADS are so far in the early experimental and design stage.
One of the requirements in the design of future ADS is the ability to predict the behaviour of such systems with the Monte Carlo (MC) codes. Experiments on smaller scale ADS facilities are therefore performed and the results are being reproduced with MC codes. Most nuclear processes and necessary cross-sections in such experiments are qualitatively known and simulations are able to reproduce experiments inside the accuracy of tens of percents. One way to increase the accuracy of simulations is to improve the precision of the cross-section data.

## JINR ADS research

Several groups in the world scale perform ADS relating experiments (MUSE, TRADE, MEGAPIE [1-3]). Among them is the Joint Institute for Nuclear Research (JINR), where new series of such experiments started in the 90's with the cross-section measurements for the ADS construction material in the high energy proton beams, and were continued with the studies of neutron production on thick targets.

### Gamma-2 to Gamma-MD

Gamma-2 was the experiment focused to the studies of production of neutrons in the spallation process and their moderation/transport in the neutron moderator. The setup consisted of a thick, lead target (diameter 8 cm, length 20 cm) surrounded with 6 cm thick paraffin moderator which slowed spallation neutrons to resonance energies. Neutrons were detected by radiochemical detectors placed on top of the polyethylene along the setup length. One experiment with the 660 MeV protons directed to the target was performed. Gamma-2 was a simple setup providing results which are very useful for comparison with computer codes predictions [4].
Extended target of lead (diameter 8 cm, length 60 cm) is nowadays used in another setup with similar name, Gamma-MD, in which graphite is used as the moderator (1.1x1.1x0.6m$^{3}$). The experiments are focused on the studies of fast neutron moderation in the graphite. The setup was by now irradiated with 2.33 GeV deuterons, more irradiations are planned.

Activation detectors, solid state nuclear track detectors and transmutation samples are used to measure the spectral fluences of the neutron field and its transmutation properties.

***Figure 1.*** *Photo of the Gamma-MD setup. Lead target is in the centre of the graphite cube. Detectors and transmutation samples can be placed inside the graphite, place for them is reserved in removable cylinders.*

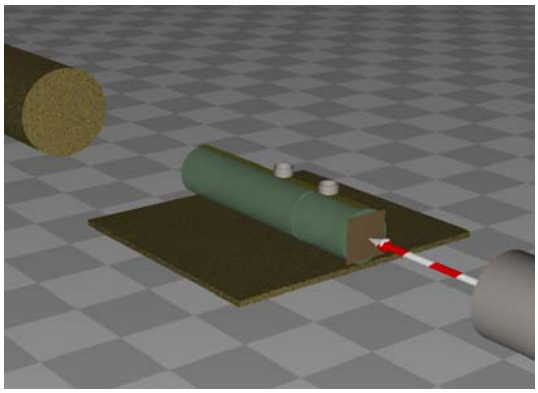

***Figure 2.*** *Schematic drawing of the Phasotron setup. Activation detectors and two transmutation samples are placed on top of the target along its length.*

**Phasotron experiment**

The focus of the Phasotron experiment was on the spatial distribution of high energy spallation neutrons (>10 MeV) along the target. Transmutation properties of radioactive iodine $^{129}$I in fast neutron spectrum were also measured. A bare, lead target (diameter 9.6 cm, length 45.2 cm) was irradiated with 660 MeV protons from the Phasotron accelerator. Activation detectors were placed on top of the target along its whole length together with the iodine transmutation samples. This setup was successfully simulated with several codes [5].

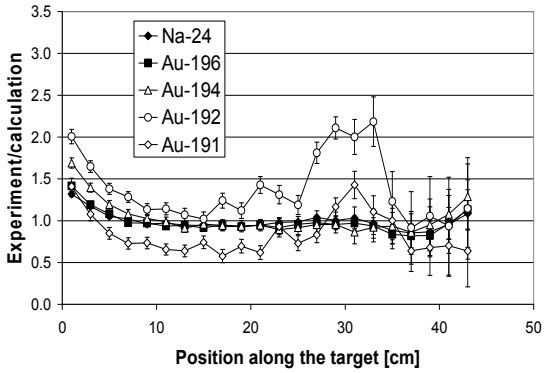


***Figure 3.*** *Comparison of experiment and FLUKA simulation. The ratios between the numbers of produced isotopes in Al and Au activation detectors measured experimentally and simulated are shown.*

### Energy Plus Transmutation

The production of neutrons and their transport in the uranium “core” became possible with the "Energy plus Transmutation" (EPT) setup. It consists of a thick, lead target (diameter 8.4 cm, length 48 cm) surrounded with the uranium blanket (206.4 kg) and placed in a polyethylene box. In series of experiments, relativistic protons and deuterons of energies from 0.7 to 2.52 GeV were directed to the target. Produced neutron flux and its transmutation capabilities were studied at different places of the setup with activation, solid state nuclear track, $^{3}$He and other detectors. The EPT setup consists of several parts, which all influence the produced neutron field. MC codes are describing successfully the experiments with this complicated setup, with the exception of the distribution of 10-100 MeV neutrons at the beam energies higher than 1 GeV [6]. It seems that distribution of neutrons with either higher energies (>100 MeV) or lower energies (<1 MeV) are predicted well at the same experiments [7].

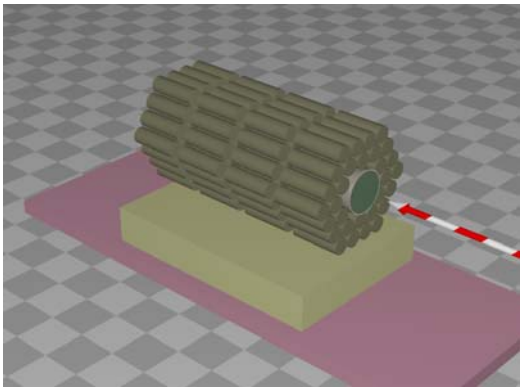

***Figure 4.*** *The EPT setup. Lead target is surrounded with uranium blanket. Polyethylene moderator is not shown in the figure. The detectors are placed in the gaps between the target/blanket sections, transmutation samples are placed on top of the setup.*

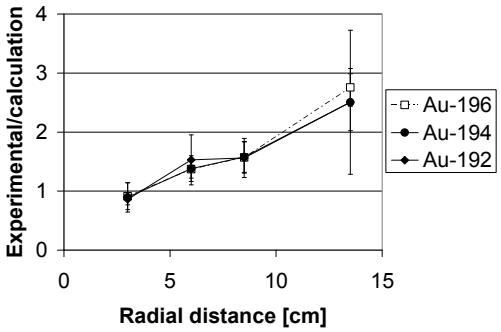


***Figure 5.*** *Comparison of the experiment and MCNPX simulation. The $^{197}$Au detectors were placed at different radial distances from the central axis in the first gap. The experimental/calculation ratios clearly increase with the radial distance.*

## Measurement methods

### Activation detectors and solid state nuclear track detectors

Both types of the detectors are mainly used for their small size (less than 1g of material is sufficient). They can be placed almost anywhere inside the setup without significant influence to the produced neutron field. During the irradiation in the neutron field, the neutrons interact with the detector material, which is analyzed offline for the traces that the neutrons left in the material.

In the case of the activation detectors, the neutrons interact with the detector material via reactions of type (n,$\gamma$), (n,$\alpha$), and (n,xn), exciting a small part of the nuclei in the detector. Providing that the decay times of the excited isotopes are in orders of minutes-days and that during the de-excitation they emit photons (>100 keV), their number can be determined with gamma-spectroscopy methods. Activation detectors cover a wide range of neutron spectrum: eV-MeV neutrons via (n,$\gamma$) reaction, 1 MeV - 100 MeV neutrons via (n,$\alpha$) and (n,xn) reactions. Materials that were used in mentioned experiments were Au, Al, Bi, Y, In, Ta, Co, Cu, and others.

Transmutation samples consist of small amount of the material from the nuclear waste (Am, Np, Pu, I, ..), which is sealed in a safety container. These samples are as well studied by the gamma-spectrometry methods after the irradiation, and transmutation characteristics of nuclear waste materials in the spallation neutron field are determined.

Solid state nuclear track (SSNT) detectors consist of two parts: of the heavy metal that interacts with neutrons via nuclear fission (irradiator) and of the material in which fission fragments leave tracks. The second material (plastic or mica foil) is chemically processed,

and the tracks are counted with optical microscope. Materials that were used in the mentioned experiments as iiradiators are U, Pb, W, Au, and others. While different isotopes of U are fissioned by neutrons of a wide range of energies (thermal-fast), Pb, W, Au ... irradiators are sensible mostly to neutrons with energies >100 MeV.

## Monte Carlo simulations

**Neutron spectral fluence**
All mentioned setups were implemented in Monte Carlo codes MCNPX and FLUKA (KASKAD MC code was also used some calculations). The codes simulate the spallation reactions of primary ions with the target material, all subsequent neutron reactions, and tally the spectral fluences of secondary neutrons, protons, pions, photons … at the places where the detectors were placed at the experiment. Tallied spectral fluences are folded with appropriate cross-sections to obtain the numbers of activated nuclei/fissions in activations/SSNT detectors.

**Cross-sections**
Cross-sections implemented in the MC codes are taken from evaluated cross-sections databases (ENDF, JEFF …), which usually extend up to 20 MeV (150 MeV in LA150 libraries), above which the cross-sections are calculated by the nuclear model currently used by the code.
The folding of the spectral fluences with the cross-sections is performed manually with the cross-section calculated with TALYS (<150 MeV) and MCNPX (>150 MeV) codes. These cross-sections are additionally checked against the experimental values found in EXFOR and commonly the values for the same cross-sections differ for tens of percents. With few exceptions, there is a lack of experimentally measured cross-sections for activation and SSNT detectors, especially at energies above 20 MeV.

**Comparison with the experiment**
With some exceptions (see Figure 5) MC codes are able to reproduce the experimental results qualitatively well (Figure 3). There are however differences on quantitative scale in the range of tens of percents [7, 5]. These differences can be due to calculated neutron distribution or wrong cross-sections. For better accuracy of the ADS simulations, the MC codes will have to be improved, and the wide range of missing cross-sections will have to be experimentally measured.

## Conclusion

At the ADS connected experiments in the JINR Dubna, the neutron distributions are measured with activation and SSNT detectors. For the reproduction of experimental values with the MC codes, good cross-sections data is needed, especially at energies higher than 20 MeV. The accuracy of today cross-sections in this energy region is not satisfactory for accurate simulations of the mentioned experiments or future ADS systems.

**Acknowledgements**
Authors are grateful to the METACentrum (the Czech Republic) for offering computers for the calculations. This work was carried out partly under support of the Grant Agency of the Czech Republic (grant No. 202/03/H043) and IRP AV0Z10480505 (the Czech Republic).

**References**
[1] RUGAMA, et al., Some Experimental Results from the Last Phases of the MUSE Program, Proceedings of Physor 2004, Chicago, Ill., 2004.
[2] M. SALVATORES, et al., TRADE (TRIGA Accelerator Driven Experiment): A Full Experimental Validation of the ADS Concept in a European Perspective, Proc. of the Sixth International Meeting on Nucl. Appl. of Accelerator Tech., AccApp'03, American Nuclear Society, 2004, p. 8-16.
[3] Juanita Schlaepfer-Miller, MEGAPIE leads the way to waste transmutation, CERN Courier, (April 2007), 29.
[4] Westmeier W. et al., Transmutation experiments on $^{129}$I, $^{139}$La and $^{237}$Np using the Nuclotron accelerator, Radiochimica Acta 93 (2/2005) 65-75.
[5] M. Majerle, et al. JINR Preprint E15-2008-94.
[6] F. Křížek, et al, Czech. J. of Phys. 56 (2006) 243.
[7] S.R. Hashemi-Nezhad, et al., NIM A, Volume 591, Issue 3, 1 July 2008, Pages 517-529

# Advanced analysis of $^{237}$Np neutron data

*V.M. Maslov*

Joint Institute for Nuclear & Energy Research, 220109, Minsk-Sosny, Belarus
maslov@bas-net.by;

***Abstract:*** Important constraints for the $^{237}$Np capture cross section come from the average radiation width, neutron strength functions $S_0$ and $S_1$ and consistent description of the total, fission and partial inelastic scattering data in 1-3 MeV energy. Inelastic data shape at $E_n$ ~1.5 MeV evidence the onset of three-quasi-particle excitations in $^{237}$Np. Strong influence of pre-fission (n, xnf) neutrons on prompt fission neutrons average energy $\langle E \rangle$ is demonstrated.

## Introduction

In recent years neutron data of $^{237}$Np have attracted much attention [1-9]. Either repository or transmutation of that major constituent of the spent fuel needs rather precise knowledge of the $^{237}$Np fission [3, 4], capture [5], inelastic scattering [6] cross sections and prompt fission neutron spectra [7, 8, 9]. The improvements of the nuclear reaction modeling and nuclear parameter systematic, developed based on neutron data description of major actinides $^{232}$Th, $^{233}$U, $^{235}$U, $^{238}$U and $^{239}$Pu provide a sound basis for critical assessment of the (n, F), (n, γ) and (n, n') of $^{237}$Np. The main reasons of improvement might be consistent description of total, fission, inelastic scattering and capture data in 0.1 keV – 5 MeV energy range. For neutron capture reaction on $^{237}$Np target nuclide in the unresolved resonance and fast neutron energy ranges the methods, proven in case of $^{232}$Th(n,γ) and $^{238}$U(n, γ) data analysis would be used. At higher energies consistent description of $^{237}$Np(n, 2n)$^{236s}$Np and $^{237}$Np(n, F) cross sections and the latter as a superposition of (n, f) and (n, xnf) reactions, with simultaneous calculation of exclusive neutron spectra of (n,xn) and (n,xnf) reactions may provide robust estimates of prompt fission neutron spectra and their average energies [8, 9, 10].
Disentangling of the model deficiencies and model parameter uncertainties, when measured cross section data fits are rather poor, especially when the data are scattering and there are systematic shifts between different data sets, turns out to be a major problem in case of $^{237}$Np+n data analysis and prediction. Important constraints for the calculated capture cross section would come from the average radiation width and neutron strength functions $S_0$ and $S_1$. Consistent description of the total, fission and partial inelastic scattering data in 1~3 MeV energy range would provide important constraint for the absorption cross section, which is quite important for the robust estimate of the capture cross section in keV energy range.
The comparison of average energies of prompt fission neutron spectra for $^{237}$Np(n, F) reaction of different evaluated data libraries with present calculated and measured data give an impetus for a new evaluation of PFNS.
Realistic assessment of the uncertainties of $^{237}$Np evaluated data should take into account the results of the consistent description of total, fission, capture and inelastic scattering cross sections with nuclear reaction theory. Purpose of the present analysis is to clear out whether the available data on total and partial cross sections and average resonance parameters could be described/reproduced consistently.

## Total cross section and elastic scattering

Auchampaugh et al. [11] measured $^{237}$Np+n total cross section in the energy range 20-200 keV, Kornilov et al. [6] - in the energy range of 0.5-9 MeV and Grigoriev et al. [12] at energies below 50 keV. Fig. 1 shows that data sets of [6] and [11] appear to be mutually consistent, while systematic discrepancy with data [12] is obvious. Calculated total, elastic scattering and absorption cross sections were obtained with the coupled-channel potential parameters by Maslov et al. [13, 14], obtained for the $^{238}$U. The experience of describing the capture cross section of $^{232}$Th [15, 16] is the motivation to decrease the real volume potential term $V_R$ by 0.5 MeV. Four ground-state rotational band levels $5/2^+$-$7/2^+$-$9/2^+$-$11/2^+$ are assumed coupled. Deformation parameters were tuned to fit $S_o$ and $S_1$ strength function values of [17]. It will be shown below that the description of newest capture cross section data by Esch et al. [5] at 1 keV–200 keV is very sensitive to the shape of the absorption cross section. Fig. 1 shows, that

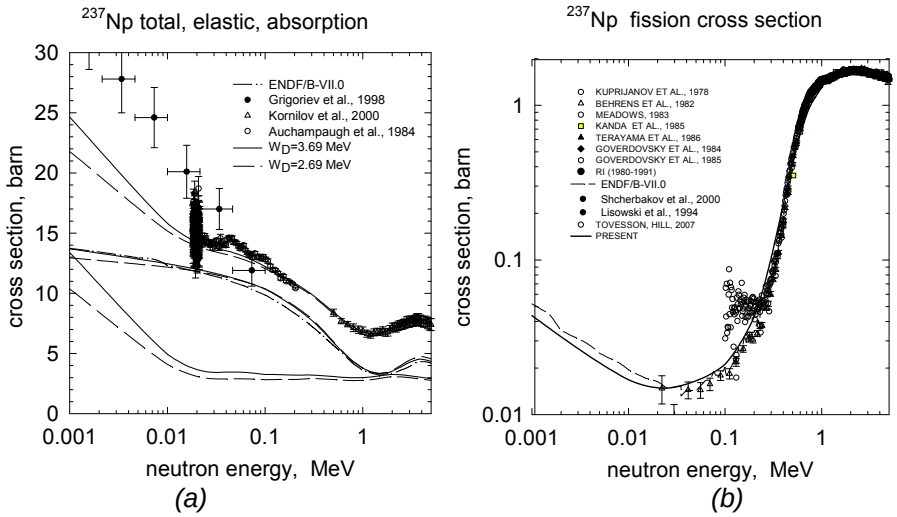


***Figure 1.*** *Total absorbtion and elastic scattering (a) and fission (b) cross sections of $^{237}$Np+n.*

around 1 MeV the total cross section is virtually insensitive to the decrease of the imaginary surface potential term $W_D$, while the lowering of the absorption cross section could be cross checked by consistency of fission and inelastic scattering cross sections. In case of ENDF/B-VII.0 [1] the elastic scattering was adjusted to balance total and partial cross sections.

## Fission cross section

In case of $^{237}$Np(n, f) cross section, for which there are systematic discrepancies in measured data [18-29], which are still not removed by recent measurement by Tovesson et al. [3, 4]. However, the overall consistency of time-of-flight data [3, 4, 27, 28] with the absolute measurements [29] is the indication of the higher 'true' cross section level. Fig. 1(a) demonstrates the fission data fit from 1 keV to 6 MeV.

## Inelastic scattering

It seems that $E_n$~1 MeV is a "stabilization point" of inelastic scattering cross section. Present calculation based on the fits of total and fission cross sections. The evaluated inelastic cross sections of ENDF/B-VII.0 evaluations is in severe disagreement with data by Kornilov et al. [6] on the inelastic scattering of neutrons with excitation of specific groups of levels (see Fig. 2a). Upward trend of the inelastic data at $E_n \geq 1.5$ MeV might be explained by the sharp increase of the level density of the residual nuclide $^{237}$Np due to the onset of three-quasi-par-ticle excitations [30]. The calculation with the decreased absorption cross section undershoots the measured data [6]. The total inelastic scattering cross section is much lower, than that corresponding to higher absorption cross section That is the sound proof of the adopted estimate of the absorption cross section, which is supported both by the $S_0$ strength function value at low energies and consistent description of fission and inelastic scattering data.

## Capture cross sections

Measured data for the $^{237}$Np(n, γ) reaction cross section [5, 31-35] shown on Fig. 2b, are scattering a lot. The important feedback from the consistent description of total, fission and inelastic scattering data might be the prediction of the capture cross section shape based on the reliable estimate of radiation strength function and absorption cross section. Fig. 2b shows the calculated curve, corresponding to the consistent description of the total, fission and inelastic scattering cross section with $\langle\Gamma_\gamma\rangle$ =40.7 meV and $\langle D_{obs}\rangle$=0.52 eV. Recent measured data [5] predict distinctly different cross section shape than the other data [31-35]. Relatively low cross section level in 20-200 keV energy range could be reproduced with rather low value of $\langle\Gamma_\gamma\rangle$ = 30 meV or decreased by 1 MeV $W_D$=2.69 MeV. Combined influence of both factors brings the calculated cross section in consistency with the data by Esch et al. [5] in the 4 keV – 300 keV energy range. However, the resulting value of $S_o = 0.78 \times 10^{-4}$ is much lower than the established value [17]. Obviously, the $S_o$ value could be increased by increasing the $\beta_2$,

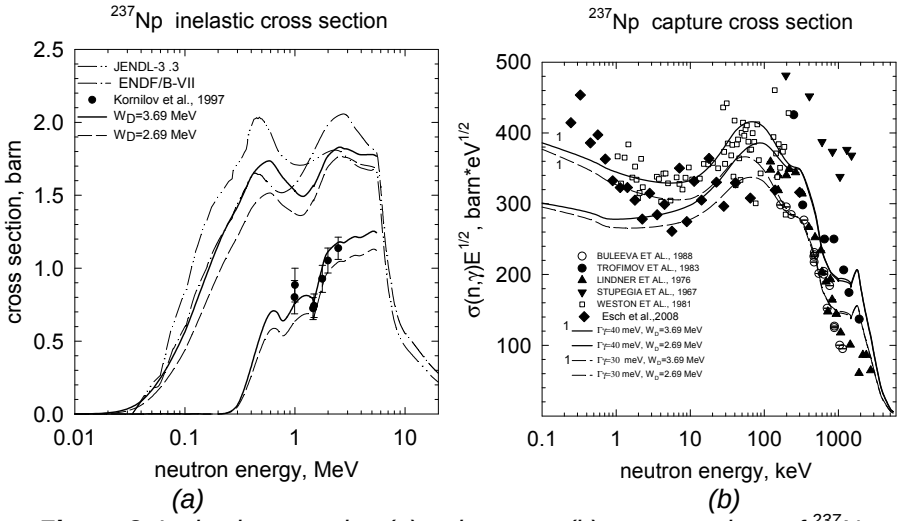


***Figure 2.*** *Inelastic scattering (a)and capture (b) cross sections of $^{237}$Np*

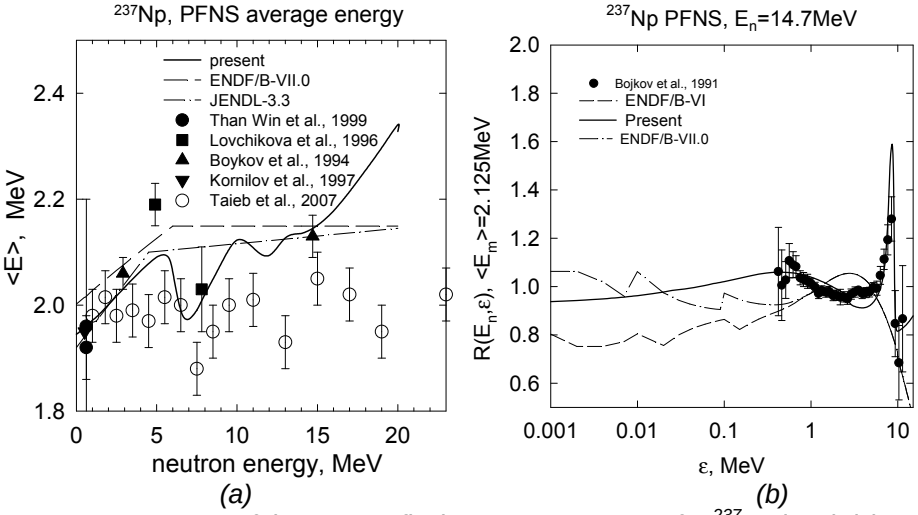


***Figure 3.*** *Average energy of the prompt fission neutron spectra for $^{237}$Np(n, F) (a);measured and calculated PFNS of $^{237}$Np(n, F) at $E_n$=14.7 MeV, relative to Maxwell PFNS.*

quadrupole deformation parameter value, but after that the calculated capture cross section will again misfit the newest data [5], shown on Fig. 2b. The high cross section at $E_n$<1 keV is reproduced only with increased of the absorption cross section and $S_0$=1.3x10$^{-4}$.

## Prompt Fission Neutron Spectra

Measured differential data on PFNS are available for the $^{237}$Np(n, F) for a few incident neutron energies [36-39]. In case of $^{237}$Np the evaluated data files of ENDF/B-VII.0, JENDL-3.3 and BROND ignore the influence of (n, xnf) pre-fission neutrons even on their average energy $\langle E \rangle$, to tell nothing about prompt fission neutron spectra shapes (see Figs. 3, 3b). Fission neutron spectra of $^{237}$Np(n, F) were measured in the vicinity of (n, xnf)-reaction thresholds. At $E_n \geq E_{nnf}$, where $E_{n,nf}$ - threshold of the (n, nf) reaction, the theoretical estimate of PFNS is obtained combining exclusive pre-fission and post-fission neutrons.

Contributions of emissive/non-emissive fission and exclusive spectra of (n, xnf) reactions are defined by consistent description of $^{237}$Np(n, F) and $^{237}$Np(n, 2n)$^{236s}$Np reactions. Energy dependence of PFNS for $^{237}$Np(n, F) at $\varepsilon < E_{th} \sim E_n - B_f$, where $B_f$ – fission barrier of $^{237}$Np, is defined by fission probability of residual nuclide $^{237}$Np. Relative contribution of the (n, nf) and (n, 2nf) reactions to the fission cross section of $^{237}$Np(n, F) are substantially lower, than in case of $^{235}$U(n, F), nonetheless, 1$^{st}$ and 2$^{nd}$ neutrons influence the PFNS shape still appreciably (see Figs. 3a(b)). The newest measurement of prompt fission neutron spectra for $^{237}$Np(n, f) [9] is quite consistent with the shape of independent model prediction (see Fig. 3a).

## Conclusion

Present approach produces consistent description of total, (n, f) and (n, 2n) measured data. Estimate of inelastic scattering cross section is supported by the data [6] on the partial inelastic scattering of neutrons. The constrained by the values of radiation strength function $S_\gamma$ and neutron strength functions $S_o$ and $S_1$ of [17] calculated capture cross section could not follow the trend, predicted by the newest measured data of [5]. The job is supported by International Science and Technology Center (Moscow) under B-1604 Project Agreement and International Atomic Energy under Research Contract 14309.

**References**

[1] M.B. Chadwick, P. Oblozinsky, M. Herman et al., Nucl. Data Sheets, 107 (2006) 2931.
[2] R. Sanchez, D. Loaiza, R. Kimpland et al. Nucl. Sci. Eng. 158 (2008) 1.
[3] F. Tovesson, T.S.Hill, Nucl.Sci.Eng. 159 (2008) 94.
[4] F.Tovesson, T.S. Hill Phys. Rev. C 75 (2007) 034610.
[5] E.-I. Esch, R. Reifarth, E.M. Bond et al. Phys. Rev. C 77 (2008) 034309.
[6] N.V. Kornilov, A.B. Kagalenko, V.Ya. Baryba et al., Ann. Nucl. Energy, 27 (2000) 1643.
[7] N.V. Kornilov, A.B. Kagalenko, F.-J. Hambsch, Phys. Atom. Nucl., 62 (1999) 209.
[8] V.M. Maslov, Atomic Energy, 104 (2008) 330.
[9] J. Taieb et al., in Proc. of the Inter. Conf. on Nuclear Data for Science and Technology (O. Bersillon, F. Gunsing, E. Bauge, R. Jacqmin and S. Leray, eds.), pp. 429-432, Nice, France, April 22-27, 2007, EDP Sciences.
[10] V.M. Maslov, Phys. Atom. Nucl. 71 (2008) 9.
[11] F. Auchampaugh, M.S. Moore, J.D. Moses et al., Phys. Rev. C29 (1984) 174.
[12] Yu.V. Grigoriev, V.V. Sinitsa, N.A. Gundorin et al., JINR-E3-98-202, 194, 1998.
[13] V.M. Maslov, Yu.V Porodzinskij, N.A. Tetereva et al., Nucl. Phys. A736 (2004) 77.
[14] V.M. Maslov, Yu.V Porodzinskij, M. Baba et al., in: Proc. of Intern. Conf. on Nuclear Data for Science and Technology, October 7-12, 2001, Tsukuba, Japan, p. 148, 2002.
[15] V.M. Maslov, Yu.V Porodzinskij, M. Baba, A. Hasegawa, Nucl. Sci. Eng. 143 (2003) 177. [16]V. M. Maslov, in Proc. of the 13th International Seminar on Interaction of Neutrons with Nuclei, May 25-28, 2005, Dubna, Russia, p. 43.
[16] S. F. Mughabghab Atlas of neutron resonances.2006, NNDC, BNL, Upton, USA.
[17] J.W. Meadows, Ann. Nucl. Energy, 15 (1988) 421.
[18] V.M. Kuprijanov, B.I. Fursov, V.I. Ivanov, G.N.Smirenkin, Atom. Energiya, 45 (1978) 440.
[19] J.W. Behrens, J.C. Browne, J.C. Walden, Nucl. Sci. Eng., 80 (1982) 239.
[20] .W. Meadows, Nucl. Sci. Eng., 85 (1983) 271.
[21] K. Kanda, O. Sato, K. Yoshida et al., JAERI-M-85-035, 1985, p. 220.
[22] H. Terayama, Y. Karino, F. Manabe et al.. NEANDC(J)-122, 1986.
[23] A.A. Goverdovskij, A.K. Gordyushin, B.D. Kuz'minov et al., Atom. Energ. 58 (1985) 137.
[24] A.A. Goverdovskij, A.K. Gordyushin, B.D. Kuz'minov et al., Proc. 6th All-Union Conf. on Neutron Physics, Kiev, 1983, vol.3, 115 (1983).
[25] I.D. Alkhazov, E.A. Ganza, L.V. Drapchinskij et al., Proc. of the 3d All-Union Conf.Neutron Radiation Metrology, Moscow, 1983, CNIIAtominform, 1983, vol. 2., p. 201.
[26] P.W. Lisowski et al., Proc. Spec. Meeting on Neutron CrossSection Standards for the Energy Region above 20 MeV, Uppsala, Sweden, May 21-23, 1991, p. 177, OECD, 1991.
[27] O.A. Shcherbakov, A. Donets, A. Evdokimov et al., Proc. Intern. Conf. on Nuclear Data for Science and Technology, October 7-12, 2001, Tsukuba, Japan, p. 230, 2002.
[28] R. Arlt et al., Sov J. At. Energy, 55 (1884) 656.
[29] V.M. Maslov, INDC(BLR)-013/L, 1998, IAEA, Vienna.
[30] N.N. Buleeva, A.N. Davletshin, O.A. Tipunkov et al., Atomnaya Energya, 65 (1988) 348.
[31] M. Lindner, R.J. Nagle, J.H. Landrum, Nucl. Sci. Eng., 59 (1976) 381.
[32] D.C. Stupegia, M. Schmidt, C.R. Keedy, Nucl. Sci. Eng., 29 (1967) 218.
[33] Yu. N. Trofimov et al. Proc. 6th All-Union Conf. on Neutron Phys. Kiev, 1983, vol. 2, 142.
[34] L.W. Weston, J.H. Todd, Nucl. Sci. Eng., 79 (1981) 184.
[35] G.S. Bojkov, V.D. Dmitriev, M.I. Svirin et al., Phys. Atom. Nucl., 57 (1994) 2126.
[36] Kornilov N.V., Kagalenko A.B., Baryba V.Ya. et al., 1997, in: Proc. of Intern. Conference on Nuclear Data for Science and Technology, May 19-24, Trieste, Italy, pp.577-579.
[37] Than Win, M. Baba, M. Ibaraki et al., Journ. Nucl. Sci. Technol., 36 (1999) 486.
[38] A.M. Trufanov, G.N. Lovchikova et al., Phys. Atom. Nucl., 55 (1992) 289.

# Validation of PWR spent fuel decay heat considering new SKB measurements.

*R.W. Mills, C.H.Zimmerman, C.Shearer*

National Nuclear Laboratory, Sellafield, Seascale, Cumbria CA20 1PG. U.K.
robert.w.mills@nnl.co.uk

***Abstract:*** The decay heat produced by spent nuclear fuel is an important parameter of safety analyses for its storage, transport, reprocessing and waste management. Current decay heat validation using the UK inventory code FISPIN10 for PWR fuel is based upon 12 calorimetric measurements reported by Schmitroth [1]. Reported results using JEF-2.2 and JEFF-3.1.1 decay and fission yield libraries using the FISPIN code [2] give good agreement; the mean calculated over experimental (C/E) values being 1.03±0.03 and 1.01±0.03 respectively. However, the data has a limited range of irradiation (25.6 to 39.4 GWd/t), cooling (2.3 to 5.7 years) and enrichment (2.5 to 3.4%) [3].
This paper considers recent PWR measurements carried out at the Swedish Nuclear Fuel and Waste Management Company (SKB) where calorimetric measurements have been performed of decay heat from BWR and PWR assemblies at the Swedish Interim Spent Fuel Storage Facility, CLAB, at Oskarshamn [4]. These include 43 measurements of decay heat from PWR spent fuel and 66 of BWR. The PWR measurements range in enrichment between 2.1 to 3.4%, irradiation of 19.7 to 51.0 GWd/t and cooling of 13 to 23 years. This considerably extends the current FISPIN decay heat validation in irradiation and cooling.
These new calculations of the SKB PWR data use the FISPIN graphical user interface, FISGUI [5], which include generic JEF-2.2 [6] and JEFF-3.1 [7] libraries for Magnox, AGR, PWR and BWR fuels. The effect of using generic libraries for PWR decay heat, rather than cross-section libraries based upon modelling a specific PWR reactor is discussed. These validation results are compared to an independent method of determining uncertainties and possible improvements discussed.

## Background

Up until recently the validation of spent fuel decay heat after 1 day of cooling relied upon measurements of the decay heat from irradiated PWR assemblies reported and compared against ORIGEN2 by Schmittroth [1]. This included 20 measurements of assemblies irradiated in the San Onofre, Point Beach and Turkey Point reactors; note that 4 measurements were reported as suspect and were ignored. The stainless steel clad fuel from San Onofre did not have a measured value for the cobalt impurity and as natural variation can result in variation in total decay heat of 10 to 20% in these cases, they could not be used for validation. Previous validation using these data with FISPIN and JEFF based libraries are shown in Table 1 [8]. The reactor physics models were based on design data reported in World Nuclear Industry Handbook [9]. These results show good agreement between experiment and calculations, all within ±5%. The overall mean C/E for JEF-2.2 and JEFF-3.1 are 1.01 ± 0.03 and 1.00 ± 0.03 respectively. It is noted that the uncertainties on the measurements were ± 2%.

## New SKB results

In this work the new SKB PWR assembly decay heat measurements have been considered [4]. The irradiation histories of these assemblies' on-power and shutdown days are given in Table 2. The irradiations in MWd/t calculated for these assemblies, the masses of the assembly components, the uranium masses and enrichments, the irradiation histories and the cooling times to each measurement were used with the FISPIN Graphical User Interface (FISGUI) to calculate the decay heat expected from the fuel, zircalloy cladding and the small amount of stainless steel and inconel assembly components. The cross-section files used were generic PWR libraries based upon design information for the Unterweser PWR. The measured heat and its C/E ratios are given in Table 3 with details of the irradiation, enrichment and cooling.

These results show good agreement with the calculations JEF-2.2 data giving 0.995 ± 0.013 and JEF-3.1.1 giving 0.985 ± 0.012. The uncertainty on the heat measurements are reported as ± 2% [4]. It is noted that using other available PWR libraries give mean C/E values of 0.987 and 1.032, and the mean C/E are different between the Ringhals 2 and 3 results. This suggests that reactor specific cross-section libraries need to be developed using the design information of these reactors to properly validate the codes and data.
The overall uncertainty from these new results is around ± 1.5%, very close to the expected measurement uncertainties of ± 2%.

## Expected uncertainties on decay heat

Validation studies of this type are based upon measurements for assemblies from specific reactors and fuel parameters (enrichment, irradiation history, cooling). Their validity outside of these ranges are less certain for safety cases. An alternative is to consider the uncertainties of the underpinning nuclear data and the biases of calculation methods including validation of spent fuel composition to calculate the decay heat with its biases and uncertainties. This type of approach has been used for a typical PWR UOX fuel and results are shown in Table 4 [10]. This shows biases of less than 1% from 3 days to 30 years of cooling and an expected uncertainty of around 5% between 5 and 100 years, whereas the above validation suggests calculations are within about 1 to 2% of the experimental measurements.

## Conclusions

These new measurements considerably increase the range of validation data available for decay heat from LWR fuel assembles and these preliminary results give very good agreement with both JEF-2.2 and JEFF-3.1.1 data. It is interesting to note that the validation results are considerably better than estimates of the uncertainties from nuclear data and chemical analysis data would suggest. It is possible that this is a result of the highly correlated nuclear data uncertainties that would be expected in decay heat calculations where a few highly correlated fission products dominate (e.g. Cs137/Ba137m, Sr90/Y90, Ce144/Pr144, Ru106/Rh106).

## Acknowledgements

The authors gratefully acknowledge support from the UK Nuclear Decommissioning Authority and the European Commission's Euratom FP6 CANDIDE project.

**References**

[1] F. Schmittroth "ORIGEN2 Calculations of PWR spent fuel decay heat compared with calorimetric data" HEDL-TME 83-32 UC-85 (1984).
[2] The FISPIN10 spent fuel inventory code is developed by the UK National Nuclear Laboratory (www.nnl.co.uk) and available through Serco Assurance (www.sercoassurance.com).
[3] R.W. Mills and C. Shearer, "Testing of the JEFF-3.1.1 radioactive decay data file for consistency and comparison with JEFF-3.1 results.", JEF/DOC-1220 (2007).
[4] Svensk Kärnbränslehantering AB, "Measurements of decay heat in spent nuclear fuel at the Swedish interim storage facility, Clab", SKB Report R-05-62, ISSN 1402-3091 (2006).
[5] C. Hoggett-Jones , C. Robbins, G. Gettinby and S. Blythe, "Modelling the inventory and impact assessment of partitioning and transmutation approaches to spent nuclear fuel management" Annals of Nuclear Energy Volume 29, Issue 5, March 2002, Pages 491-508
[6] "JEFF Report 17: The JEF-2.2 Nuclear Data Library" NEA Data Bank report OECD, Paris (2000).
[7] "JEFF Report 21: The JEFF-3.1 Nuclear Data Library", NEA Data Bank report, OECD, Paris (2006).
[8] R.W. Mills and C. Shearer, "Testing of the JEFF-3.1.1 radioactive decay data file for consistency and comparison with JEFF-3.1 results", JEF/DOC- 1220 (2007).
[9] Nuclear Engineering International World Nuclear Industry Handbook 1987 (ISSN 0029-5507).
[10] R.W. Mills, C.H. Zimmerman and R.G. Moore, "Uncertainties on spent fuel inventories in the application of nuclear fuel cycles", NEMEA-4 workshop, 16-18 October 2007, Prague, Czech Republic.

***Table 1.*** *Comparison of PWR assembly decay heat measurements with calculations using JEFF data.*

| Reactor | Initial $^{235}U$ (Wt%) | Burnup (GWd/t) | Cooling (d) | Measured heat (W) | JEF-1 C/E | JEF-2.2 C/E | JEFF-3.1 C/E |
|---|---|---|---|---|---|---|---|
| Point Beach | 3.397 | 31.914 | 1635 | 724 | 1.04 | 0.98 | 0.97 |
| | | 31.914 | 1635 | 723 | 1.04 | 0.98 | 0.97 |
| | | 38.917 | 1634 | 921 | 1.04 | 1.01 | 1.00 |
| | | 39.384 | 1633 | 931 | 1.04 | 1.01 | 1.00 |
| | | 35.433 | 1630 | 846 | 1.03 | 0.97 | 0.96 |
| | | 38.946 | 1629 | 934 | 1.03 | 1.00 | 0.99 |
| | | 37.057 | 1630 | 874 | 1.04 | 1.00 | 0.99 |
| Turkey Point | 2.556 | 28.430 | 962 | 1423 | 1.05 | 1.05 | 1.04 |
| | | 28.430 | 2077 | 625 | 1.02 | 1.03 | 1.01 |
| | | 26.485 | 963 | 1284 | 1.06 | 1.06 | 1.05 |
| | | 27.863 | 864 | 1550 | 1.07 | 1.06 | 1.05 |
| | 2.559 | 25.595 | 1782 | 637 | 0.99 | 1.00 | 0.98 |
| Mean and Standard Deviation of C/E values | | | | Point Beach | 1.04 ± 0.01 | 0.99 ± 0.02 | 0.98 ± 0.02 |
| | | | | Turkey Point | 1.04 ± 0.03 | 1.04 ± 0.03 | 1.02 ± 0.03 |
| | | | | Combined | 1.04 ± 0.02 | 1.01 ± 0.03 | 1.00 ± 0.03 |

***Table 2.*** *Irradiation histories of the measured SKB PWR assemblies.*

| Assembly | Reactor | Cycle 1 on-power days | Shut down days | Cycle 2 on-power days | Shut down days | Cycle 3 on-power days | Shut down days | Cycle 4 on-power days | Shut down days | Cycle 5 on-power days | Shut down days | Cycle 6 on-power days |
|---|---|---|---|---|---|---|---|---|---|---|---|---|
| 0C9 | Ringhals 3 | 1038 | 104 | 240 | 74 | 305 | 47 | 323 | | | | |
| 0E2 | | 305 | 47 | 323 | 49 | 335 | 47 | 338 | | | | |
| 0E6 | | 323 | 49 | 335 | 47 | 338 | | | | | | |
| 1C2 | | 1038 | 104 | 240 | 74 | 305 | 47 | 323 | | | | |
| 1C5 | | 1038 | 104 | 240 | 74 | 305 | 47 | 323 | | | | |
| 1E5 | | 323 | 49 | 335 | 47 | 338 | | | | | | |
| 2A5 | | 1038 | 104 | 240 | | | | | | | | |
| 2C2 | | 1038 | 104 | 240 | 74 | 305 | 47 | 323 | | | | |
| 3C1 | | 1038 | 104 | 240 | 74 | 305 | 47 | 323 | | | | |
| 3C4 | | 1038 | 104 | 240 | 74 | 305 | 47 | 323 | | | | |
| 3C5 | | 1038 | 104 | 240 | 74 | 305 | 47 | 323 | | | | |
| 3C9 | | 1038 | 104 | 240 | 74 | 305 | 47 | 323 | | | | |
| 4C4 | | 1038 | 104 | 240 | 74 | 305 | 47 | 323 | | | | |
| 4C7 | | 1038 | 104 | 240 | 74 | 305 | 47 | 323 | | | | |
| 5A3 | | 1038 | 104 | 240 | | | | | | | | |
| 5F2 | | 335 | 47 | 338 | 38 | 312 | 40 | 310 | 34 | 337 | | |
| C01 | Ringhals 2 | 1029 | 85 | 267 | 56 | 312 | 83 | 281 | 78 | 290 | | |
| C12 | | 1029 | 85 | 267 | 56 | 312 | 83 | 281 | 78 | 290 | | |
| C20 | | 1029 | 85 | 267 | 56 | 312 | 1927 | 266 | | | | |
| C42 | | 1029 | 1532 | 317 | 84 | 273 | 1512 | 329 | | | | |
| D27 | | 312 | 83 | 281 | 78 | 290 | 481 | 273 | | | | |
| D38 | | 267 | 56 | 312 | 83 | 281 | 78 | 290 | 80 | 317 | | |
| E38 | | 312 | 83 | 281 | 78 | 290 | 80 | 317 | | | | |
| E40 | | 312 | 83 | 281 | 78 | 290 | 80 | 317 | | | | |
| F14 | | 281 | 78 | 290 | 80 | 317 | 84 | 273 | | | | |
| F21 | | 281 | 78 | 290 | 80 | 317 | 84 | 273 | 91 | 260 | | |
| F25 | | 281 | 78 | 290 | 80 | 317 | 84 | 273 | | | | |
| F32 | | 290 | 80 | 317 | 84 | 273 | 778 | 320 | 63 | 297 | 54 | 329 |
| G11 | | 290 | 80 | 317 | 84 | 273 | 91 | 260 | 90 | 266 | | |
| G23 | | 317 | 84 | 273 | 91 | 260 | 90 | 266 | | | | |
| I09 | | 260 | 90 | 266 | 71 | 320 | 63 | 297 | 54 | 329 | | |
| I20 | | 273 | 91 | 260 | 90 | 266 | 71 | 320 | | | | |
| I24 | | 273 | 91 | 260 | 90 | 266 | 71 | 320 | | | | |
| I25 | | 273 | 91 | 260 | 90 | 266 | 71 | 320 | 63 | 297 | | |

***Table 3.*** *Details of measured decay heats and FISPIN calculations using generic libraries.*

| Assembly | Reactor | U235 Wt% | U236 ppm | Final Irradition MWd/t | Cooling (days) | Cooling (years) | Irradiation step 1 MWd/t | Irradiation step 2 MWd/t | Irradiation step 3 MWd/t | Irradiation step 4 MWd/t | Irradiation step 5 MWd/t | Irradiation step 6 MWd/t | Measured heat (W) | JEFF-2.2 C/E | JEFF-3.1.1 C/E |
|---|---|---|---|---|---|---|---|---|---|---|---|---|---|---|---|
| 0C9 | Ringhals 3 | 3.101 | 150 | 38442 | 6551 | 17.94 | 9884 | 8192 | 10350 | 10016 | | | 491.2 | 1.000 | 0.991 |
| 0E2 | | 3.103 | 150 | 41628 | 5823 | 15.94 | 7496 | 13034 | 11308 | 9790 | | | 587.9 | 0.974 | 0.967 |
| 0E6 | | 3.103 | 150 | 35993 | 5829 | 15.96 | 12490 | 13031 | 10472 | | | | 487.7 | 0.986 | 0.975 |
| 1C2 | | 3.101 | 150 | 33318 | 6559 | 17.96 | 6249 | 5019 | 11509 | 10541 | | | 417.7 | 0.999 | 0.988 |
| 1C5 | | 3.101 | 150 | 38484 | 6593 | 18.05 | 9884 | 8102 | 10411 | 10087 | | | 499.2 | 0.983 | 0.974 |
| 1E5 | | 3.103 | 150 | 34638 | 5818 | 15.93 | 10556 | 13134 | 10948 | | | | 468.8 | 0.986 | 0.975 |
| 2A5 | | 2.1 | 150 | 20107 | 7297 | 19.98 | 12228 | 7879 | | | | | 233.7 | 1.015 | 1.000 |
| 2C2 | | 3.101 | 150 | 36577 | 6550 | 17.93 | 7783 | 8345 | 9932 | 10517 | | | 466.5 | 0.998 | 0.988 |
| 3C1 | | 3.101 | 150 | 36572 | 6545 | 17.92 | 7783 | 8341 | 9931 | 10517 | | | 470.2 | 0.988 | 0.978 |
| 3C4 | | 3.101 | 150 | 38447 | 6544 | 17.92 | 9884 | 8192 | 10354 | 10017 | | | 497.3 | 0.984 | 0.976 |
| 3C5 | | 3.101 | 150 | 38373 | 6543 | 17.91 | 9884 | 8113 | 10343 | 10033 | | | 501.4 | 0.980 | 0.971 |
| 3C9 | | 3.101 | 150 | 36560 | 6552 | 17.94 | 7783 | 8377 | 9876 | 10524 | | | 468.4 | 0.992 | 0.982 |
| 4C4 | | 3.101 | 150 | 33333 | 6572 | 17.99 | 6249 | 4991 | 11030 | 11063 | | | 422 | 0.989 | 0.978 |
| 4C7 | | 3.101 | 150 | 38370 | 6549 | 17.93 | 9884 | 8101 | 10347 | 10038 | | | 498.7 | 0.983 | 0.975 |
| 5A3 | | 2.1 | 150 | 19699 | 6972 | 19.09 | 11696 | 8003 | | | | | 237.7 | 0.991 | 0.976 |
| | | | | | 6975 | 19.10 | | | | | | | 236.6 | 0.996 | 0.981 |
| | | | | | 6977 | 19.10 | | | | | | | 243.4 | 0.968 | 0.953 |
| | | | | | 7291 | 19.96 | | | | | | | 230.9 | 1.005 | 0.990 |
| | | | | | 7304 | 20.00 | | | | | | | 230.2 | 1.007 | 0.992 |
| 5F2 | | 3.404 | 150 | 47308 | 4724 | 12.93 | 13475 | 6922 | 10337 | 8930 | 7644 | | 714 | 0.976 | 0.971 |
| C01 | Ringhals 2 | 3.095 | 150 | 36688 | 8468 | 23.18 | 11247 | 9403 | 7569 | 8469 | | | 415.7 | 1.006 | 0.998 |
| C12 | | 3.095 | 150 | 36385 | 8403 | 23.01 | 11247 | 9318 | 7390 | 8430 | | | 410.3 | 1.009 | 1.000 |
| C20 | | 3.095 | 150 | 35720 | 6950 | 19.03 | 11247 | 9377 | 7454 | 7642 | | | 415.8 | 1.034 | 1.026 |
| | | | | | 6951 | 19.03 | | | | | | | 426.1 | 1.009 | 1.001 |
| | | | | | 6952 | 19.03 | | | | | | | 428.9 | 1.003 | 0.994 |
| | | | | | 6959 | 19.05 | | | | | | | 435.6 | 0.987 | 0.979 |
| C42 | | 3.095 | 150 | 35639 | 5803 | 15.89 | 16565 | 7619 | 8126 | 3329 | | | 442.3 | 0.991 | 0.983 |
| | | | | | 5804 | 15.89 | | | | | | | 448.4 | 0.978 | 0.970 |
| D27 | | 3.252 | 150 | 39676 | 7669 | 21.00 | 9510 | 12889 | 9267 | 8010 | | | 456 | 0.991 | 0.983 |
| D38 | | 3.252 | 150 | 39403 | 8005 | 21.92 | 6367 | 9331 | 7358 | 8701 | 7646 | | 442.4 | 1.001 | 0.992 |
| E38 | | 3.199 | 150 | 33973 | 7999 | 21.90 | 7568 | 8458 | 9879 | 8068 | | | 376.3 | 0.995 | 0.984 |
| | | | | | 8000 | 21.90 | | | | | | | 374.3 | 1.000 | 0.989 |
| E40 | | 3.199 | 150 | 34339 | 8075 | 22.11 | 7705 | 7249 | 10655 | 8730 | | | 381.2 | 0.992 | 0.982 |
| F14 | | 3.197 | 150 | 34009 | 7722 | 21.14 | 5069 | 10755 | 9898 | 8287 | | | 381.8 | 1.003 | 0.992 |
| F21 | | 3.197 | 150 | 36273 | 7376 | 20.19 | 4767 | 6317 | 10046 | 8255 | 6888 | | 420.9 | 0.992 | 0.982 |
| F25 | | 3.197 | 150 | 35352 | 7725 | 21.15 | 8307 | 10749 | 8316 | 7980 | | | 396.7 | 1.011 | 1.000 |
| F32 | | 3.197 | 150 | 50962 | 5860 | 16.04 | 10553 | 10609 | 8391 | 7761 | 6629 | 7019 | 692 | 0.994 | 0.990 |
| G11 | | 3.188 | 150 | 35463 | 6990 | 19.14 | 6890 | 10422 | 7868 | 6943 | 3340 | | 416.3 | 0.992 | 0.982 |
| G23 | | 3.206 | 150 | 35633 | 6984 | 19.12 | 10268 | 10035 | 7618 | 7712 | | | 420.7 | 0.996 | 0.986 |
| I09 | | 3.203 | 150 | 40188 | 5849 | 16.01 | 6727 | 8950 | 9065 | 7568 | 7878 | | 507.9 | 1.011 | 1.003 |
| I20 | | 3.203 | 150 | 34313 | 6588 | 18.04 | 8300 | 9010 | 9108 | 7895 | | | 403.5 | 0.987 | 0.976 |
| I24 | | 3.203 | 150 | 34294 | 6601 | 18.07 | 8245 | 8967 | 9144 | 7938 | | | 410 | 0.983 | 0.972 |
| I25 | | 3.203 | 150 | 36859 | 6198 | 16.97 | 5207 | 4991 | 9803 | 8998 | 7860 | | 445.8 | 1.000 | 1.000 |
| Mean and Standard Deviation of C/E values | | | | | | | | | | Ringhals 3 | | | | 0.990 ± 0.012 | 0.979 ± 0.010 |
| | | | | | | | | | | Ringhals 2 | | | | 0.999 ± 0.012 | 0.990 ± 0.012 |
| | | | | | | | | | | Combined | | | | 0.995 ± 0.013 | 0.985 ± 0.012 |

***Table 4.*** *Expected decay heat biases and uncertainty from JEFF-3.1.1 FISPIN calculations.*

| Cooling time (Years unless stated) | Shutdown | 3 days | 5 | 10 | 15 | 20 | 25 | 30 | 100 | 1000 | 50000 | $10^5$ | $10^6$ |
|---|---|---|---|---|---|---|---|---|---|---|---|---|---|
| Expected bias (%) | 0.26 | 0.74 | -0.31 | 0.50 | 0.27 | 0.23 | 0.35 | 0.62 | 7.32 | 12.35 | 7.05 | 5.07 | -8.59 |
| Expected uncertainty (%) | 93.5 | 49.4 | 4.8 | 4.8 | 4.7 | 4.6 | 4.4 | 4.3 | 4.8 | 5.8 | 6.3 | 5.0 | 4.9 |

# Fission reaction data at intermediate energies: measurement techniques

*I.V. Ryzhov*

Khlopin Radium Institute, 2nd Murinski pr. 28, 194021 St. Petersburg, Russia
ryzhov@khlopin.ru

***Abstract:*** A review is presented of recent experimental works on intermediate-energy neutron-induced fission. The emphasis is placed on the experiments carried out at the TSL, LLN and GNEIS neutron beam facilities. Experimental setups dedicated to measurements of neutron-induced fission cross-sections as well as to measurements of fission fragment mass distributions are considered. Technical aspects of using the experimental setups at the neutron beams with quasi-monoenergetic and "white" spectra are discussed. A strategy is outlined for further experiments in this field.

## Introduction

Over the past ten years a large body of experimental research has been focused on neutron-induced fission at so-called intermediate energies, i.e. in the range from 20 to 200 MeV. A motivation of this activity stems from the nuclear data needs for accelerator-driven systems (ADS), which address such problems as transmutation of nuclear waste, energy amplification, incineration of weapon plutonium, etc. Feasibility studies for ADS require the fission reaction data for a wide set of nuclides ranging from tungsten to heavy actinides. A comprehensive measurement of these data is a challenge for the nuclear research community, so it is not surprising that teamwork through international collaborations became a necessity. The present paper makes an attempt to review a series of fission experiments carried out by Khlopin Radium Institute and Petersburg Nuclear Physics Institute in collaboration with Uppsala University and Université Catholique de Louvain. The experimental campaign has been performed at neutron beams of the The Svedberg Laboratory (TSL), of the Louvain-la-Neuve (LLN) cyclotron facility CYCLONE, and of the neutron time-of-flight spectrometer GNEIS (PNPI). The investigated nuclides, the data measured and the covered energy ranges are summarized in Table 1 together with the neutron beam facilities, the detector setups, and the monitor reactions used. All the measurements have been carried out making use of various multi-section ionization chambers (MIC), and thin-film breakdown counters (TFBC). The emphasis in this paper is placed on MIC's including Frisch-gridded (MFGIC) and parallel plate ionization chambers whereby the most data have been obtained.

***Table 1.*** *Overview of the experimental campaign*

| Target nuclide | Data measured | Energy range MeV | Facility | Detector setup | Monitor reaction |
|---|---|---|---|---|---|
| $^{181}$Ta | σ (n,f) | 94-174 | TSL | TFBC | $^{209}$Bi(n,f) |
| $^{182,183,184,186,\ nat}$W | σ (n,f) | 45-175 | TSL | MIC(mini),TFBC | $^{209}$Bi(n,f) |
| $^{nat}$W | σ (n,f) | 66-200 | GNEIS | MIC (large) | $^{235}$U(n,f) |
| $^{205}$Tl | σ (n,f) | 33-175 | LLN,TSL | MFGIC,TFBC | $^{238}$U(n,f) |
| $^{196}$Au | σ (n,f) | 65-160 | TSL | TFBC | $^{209}$Bi(n,f) |
| $^{204,206,207,208,\ nat}$Pb | σ (n,f) | 33-175 | LLN,TSL | MFGIC, TFBC | $^{238}$U(n,f) |
| $^{nat}$Pb | σ (n,f) | 40-200 | GNEIS | MIC(large) | $^{235}$U(n,f) |
| $^{209}$Bi | σ (n,f) | 33-175 | LLN,TSL | MFGIC, TFBC | $^{238}$U(n,f) |
| $^{209}$Bi | σ (n,f) | 27-200 | GNEIS | MIC (large) | $^{235}$U(n,f) |
| $^{232}$Th | σ (n,f) | 1-200 | GNEIS | MIC (large) | $^{235}$U(n,f) |
| $^{233}$U | σ (n,f) | 1-200 | GNEIS | MIC (large) | $^{235}$U(n,f) |
| $^{238}$U | σ (n,f) | 1-200 | GNEIS | MIC (large) | $^{235}$U(n,f) |
| $^{237}$Np | σ (n,f) | 1-200 | GNEIS | MIC (large) | $^{235}$U(n,f) |
| $^{239}$Pu | σ (n,f) | 1-200 | GNEIS | MIC (large) | $^{235}$U(n,f) |
| $^{240}$Pu | σ (n,f) | 1-200 | GNEIS | MIC (large) | $^{235}$U(n,f) |
| $^{243}$Am | σ (n,f) | 1-200 | GNEIS | MIC (large) | $^{235}$U(n,f) |
| $^{232}$Th | FFY | 30-60 | LLN | MFGIC | - |
| $^{238}$U | FFY | 30-60 | LLN | MFGIC | - |

## Detector setups for the (n, f) cross section measurements

### Typical background problems

Ionization chambers, in general, are well suited to the (n,f) cross section measurements at intermediate energies. These detectors allow neutron TOF measurements with a time resolution of 1-5 ns and have almost 100% efficiency for fission fragment detection. In addition, the detector sensitivity can be increased, if necessary, using multi-section assemblies and (or) large fissile targets. At the same time, there some background problems related to features of both ionization chambers and neutron beam facilities. The first problem is an overlap between energy deposition spectra of fission fragments and other charged particles (CPs). The latter are produced by energetic neutrons in upstream materials and by heavy target nuclei decaying spontaneously by alpha emission. The "overlap" problem becomes especially complicated for short-lived alpha emitters as well as for light nuclei characterized by small fission cross sections and low fission fragment energies.

The other problem is typical for measurements at the GNEIS facility where each neutron burst is accompanied by an intense gamma flash. The gamma flash results in a baseline distortion that complicates a threshold discrimination against the CPs and electronic noise.

Finally, the measurements at pulsed neutron sources with short micropulse spacing (TSL, LLN) suffer from so-called wraparound background caused by slow neutrons arriving at the detector simultaneously with fast neutrons from the next micropulses. In the presence of the wrap-around neutrons the measured TOF distributions have a frame–overlapping structure that prevents a proper TOF analysis of fission events. In what follows several ways to mitigate the background problems are illustrated by the example of the detector setups developed.

### A miniature MIC

A new TSL facility placed in operation in 2003-2004 offers an additional "parasitic" irradiation position with increase in neutron flux, but at the cost of limited size of irradiated objects. To measure the (n,f) cross sections of W relative to Bi a miniature MIC has been developed (see the left part of Fig. 1). The detector holds up to 17 double-sided fissile targets (with a diameter of 22 mm) deposited on 300 μm thick aluminum backings. A blank section (without a fissile sample) has been used to measure a shape of the background due to the CPs and gamma radiation. The background subtraction is shown at the right of Fig. 1.

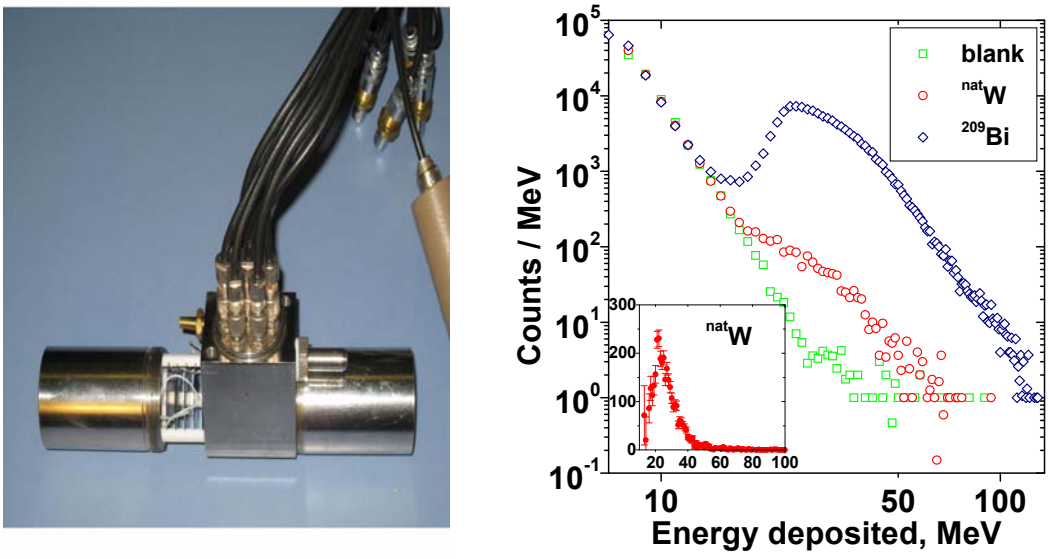


***Figure 1.*** *Left: a picture of a miniature MIC used at a "parasitic" irradiation position at the new TSL facility. Right: energy deposition spectra measured with the miniature MIC.*

### A multi-section Frisch-gridded ionization chamber (MFGIC)

A Frisch-gridded ionization chamber permits both pulse height (PH) and so-called angular discrimination against the background particles. In Fig 2 a MFGIC used for the (n,f) cross section measurements at the TSL and LLN neutron beams is shown. The electrode assembly of the MFGIC consists of seven sections. Each section comprises two gridded ionization

chambers with a common cathode. The fissile materials ($^{205}$Tl, $^{204, 206, 207, 208}$Pb, $^{209}$Bi, and $^{nat}$U) were deposited by thermal vacuum evaporation on both sides of each cathode. A detailed description of the detector setup and the electronic equipment is given elsewhere [1]. The left part of Fig. 3 shows a scatter plot of PH of cathode signal versus PH of anode signal that elucidates the discrimination techniques. A result of the angular discrimination against the CPs is also given in Fig. 3 (the right part).

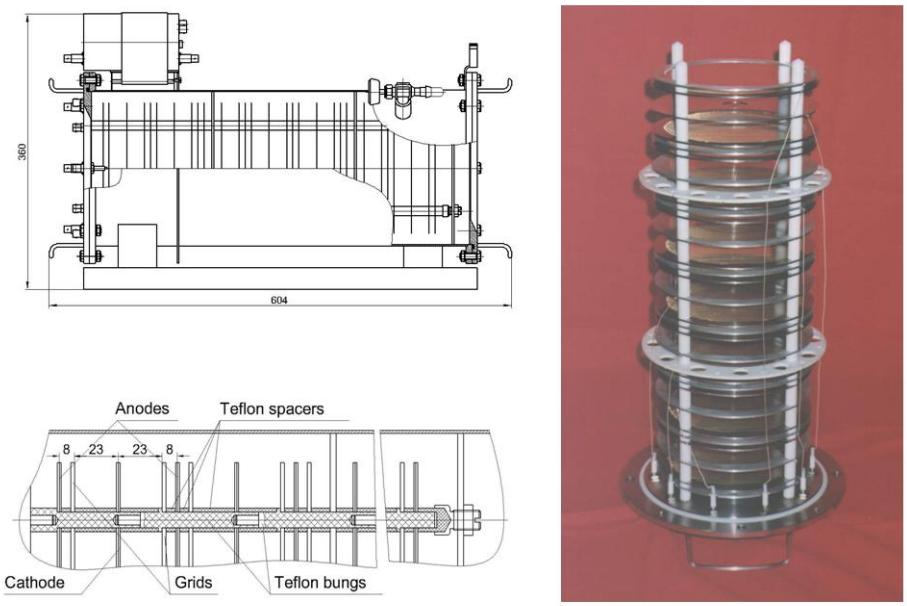


***Figure 2.*** *Cross section views (left) and picture (right) of the MFGIC.*

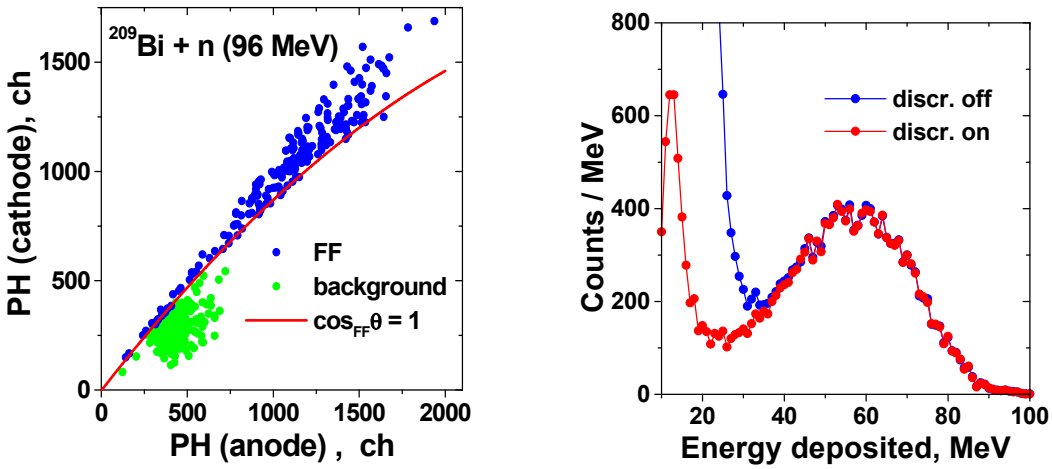


***Figure 3.*** *PH of cathode signal vs PH of anode signal (left) and energy deposition spectra (right) with (red) and without (blue) the angular discrimination against the CPs.*

**A large-sized MIC**

To take full advantage of neutron beam at the GNEIS facility the large sized MICs were used for the (n,f) cross section measurements [2,3]. All targets (see Table 1) were 180mm in diameter and deposited on one side of the 50 μm thick Al backing. Most of the targets were 150-550 μg/cm$^2$ thick with the exception of $^{240}$Pu and $^{243}$Am. The latter were 5-7 μg/cm$^2$ thick only. The use of flash ADCs made it possible to handle multiple events from each neutron burst. In addition, the digital signal processing allowed for an identification of fission events against the background of CPs and electronic noise in the present of the baseline distortion caused by an intense gamma flash. An example of the waveforms and the pulse height spectra obtained is shown in Fig. 4.

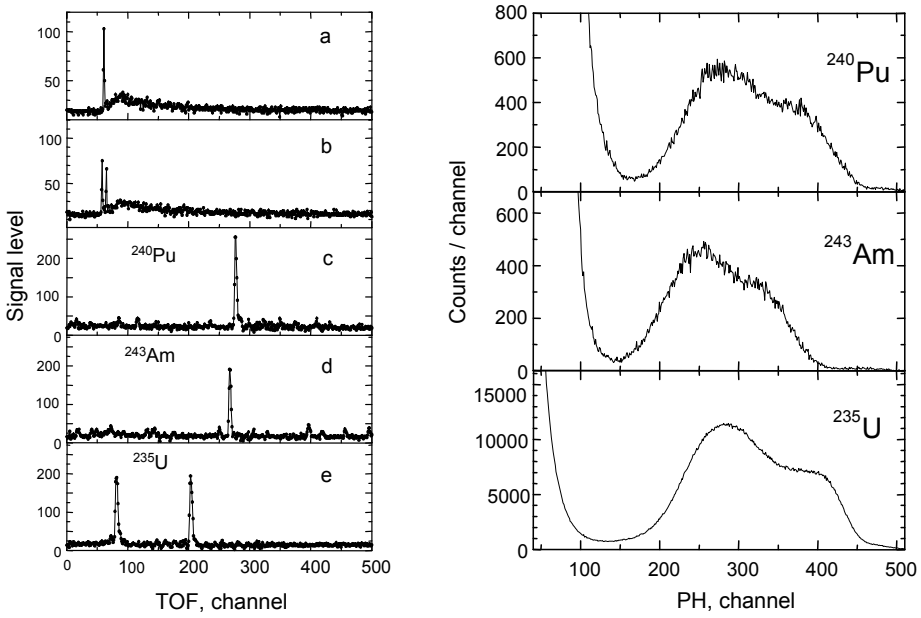


***Figure 4.*** *Left: waveforms of a gamma flash detector (a,b) and of the MIC (c,d,e), the channel width is 10 ns. Right: pulse height spectra obtained for the fissile targets with a high specific radioactivity.*

**Parallel plate avalanche counters (PPACs)**

Whenever feasible, detection of both fission fragments in coincidence and measurement of their kinetic energies should be done to attain the best discrimination against the CPs. This approach has recently been implemented in the (p,f) cross section measurements at the PNPI synchrocyclotron [4]. The experimental setup consisted of six detecting assemblies. Each assembly comprised two PPACs and a thin fissile target placed in between them. The right part of Fig. 5 shows a 2D amplitude distribution of the coinciding events detected by the PPACs for proton-induced fission of $^{238}$U at 1 GeV. One can see that a correlation analysis of these events allows rejection of almost all the background events.

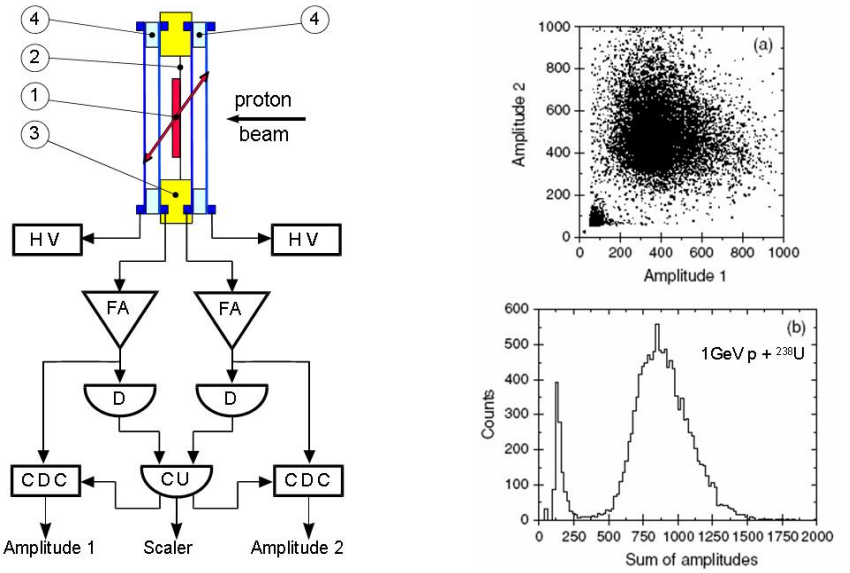


***Figure 5.*** *Left: fission fragment registration with PPACs. 1 - target; 2 - backing; 3 - target support; 4 -PPAC; HV - high voltage; FP- fast amplifier; D - discriminator; CU - coincidence unit; CDC - charge-to-digital converter. Right (a): an amplitude scatterplot of the coinciding events. Right (b): distribution over the sum of the amplitudes.*

## Detector setups for measurements of fragment mass yields

### A MFGIC

Pre-neutron emission fragment mass yields have been recently measured for the $^{232}$Th(n,f) and $^{238}$U(n,f) reactions in the energy range 30-60 MeV . The measurements have been carried out at quasi-monoenergetic neutron beam of the LLN accelerator facility making use of a MFGIC similar to that described in [1]. A measured time distribution of fission events relative to the RF signals (see Fig. 6) reveals that fission events induced by wrap-around neutrons can not be rejected by imposing a cut on the time intervals. A time distribution simulated by a Monte-Carlo folding of the fission cross section [5] with the neutron spectrum [6] is also shown. In the right part of Fig. 6 a pre-neutron emission fragment mass distribution measured for the peak neutrons is shown along with the distributions from low-energy fissions falling into the same time cut. For the sake of simplicity, the "background" distributions have been shaped using the Wahl systematics [6].

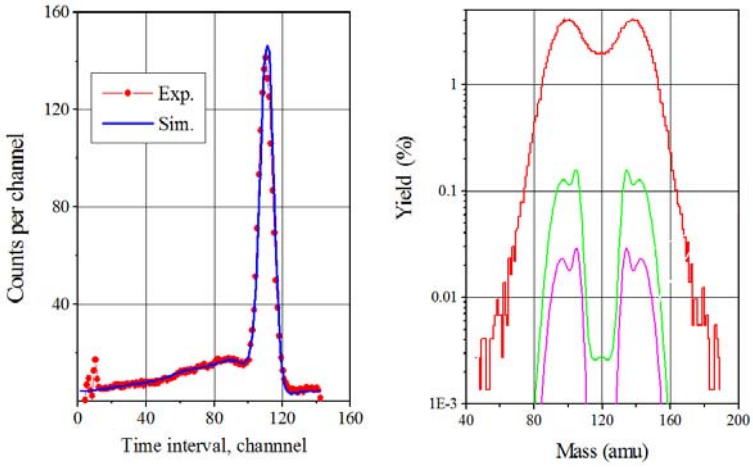


***Figure 6.*** *Left: measured and simulated TOF spectra of fission events for the $^{238}$U(n,f) reaction induced by quasi-monoenergetic neutrons with peak energy of 32.8 MeV. Right: pre-neutron emission fragment mass distribution measured for the peak neutrons (red) and the "background" distributions from the wrap-around neutrons.*

### Time-of-flight spectrometer of fission fragments

A recently developed TOF spectrometer of fission fragments is shown in Fig. 7. The E,V method is applied to measure the post-neutron emission fragment mass yields for two thick targets.

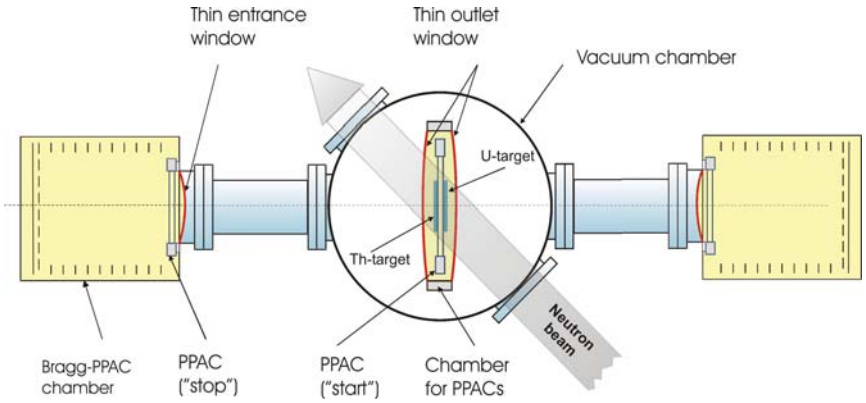


***Figure 7.*** *Schematic drawing of the TOF spectrometer of fission fragments.*

The targets are deposited onto electrodes of the central PPAC. When a binary fission happens, one of the fragments is instantly detected by the central PPAC providing a "start" signal with a time resolution of about 300 ps (FWHM). The other fragment travels in vacuum a distance of 50 cm and arrives at the Bragg-PPAC hybrid detector which is a wide-aperture ionization chamber housed in a common value with a thin PPAC. The hybrid detector provides a "stop" signal and the energy of the second fragment. Testing experiments with the TOF spectrometer are under way.

## Outlook

The detector setups developed and the experience accumulated open up possibilities for new measurements of the fission reaction data at intermediate energies. At this point it should be remarked that a commercialization of the TSL accelerator facility will result in a limitation of this sort of experiments for the years to come. Moreover, the TSL destiny after 2011 is uncertain. Because of this, the most part of the collaborative activity could be connected with the GNEIS and LLN facilities. In summer 2008, the PPACs and the MFGIC were tested at the GNEIS facility making use of the data acquisition system based on commercially available 8 bit, 500 MHz flash ADCs for the signal treatment. It was concluded that the PPACs can be efficiently used for measurement of the (n,f) cross sections of actinides with $T_{1/2} \geq 10^4$ yr in the energy range 1-200 MeV. It was also found that a twin ionization chamber with Frisch grids being used at the GNEIS facility provides a means for measurements of fission fragment mass yields for actinides with $T_{1/2} \geq 2 \cdot 10^6$ yr at neutron energies at least up to 100 MeV. To make good use of the TOF spectrometer of fission fragments, the neutron beams with a fluence rate not less than $10^7$ $s^{-1}cm^{-2}$ are necessary. At the same time, the TOF spectrometer permits measuring of fragment mass yields in proton-induced fission in the energy range 200 -1000 MeV covered by the PNPI accelerator.

**Acknowledgements**
The greater part of the experimental activity reviewed in this paper was supported by International Science and Technology Center (projects nos. 609, 1309, 1405, 1971, 2213 and 3192). Measurements of fragment mass yields at the LLN neutron beam facility were supported by the European Commission within the Sixth Framework Programme through I3-EURONS (contract no. RII3-CT-2004-506065).

**References**

[1] I.V. Ryzhov, G.A. Tutin, A.G. Mitryukhin, V.S. Oplavin, S.M. Soloviev, J. Blomgren, P . U. Renberg, J.P. Meulders, Y.El Masri, Th. Keutgen, R. Prieels and R. Nolte, “Measurements of neutron-induced fission cross sections of $^{205}$Tl, $^{204, 206, 207, 208}$Pb and $^{209}$Bi with a multi-section Frisch-gridded ionization chamber”, Nucl. Instrum. and Meth. A562, 439 (2006).

[2] O.A. Shcherbakov, A.Yu. Donets, A.V. Evdokimov, A.V. Fomichev, T. Fukahori, A. Hasegawa, A.B. Laptev, V.M. Maslov, G.A. Petrov, S.M. Soloviev, Yu.V. Tuboltsev, A.S. Vorobyev, "Neutron-Induced Fission of $^{233}$U, $^{238}$U, $^{232}$Th, $^{239}$Pu, $^{237}$Np, $^{nat}$Pb and $^{209}$Bi Relative to $^{235}$U in the Energy Range 1-200 MeV", Proc. Int. Conf. on Nuclear Data for Science and Technology, October 7-12, 2001, Tsukuba, Ibaraki, Japan. J. Nucl.Sci.and Tech., Suppl.2, v.1, 2002, pp.230-233.

[3] A.B. Laptev, A.Yu. Donets, A.V. Fomichev, A.A. Fomichev, R. Haight, O.A. Shcherbakov, S.M. Soloviev, Yu.V. Tuboltsev, A.S. Vorobyev, “Neutron-induced fission cross sections of $^{240}$Pu, $^{243}$Am and $^{Nat}$W in the energy range 1-200 MeV”, Proc. Int. Conf. on Nuclear Data for Science and Technology, September 26-October 1, 2004, Santa Fe, New Mexico, USA. Editors: R. Haight, M. Chadwick, T. Kawano, P. Talou, AIP Conf. Proc., Vol. 769, Melville, New York, 2005, Part 1, pp.865-869.

[4] A.A. Kotov, L.A. Vaishnene, V.G. Vovchenko, Yu.A. Gavrikov, V.V. Poliakov, M.G. Tverskoy, O.Ya. Fedorov, Yu.A. Chestnov, A.I. Shchetkovskiy, A.V. Shvedchikov, A.Yu. Doroshenko, T. Fukahori, “Energy dependence of proton induced fission cross sections for heavy nuclei in the energy range 200–1000 MeV”, Phys. Rev. C 74, 034605 (2006).

[5] ENDF/B-VI; A.D. Carlson, S. Chiba, F.-J. Hambsch, A.N. Smirnov, “Update to nuclear data standards for nuclear measurements”, Proc. Int. Conf. on Nuclear Data for Science and Technology, May 9-13, 1997, Trieste, Italy, Bologna, IPS, 1997, part II, pp.1223-1229.

[6] H. Schuhmacher, H.J. Brede, V. Dangendorf, M. Kuhfuss, J.P. Meulders, W.D. Newhauser, R. Nolte, “Quasi-monoenergetic neutron beams with energies from 25 to 75 MeV”, Nucl. Instrum. and Meth. A 421, 284 (1999).

[7] A.C. Wahl, “Systematics of Fission-Product Yields”, Los Alamos National Laboratory report LA-13928 (2002).

# High resolution neutron cross section measurements on $^{241}$Am

*C. Sage[1,2,3,4], A. Borella[1], C. Brossard[5], O. Bouland[3,6], A. Fernandez[5], F. Gunsing[2], M. Holzhäuser[5], R. Jaime Tornin[1], S. Kopecky[1], C. Nästren[5], G. Noguère[3], H. Ottmar[5], A.J.M. Plompen[1], P. Schillebeeckx[1], V. Semkova[1], P. Siegler[1], J. Somers[5], F. Wastin[5]*

1) European Commission, Joint Research Centre, Institute for Reference Materials and Measurements, Retieseweg 111, B-2440 Geel, Belgium
2) CEA Saclay, DSM/IRFU/SPhN, F-91191 Gif-sur-Yvette, France
3) CEA Cadarache, DEN/CAD/DER/SPRC/LEPh, F-13108 St-Paul-lez-Durance, France
4) IPHC Strasbourg, IN2P3, F-67037 Strasbourg, France
5) European Commission, Joint Research Centre, Institute for Transuranium elements, Postfach 2340, D-76125 Karlsruhe, Germany
6) Los Alamos National Laboratory, T-2 group, theoretical division, NM 87545, USA

christophe.sage@cea.fr

***Abstract:*** An extensive programme of measurements of several neutron induced reactions on $^{241}$Am is being carried out at the JRC-IRMM in the frame of a collaboration between the JRC and French laboratories from CNRS and CEA. Raw material coming from the Atalante facility of CEA Marcoule has been transformed by JRC-ITU Karlsruhe into suitable $^{241}AmO_2$ samples embedded in $Al_2O_3$ and $Y_2O_3$ matrices. They were specifically designed for activation and time-of-flight measurements.
The $^{241}$Am(n,2n)$^{240}$Am reaction cross section was measured at the 7 MV Van de Graaff accelerator using the activation technique. The irradiations were performed in four sessions, using quasi mono-energetic neutrons with energies ranging from 8 to 21 MeV produced via the D(d,n)$^3$He and the T(d,n)$^4$He reactions. For the first time, these measurements allowed the experimental investigation of the $^{241}$Am(n,2n) reaction cross-section above 15 MeV. The induced activity was measured off-line after the irradiation by standard gamma-ray spectrometry using a high purity germanium detector.
A different sample of the same isotope has been measured in transmission experiments in the resonance region at the neutron time-of-flight facility Gelina. These experiments were performed during two measurement campaigns, the second one after a recent upgrade of the data acquisition system. Finally, a capture experiment in the resonance region is currently ongoing, also at Gelina.
This paper will describe the results of the (n,2n) measurement campaign, compared with previously existing data and the current evaluated data libraries JEFF-3.1, BROND-2.2, JENDL-3.3 and ENDF/B-VII, as well as some preliminary results from the transmission measurements.

## Introduction

Very precise neutron-induced reaction cross-section data are required for many practical applications, especially to predict reliably the behaviour of reactor cores in both present fission and future fusion reactors. The present evaluated data files of $^{241}$Am do not fulfil these requirements, and an ambitious programme of measurements has been developed to address two of the problems encountered in these files.
Only a few measurements on the $^{241}$Am(n,2n) reaction exist, most of them obtained at neutron energies around 14 MeV [1-3], with another recent set of measurements going from the threshold up to 14 MeV [4]. These data reveal huge discrepancies and none of them are going above 15 MeV. Moreover, the evaluations show a large spread in the predicted excitation function [5] (see Fig. 1a). Thus, measurements of this reaction cross section were performed at the 7 MV Van de Graaff accelerator at JRC-IRMM using the activation technique.
The second problem to be looked at concerns the resonance parameters of the low energy

americium resonances, as it has been observed that the resonance integral as calculated from the resonance parameters of the evaluated data files is smaller than the value determined by integral measurements. The evaluations for the lowest resonances are based essentially on three measurements (Adamchuck [6], Belanova [7,8], Slaughter [9]) like for instance JEFF3.1 [10]. As already observed and mentioned by O. Bouland [11], the agreement for the lowest resonances between Adamchuck et al., and Belanova et al. are satisfactory, neglecting a small shift in the energies of the lowest resonance, but the results by Slaughter et al. are different (see Fig. 1b). The peak cross sections of the resonances are about 30% higher than for the two other measurements. The cross sections as suggested in the evaluation are typically somewhere in between those two curves. To explain these rather large discrepancies, the influence of the sample properties when powder materials are used is under investigation. Therefore, a set of transmission and capture measurements using a novel sample type have been performed at GELINA, the white neutron source at JRC-IRMM.

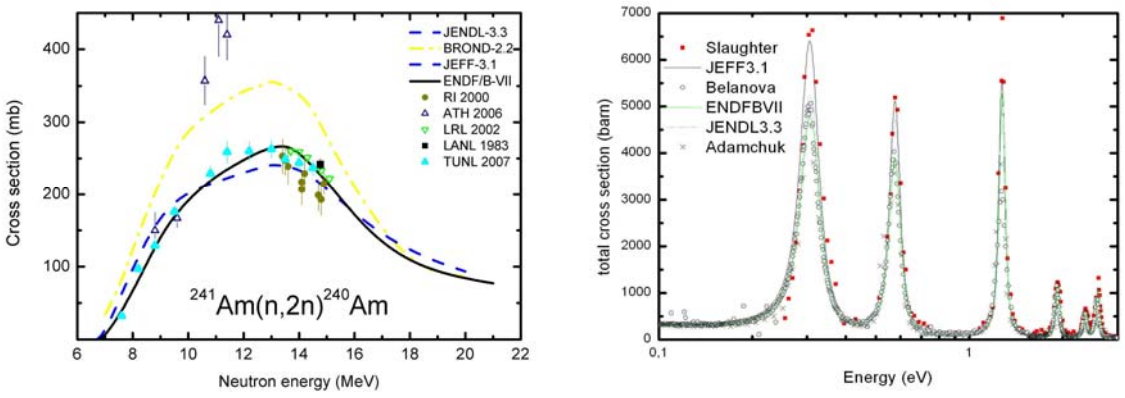


***Figure 1.*** *a) Status of the (n,2n) cross section data and evaluations.*
*b) Status of the total cross section data and evaluations.*

## Activation measurements

### Samples and experimental procedure

The samples were prepared by a method especially developed for this present study by JRC-ITU. This method is based on the production of porous alumina granules by powder metallurgy. The americium (originally provided by CEA) was then introduced into the porous particles by infiltration of the nitrate solution. Following drying to eliminate water, and calcination to convert to oxide, the resulting powder was pressed into pellets of 12 mm diameter and 2 mm thickness. The samples' weight is in average 400 mg and the average americium content is 40 mg. The americium-alumina material was then encapsulated into aluminium containers. The samples' geometries were examined by X-ray radiography and the Am content determined by calorimetry. The mass of $^{241}$Am in the samples was determined by γ-spectrometry at IRMM as well and the results agree within 2% uncertainty.

Three sets of irradiations were performed. For the first one, we used the $^{2}$H(d,n)$^{3}$He reaction on a deuterium gas target for the production of quasi mono-energetic neutrons with energies of 8.8 and 9.4 MeV. The two other experiments, determining for the first time the reaction cross section above 15 MeV, used quasi mono-energetic neutrons with energies between 13.4 and 20.7 MeV produced via the $^{3}$H(d,n)$^{4}$He reaction, employing a solid-state Ti/T target (2 mg/cm$^{2}$ thick) on a silver backing (0.4 mm thick).

The samples, each sandwiched between monitor foils, were placed at 0° relative to the incident neutron beam and at 2 cm distance from the target. During the irradiation, a long counter was used to record the time profile of the neutron flux in order to correct for the flux fluctuation.

The neutron energy and yield distributions as a function of deuteron energy and emission angle were calculated using the program EnergySet [12], and the fluence rate was determined relative to the $^{27}$Al(n,α)$^{24}$Na reaction. To account for the contribution of low energy neutrons, various dosimetry reactions with different energy thresholds were used, such as $^{115}$In(n,n')$^{115}$In, $^{58}$Ni(n,p)$^{58}$Co, $^{27}$Al(n,p)$^{27}$Mg, $^{56}$Fe(n,p)$^{56}$Mn and $^{93}$Nb(n,2n)$^{92m}$Nb, combined with results from previous time-of-flight spectrum measurements.

**Activity measurement**

After the irradiation, the induced activity was measured off-line by standard γ-ray spectrometry using a high-purity germanium detector. The data acquisition was controlled by the Maestro system supplied by Ortec, and the γ-ray spectra were analysed using the software package Genie2000 of Canbera. The decay data for both $^{241}$Am and $^{240}$Am used for the data analysis were taken from the Nuclear Data Sheets.

A Pb/Sn/Cu shielding was used to reduce the important natural activity from the $^{241}$Am decay in order to limit the dead time of the system to less than 10%. The detector was additionally shielded from the side with a 10 mm Cu cylinder to avoid detection of scattered gamma rays. It was found out that among the two most intensive gamma lines from $^{240}$Am, at 888.8 and 987.8 keV, the first one was contaminated by the $^{241}$Am natural activity, but the region around the second one was free from such background activity.

The efficiency of the detection setup was determined by Monte Carlo simulation using the MCNP5 code. The cross sections were calculated using the activation formula. Corrections were applied for the detection efficiency, irradiation and measurement geometry, neutron flux fluctuation and secondary neutrons.

**Results and discussion**

The experimental results of this work are shown in Fig. 2. Our results agree within the uncertainty limits with the results obtained at TUNL in 2007 and with the ENDF/B-VII evaluation above 16 MeV, which is remarkable given the fact that this latter was based on knowledge about the data at 14 MeV only. Thus, the experimental data above 16 MeV provide a valuable test for the preequilibrium modelling in the presence of fission.

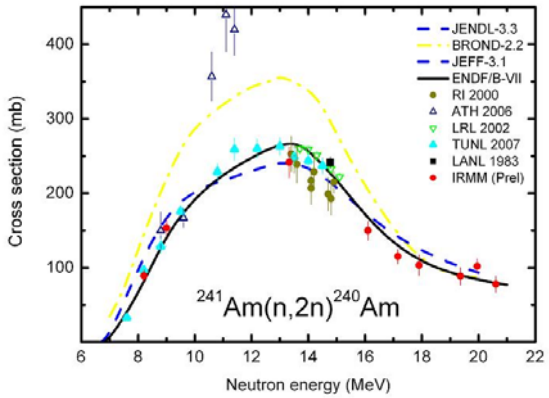


***Figure 2.*** *Experimental $^{241}$Am(n,2n) cross sections obtained at IRMM compared with previous data and evaluations.*

## Transmission measurements

One sample (22 mm diameter and 3.3 mm thickness) based on an $Y_2O_3$ matrix was infiltrated with 325 mg of $^{241}$Am oxide, providing an equal distribution of Am over the whole sample size. The characteristics of this sample, prepared at JRC-ITU like the other ones for the activation measurements, were determined in the same way as previously described.

The measurements were performed at GELINA, the white neutron source of JRC-IRMM, which is a linear electron accelerator that accelerates electrons up to 150 MeV. The electron pulses had a duration of approximately 1 ns, and the used repetition rate was 50 Hz. The chosen flight path length was 26.44 m and the beam diameter was limited to about 1.5 cm using a combination of Li-carbonate, Cu and Ni collimators. The sample was positioned at a distance of around 10 m halfway between the neutron target and the detector system, which was a 0.5 inch thick and 4 inch diameter Li-glass scintillator, viewed by two photomultipliers tubes. To reduce the impact of a variation of the neutron flux on the measured transmission, measurements of the sample and open beam were cycled every twenty minutes.

To derive the transmission from the registered data, the software package AGS [13] was used. This code performs the most important corrections, such as dead time, background subtraction, normalisation, etc. with a full propagation of the covariance matrix, starting with the uncorrelated statistical uncertainties of the counting statistics. The background is

estimated with the black resonance technique, i.e. filters are inserted into the beam, removing all the neutrons at a given energy.
The transmission was determined and analyzed using the resonance shape analysis code Refit [14]. Fig. 3 shows a preliminary result of such a shape analysis, compared to the transmission determined with the resonance parameters given in ENDF/B-VII, JEFF3.1 and JENDL. All three evaluations seem to underestimate the cross sections, but final results will only be obtained after a simultaneous analysis of the transmission and capture data.

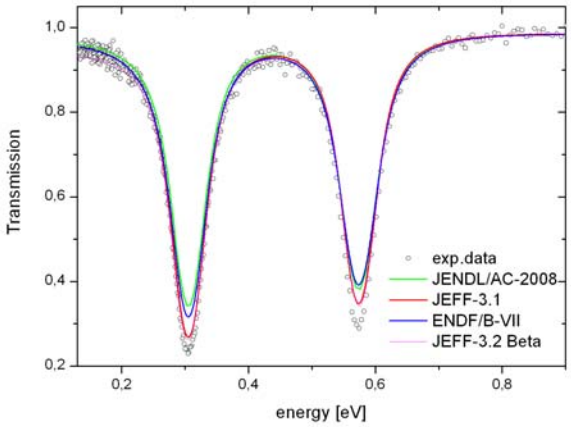


***Figure 3.*** *Experimental transmission data compared to different evaluations.*

## Conclusions

The consistency of our $^{241}$Am(n,2n) experimental points with other recent experimental data was shown for neutron energies below 14 MeV. The present work is the first to report results above 15 MeV, where a remarkable agreement was obtained with the model calculations of ENDF/B-VII.
The preliminary results of the transmission experiment for the first resonances show a probable underestimation of the capture cross section (and hence of the total cross section) by the various evaluations. Further capture experiments are ongoing, and once both types of measurements completed, the results of a detailed resonance shape analysis can be used as a basis for a new evaluation.

**References**

[1] A. A. Filatenkov and S. V. Chuvaev, Phys. At. Nucl. 63, 1504 (2000).
[2] R. W. Lougheed, W. Webster, M. N. Namboodiri, D. R. Nethaway, K. J. Moody, L. H. Landrum, R. W. Hoff, R. J. Dupzyk, J. H. McQuaid, R. Gunnink, and E. D. Watkins, Radiochimica Acta 90, 833 (2002).
[3] G. Perdikakis, C T. Papadopoulos, R. Vlastou, A. Lagoyannis, A. Spyrou, M. Kokkoris, S. Galanopoulos, N. Patronis, D. Karamanis, Ch. Zarkadas, G. Kalyva, and S. Kossionides, Phys. Rev. C 73, 067601 (2006).
[4] A. Tonchev, C.T. Angell, M. Boswell et al., Phys. Rev. C 77, 054610 (2008).
[5] NNDC Online Data Service, ENDF database, http://www.nndc.bnl.gov/exfor7/endf00.htm (2008).
[6] Adamchuck Yu. V., Gerasimov V. F., Efimov B. V.et al., Proceedings of the first UN Conference on the Peaceful Uses of Atomic Energy, Geneva 1955, p. 216 and p. 259.
[7] Belanova T. S., Kolesov A. G., Nikolaev V. M. et al., Atom. Ener. 38, 33 (1974).
[8] Kalebin S., Artamonov V. S., Ivanov R. N. et al., Atom. Ener. 40, 373 (1976).
[9] Slaughter G. G., Harvey J. A., Block R. C., ORNL Report 3085, p. 42 (1961).
[10] Bouland O. and Bernard D., JEF-DOC-1086.
[11] Bouland O., JEF-DOC-931.
[12] G. Lövestam, EnergySet, EC-JRC-IRMM, private communication (2004).
[13] Bastian C., Borella A., Gunsing F., Heyse J ., Kopecky S., Noguère G., Siegler P., Schillebeeckx P., PHYSOR-2006 – American Nuclear Society's Topical Meeting on Reactor Physics (2006).
[14] Moxon M. C., Ware T. C., Dean C. J., REFIT-2007, UKNSF P216 (2006).

# New frontiers and challenges for statistical data adjustment methods

*M. Salvatores[1,2)], G. Palmiotti[2)], H. Abdel-Khalik[3)], M. Hermann[4)], H. Hiruta[2)], P. Oblozinsky[4)],*

1) CEA-Cadarache; France
2) Idaho National Laboratory, USA
3) North Carolina State University,USA
4) Brookhaven National Laboratory, Upton, NY 11973, USA
massimo.salvatores@cea.fr

## Introduction

Data adjustment (or data « assimilation ») techniques have been proposed in the past and widely used in the core and fuel cycle neutronics field (see e.g. Refs 1- 4 ), in order to provide best estimates and reduced uncertainty values for design parameters of nuclear reactor systems. Key ingredients of that approach are a) well quantified uncertainties and associated variance-covariance data; b) well documented, high accuracy and "representative" integral experiments; c) general sensitivity methods to produce sensitivity coefficients for a wide variety of different design parameters (core and fuel cycle).
The major drawback of these techniques is the potential limitation of the domain of application of the adjusted data and the fact the statistical adjustments are made on multigroup data, which means that both the multigroup structure and the code used to process the basic data file are significant constraints.
A method to overcome these potential difficulties is proposed. In fact, the classical statistical adjustment method can be improved to "adjust" physical parameters and not multigroup nuclear data. The objective is now to correlate the uncertainties of some basic parameters that characterize the neutron cross section description, to the discrepancy between calculation and experimental value for a large number of (existing) clean (i.e. well documented with high QA standards), high accuracy (i.e. with as low as possible experimental uncertainties and systematic errors) integral experiments.

**Use of integral experiments to reduce uncertainties on design parameters.**

The use of integral experiments and uncertainties (both experimental uncertainties and cross section covariance data), to improve the prediction of reference design integral parameters and to reduce the associated uncertainties:

- The „bias factor" method (one mock-up experiment available)
- Statistical cross section adjustments (i.e. a systematic experimental program is available, see e.g. Ref. 5)

Several variants have been proposed (notably in Japan by T. Takeda et al see Refs. 6-8), but they are substantially equivalent**.**

**The bias factor method**
Given a design reference system (ref) and an experimental mock-up (exp) of it, for a specific integral parameter $B_i$ one can define:

the reference calculated value: $B_{i,ref,c}$
the mock-up calculated value: $B_{i,exp,c}$
the mock-up experimental value: $B_{i,exp,e}$

The „bias factor"method tries to improve the prediction of the design reference system as follows:

$$B_{i,ref,c,improv} = B_{i,ref,c} \times (B_{i,exp,e}/B_{i,exp,c}) = B_{i,ref,c} \times f$$

and f is the bias factor
As for uncertainty on the integral parameter $B_i$ we have the following expressions:
a) if $S_{B,i,ref}$ is the sensitivity vector of integral parameter $B_i$ in the reference system to cross sections p and $B_p$ is the associated covariance matrix, then the „a priori“ variance of $B_{i,ref}$ is given by:

$$\mathbf{V(B_{i,ref}) = S^T_{Bi\,ref} B_p S_{Bi\,ref}}$$

b) in the case of the bias factor method (one mock-up experiment), we have

$$\mathbf{V(B_{i,ref,improv}) = (S^T_{Bi\,ref} - S^T_{Bi\,exp}) B_p (S_{Bi\,ref} - S_{Bi\,exp}) + V(E)}$$

where $S_{B,i,exp}$ is the sensitivity vector of integral parameter $B_i$ in the mock-up experiment and V(E) is the experimental uncertainty.

**The statistical adjustment method**
Data adjustment (or data « assimilation ») techniques have been proposed in the past and widely used in the core and fuel cycle neutronics field, in order to provide best estimates and reduced uncertainty values for design parameters of nuclear reactor systems.

Key ingredients of that approach are:
a) well quantified uncertainties and associated variance-covariance data;
b) well documented, high accuracy and “representative” integral experiments;
c) general sensitivity methods to produce sensitivity coefficients for a wide variety of different design parameters (core and fuel cycle).

If $B_p$ is the “a priori” nuclear data covariance matrix, $S_B$ the sensitivity matrix of the performance parameters $B_i$ (i=1…..I) to the J nuclear cross sections, the “a priori” covariance matrix of the performance parameters is given by:

$$B_B = S_B^T B_p S_B$$

It can be shown that, using a set of K integral experiments A, characterized by a sensitivity matrix $S_A$, besides a set of statistically adjusted cross-section data, a new (“a posteriori”) covariance matrix can be obtained:

where $B_A$ is the integral experiment uncertainty matrix.

## 2.3 Uncertainty reduction

The previous matrix can then be used to define a new (“a posteriori”) covariance matrix for the performance parameters B:

$$\begin{aligned}
&\tilde{B}_B = S_B^T \tilde{B}_p S_B = \{B_B - \\
&- S_B^T B_p S_A \left(S_A^T B_p S_A + B_A\right)^{-1} S_A^T B_p S_B\} = \\
&= B_B \{1 - (S_B^T B_p S_B)^{-1} (S_A^T B_p S_A + B_A)^{-1} \times \\
&\times (S_A^T B_p S_B)^2\}
\end{aligned}$$

From this expression, it results that in order to reduce the performance parameter „a priori“ uncertainties, the most effective integral experiments are those with „representative“ sensitivity profiles ($S_A \sim S_B$) and small experimental uncertainties ($B_A \sim 0$).

Moreover, one can use the same equation to understand the effectiveness of a data adjustment and its “extrapolability” to a set of different reference systems.
For this purpose, one has to introduce in the previous equation the sensitivity matrix of the design parameters (i=1, … , I ; n=1, … , N) of a set of N reference systems, to the J nuclear data as matrix $S_B$.

**Features of a recent of statistical data adjustment (Ref. 9)**
A recent example of the use of a statistical adjustment method in order to reduce the uncertainties of key design parameters has been reported in Ref. 9. With respect to numerous past adjustment studies, the study of Ref. 1 presents a number of significant features:

- Use of science-based correlation matrices
- A new large scale effort, focussed on innovative systems (core and fuel cycle), accounting for a wide international integral data base
- A better understanding of experiment « representativity », of the range of applicability and extrapolation of the adjusted data and of the residual uncertainties on design integral parameters
- A better understanding of the use of the outcome of the « adjustment » (e.g. a-posteriori correlations)
- Improved/redundant calculation methods for the analysis to avoid as far as possible systematic errors

Moreover, the selected integral experiments meet a series of requirements:

a) low and well documented experimental uncertainties;
b) enabling to separate effects (e.g., capture and fission);
c) allowing validating global energy and space dependent effects.

In particular, irradiation experiments have been used to cope with requirement b) and use of “representative experiments”, i.e. experiments that have close enough sensitivity coefficients with respect to the reference system, in order to comply with requirement c)
Finally, specific spatial effects are singled out with appropriate experiments (e.g. experiments with or without blankets)
This preliminary study was performed in four bands of energy: 20 MeV, 0.5 MeV, 67 keV, 2 keV. The results have been discussed in detail in Ref. 1. For the purpose of the present paper, we will discuss only one aspect, i.e. the a posteriori covariance matrix.

**A posteriori correlations**
An interesting feature of a statistical adjustment is the “a posteriori” covariance matrix that is associated both to the integral experiments and to the multigroup data after adjustment. In the specific case of the adjustment study documented in Ref. 9, the a posteriori correlations for the integral experiments (originally considered fully not-correlated), underline very plausible not-zero correlations among the criticality of experimental configurations with similar fuel compositions (i.e. similar U/Pu ratios) and significant correlations among irradiation experiments and criticality, in particular as anti-correlations between experiments allowing to measure the integral capture rate of U-238 and the criticality of configurations with a U/Pu ratio ~5 (Ref. 9).
As for the new correlation matrix associated to multigroup cross sections, apart from a significant decrease of most variance data, the adjustment method indicates some modifications of the original correlation coefficients that need a careful investigation. As examples, we show in Tables 1 and 2 both the original and the new correlation factors in the case of Pu-238 and of Pu-240 capture data.
In both cases very significant modifications are proposed, introducing in some cases anti-correlations instead of correlations, or even introducing inter-isotope and reaction correlations.

***Table 1.*** *New correlation coefficients for the Capture cross section of Pu-240 in energy groups 2,3 and 4. Original correlation coefficients are shown in parenthesis.*

| | $\sigma_c^2(\mathbf{Pu-240})$ | $\sigma_c^3(\mathbf{Pu-240})$ | $\sigma_c^4(\mathbf{Pu-240})$ | $\sigma_f^3(\mathbf{Pu-241})$ |
|---|---|---|---|---|
| $\sigma_c^2(\mathbf{Pu-240})$ | 1.0 | 0.53<br>(0.97) | -0.16<br>(0.0) | 0.29<br>(0.0) |
| $\sigma_c^3(\mathbf{Pu-240})$ | | 1.0 | -0.17<br>(0.0) | 0.32<br>(0.0) |
| $\sigma_c^4(\mathbf{Pu-240})$ | | | 1.0 | 0.0<br>(0.0) |

***Table 2.*** *New correlation coefficients for the capture cross section of Pu-238 in energy groups 2, 3 and 4. Original correlation coefficients are shown in parenthesis.*

| | $\sigma_c^2(\mathbf{Pu-238})$ | $\sigma_c^3(\mathbf{Pu-238})$ | $\sigma_c^4(\mathbf{Pu-238})$ |
|---|---|---|---|
| $\sigma_c^2(\mathbf{Pu-238})$ | **1.0** | **-0.24**<br>**(0.84)** | **-0.48**<br>**(0.67)** |
| $\sigma_c^3(\mathbf{Pu-238})$ | | **1.0** | **-0.32**<br>**(0.81)** |
| $\sigma_c^4(\mathbf{Pu-238})$ | | | **1.0** |

The new correlation factors as shown in these tables are probably related to the (very broad) multigroup energy structure used in that adjustment exercise. In any case, any new proposed correlation should be investigated carefully, in order to assess their reliability.

## A new frontier: the consistent method

The major drawback of the classical adjustment method is the potential limitation of the domain of application of the adjusted data since adjustments are made on multigroup data, and both the multigroup structure and the code used to process the basic data file are significant constraints.
It can be improved by “adjusting” physical parameters and not multigroup nuclear data.
As indicated above, the objective is now to correlate the uncertainties of some basic parameters that characterize the neutron cross section description, to the discrepancy between calculation and experimental value for a large number of clean, high accuracy integral experiments.
In the past a few attempts were made [10, 11] to apply a consistent approach for improving basic nuclear data, in particular to inelastic discrete levels and evaporation temperatures data of Fe56 for shielding applications, and resolved resonance parameters (e.g. g and total widths, peak positions etc.) of actinide isotopes. Although these efforts demonstrated the validity of the approach, they clearly indicated a major drawback related to the way of getting the sensitivity coefficients. Thanks to the introduction of innovative and efficient method to compute sensitivity coefficients [12] a consistent data assimilation approach becomes practical and feasible.
As added value, the information gained in the consistent data assimilation and the resulting new covariance data can be effectively used by nuclear data evaluators as feedback and indication on where and which data (model parameters) need to be improved, within well established uncertainty limits and well understood correlations.

**Strategies towards consistent data assimilation.**
Two strategies leading to the consistent data assimilation are considered.
The first one makes use of the product of explicit sensitivity matrices so that the sensitivities of integral experiments to fundamental parameters pk are defined as:

$$\frac{\Delta R}{\Delta p_k} = \sum_j \frac{\Delta R}{\Delta \sigma_j} \times \frac{\Delta \sigma_j}{\Delta p_k}$$

where R is an integral reactor physics parameter (e. g. keff, reaction rates, reactivity coefficient, etc.), and σj a multigroup cross section and pk are the basic parameters and σj are the cross sections (the j index accounts for isotope, cross section type and energy group).
In general to compute σj one can use EMPIRE (Ref. 13) with an appropriate set of parameters pk to generate first an ENDF file for that specific isotope and successively to use NJOY, to obtain multi-group cross sections or continuous energy files for Monte Carlo transport calculations. One can then compute the variation of the cross sections Δσj resulting from a variation of each individual parameter pk variation.
These calculations would cover the needs of a large number of adjustments, using several experimental configurations and several integral experiments (e.g. keff, spectral indexes, reactivity coefficients etc) in each configuration. In fact, the sensitivity coefficients:

$$\frac{\Delta \mathbf{R}}{\Delta \sigma_{\mathbf{j}}}$$

would be provided by reactor physics calculations, using the standard Generalized Perturbation Theory.
The second strategy invokes a Monte Carlo method to produce sensitivity of the integral reactor parameters to the nuclear reaction model parameters directly without approximations.
For each random set of model parameters, a full chain of calculations will be performed starting with reaction modelling with EMPIRE, ENDF formatting, NJOY processing and transport calculations with the MCNP code.
The Efficient Subspace Method (ESM, Ref. 12) can be used to optimize number of necessary histories. For example, each run of MCNP corresponding to a specific experiment, will produce the calculated integral parameters to be compared with the experimental results. Since the sensitivity matrix is expected to be ill-conditioned, i.e. low-rank, ESM will take advantage of that by minimizing the number of required MCNP runs.
To ensure that the integral parameters statistical uncertainties estimated by MCNP are uncorrelated with uncertainties originating from fundamental parameters uncertainties, a variance reduction technique will be employed.
Moreover, a rank revealing decomposition, e.g. singular value decomposition (SVD), of the fundamental parameters covariance matrices will be performed, such that the number of perturbations required will be proportional to the rank of the covariance matrix rather than the number of fundamental parameters as in strategy #1.
This procedure will be repeated for all isotopes of interest and the reduction in computational cost relative to strategy #1 will be proportional to:

$$\sum_{i=1}^{N} r_i \Big/ \sum_{i=1}^{N} k_i$$

where r and k are the rank and dimension of the ith isotope covariance matrix, respectively.

**Cross section evaluation**
The first step in both strategies will be generation of an ENDF evaluation provided completely by the EMPIRE calculations.
To this end, an appropriate set of model parameters pk have to be found out such that when used in EMPIRE, it provides a full set of cross sections, which reproduce experimental data close enough. In the case of a trustworthy ENDF/B-VII.0 evaluation (e.g., major actinides) one may choose to substitute experimental data with the ENDF/B-VII.0 cross sections.
At this stage point-wise cross sections, cross section covariances, and, the most important, a set of model parameters along with their covariances are obtained.
11,00This set of parameters contains all needed knowledge regarding the material – when combined with the EMPIRE code it defines all relevant observables and their covariances, constrained by the considered microscopic experiments and nuclear reaction models used in the calculations.

**Proposed test of the method**
The provisional list of isotopes (~25) of interest is:
Fe-56; Fe-54 …; Cr-52 … ; Ni-59 … ; Na-23; (O-16; C-12)
U-235; U-238; Pu-238; Pu-239; Pu-240; Pu-241; Pu-242
Am-241 ; Am-242 ; Am-243; Np-237; Cm-242; Cm-244; Cm-245

As far as tests, the following strategy is envisaged, with an increasing degree of complexity:

- Apply the method to the analysis of a neutron propagation experiment in a single-isotope medium (e.g. adjustment on a single structural isotope, e.g. Na).
- Apply the method to the analysis of the JEZEBEL plutonium sphere experiment (adjustment on a single fissile isotope: Pu239)
- Apply the method to the analysis of the ZPR-6 Assembly 6A critical experiment (see e.g. Ref. 9). The use of this experiment with U-235 fuel, will allow an adjustment on a limited number of fissile and structural isotopes (~10).

## Conclusions

To meet future system design tight accuracy requirements (for safety, economics, optimization etc), extensive uncertainty quantification and robust validation methods are needed.

In this context, beside the performance of few selected differential experiments with very high experimental accuracy, the use of

- data covariances,
- clean integral experiments,
- modern sensitivity methods and
- a new method of basic parameters statistical adjustment,

allows to envisage not only to reduce uncertainties but also to dramatically enlarge the domain of validation of the next generation of improved basic nuclear data files.

**References**

[1] GP. Cecchini et al. “Analysis of integral data for few-group parameter evaluation of fast reactors.” Proc. of United Nations Geneva Conf., p. 627, 1964.
[2] M. Salvatores, “Nuclear data adjustment with integral experiments.Nucl. Sci. & Eng. 50, 345 (1973)
[3] A. Gandini, M. Petilli, “AMARA: A Code Using the Lagrange Multipliers Methods of Nuclear Data Adjustment”, RT/FI(73)39, Comitato Nazionale per l’Energia Nucleare (1973).
[4] A. Gandini, “Uncertainty Analysis and Experimental Data Transposition Methods” in Uncertainty Analysis, Y. Ronen Editor, CRC Press 1988.
[5] G. Palmiotti and M. Salvatores, “Use of Integral Experiments in the Assessment of Large Liquid-Metal Fast Breeder Reactor Basic Design Parameters”. Nucl. Sci. Eng. 87, 333 (1984).
[6] Y. Ronen et al, “Determination and Application of Generalized Bias Operators Using an Inverse Perturbation Approach”, Nucl. Sci. Eng., 77, 426 (1981).
[7] Takeda and A. Yoshimura, “Prediction Uncertainty Evaluation Method of Core Performance Parameters in Large Liquid Metal Fast Breeder Reactors”, Nucl. Sci. Eng., 103,157 (1989).
[8] T. Takeda et al. “Generalized Bias Factor Method for Accurate Prediction of Neutronics Characteristics”, PHYSOR-2006, ANS Topical Meeting on Reactor Physics, Vancouver, BC, Canada, September 2006.
[9] G.Palmiotti et al. “A Global Approach to the Physics Validation of Simulation Codes for Future Nuclear Systems” Proc. Int. Conf. PHYSOR 2008, Interlaken, Sept. 2008
[10] A. D’Angelo, A. Oliva, G. Palmiotti, M. Salvatores, and S. Zero, “Consistent Utilization of Shielding Benchmark Experiments,” Nuclear Science Engineering 65, 477 (1978).
[11] M. Salvatores, and G. Palmiotti, et al. “Resonance Parameter Data Uncertainty Effects on Integral Characteristics of Fast Reactors,” IAEA Specialist’s Meeting on Resonance Parameters, Vienna, 28 September - 2 October, 1981.
[12] H. S. Abdel-Khalik, P. J. Turinsky, and M. A. Jessee, “Efficient Subspace Methods-Based Algorithms for Performing Sensitivity, Uncertainty, and Adaptive Simulation of

Large-Scale Computational Models," Nuclear Science and Engineering, vol. 159, pp. 256-272, 2008.

[13] M. Herman, R. Capote, B. Carlson, P. Oblozinsky, M. Sin, A. Trkov, and V. Zerkin, EMPIRE nuclear reaction model code, version 2.19 (Lodi). www.nndc.bnl.gov/empire219/ (March 2005).

# Neutronic characteristics of a module of the fluoride-salt graphite-core blanket

*E. Šimečková[1)], P. Bém[1)], M. Götz[1)], M. Honusek[1)], S.Hron[2)], J. Kyncl[2)], M. Mikisek[2)]*

1) Nuclear Physics Institute of the ASCR, CZ-250 68 Řež, Czech Republic
2) Nuclear research Institute, CZ-250 68 Řež, Czech Republic
simeckova@ujf.cas.cz

***Abstract:*** A neutron transport benchmark experiment has been conducted on the fluoride-salts/graphite core module that simulates the blanket of SPHINX nuclear transmutation system. The p(19 MeV)+Be external neutron source of the NPI Řež cyclotron U-120M was placed in the front of the input surface of the module. The dosimetry-foil method was used for reaction-rate measurement at different position on the module surface. The neutron energy range from 1 to 18 MeV has been investigated using the (n,2n), (n,n') and (n,α) threshold reactions on Au, In and Al dosimetry foils. The epithermal energy region was investigated and qualitatively discussed as well using (n,γ) dosimetry reaction on Au and In. The calculation of reaction rates using the MCNP4a code with ENDF/B-6 neutron cross-section data library have been carried out and compared with measurement at fast-neutron energy region. Some aspects of present neutron transport benchmark are discussed in details.

## Introduction

The SPHINX project [1] is dealing with a solution of some principle problems of a very promising way of nuclear waste treatment by means of transmutation of radionuclides by use of a nuclear reactor with liquid fuel based on molten fluorides, which might be a subcritical system driven by a suitable neutron source. Because of the fundamental different dynamics and dissimilar settlement it is necessary to study a model of blanket in variant neutron fields (thermal and in few MeV region). The current status of the experimental program performance has been focused upon the irradiation of samples of molten-salt system as well as structural materials proposed for the blanket of the SPHINX transmutor in the field of high neutron flux of research reactor and external neutron field as well. The reliability of computerized simulation depends on neutron cross-section data whose are occasionally incomplete or hagridden by errors and dispersion of particular experiments.
The experience from the reactor physics shows that suitable analysis model suffers to perform experiments with relatively small geometry of reactor make-up. Actually there is not large difference for critical or non-critical settlement in the simulation.
The integral test of neutron database and simulation calculation of neutron response of model settlement blanket reactor (on the bases of fluoride salts) on the neutron field from external source was performed using of the U120M cyclotron-based neutron facility. The calculation of reaction rates using the MCNP4a code with ENDF/B-6 neutron cross-section data library have been carried out and compared with the measurement at fast neutron energy region.

## Experiment

### Module of the blanket

The module is assembled of six graphite hexagons surrounding the central one which contains the LiF(60%)+NaF(40%) fluoride mixture. In the centre of each external hexagon the cylinders of the 60 mm diameter are located which also contain fluoride-salts - see Figure 1. All components are shouldered by aluminium case of 5 mm thickness. The length of the module is 600 mm.

### Cyclotron based external neutron source

The reaction $^{9}$Be(p,xn) with the proton incident energy $E_p$=19.08 MeV on thick beryllium target was chosen because of the energy limit (20 MeV) of the data file in MCNP4a code. The reaction data were taken from the accurate experiment performed at PTB Braunschweig [2]. The angular distribution of spectral yield of the $^{9}$Be(p,xn) reaction is shown in Figure 2.

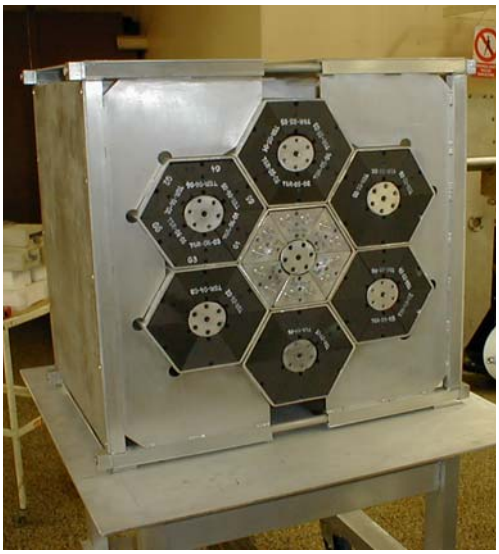

***Figure 1.*** *The view on the front (input) side of the module.*

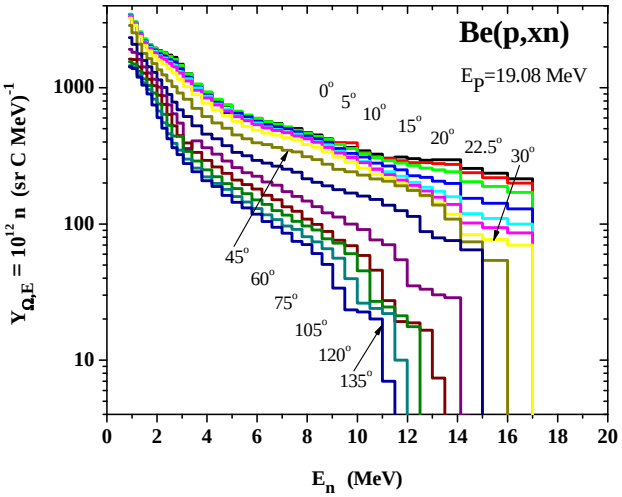


***Figure 2.*** *The angular distribution of the spectral yield of $^{9}$Be(p,xn) reaction with initial proton energy of 19.08 MeV [2].*

**Experimental set-up**

The front side of the module was located in the 23 cm distance from the neutron source target. The axially symmetrical module and beam line were sited on the identical axis. The module was irradiated by neutrons from Be(p,xn) source of about 18 hours with almost stable proton current of about 8 μA. Beam current was registered and stored in PC to restore history. The response of module to the external neutron field in the neutron energy range from 1 MeV to 18 MeV was investigated using the (n,2n), (n,n') and (n,α) threshold reactions on a set of Au, In and Al dosimetry foils – Table 1. Consequently, during the irradiation, the assembles of dosimetry foil set (diameter 12 mm) were situated in 2, 8.8, 15.5, 25.5 and 32.7 cm radial distance from axial axis on the front and back side of the module, respectively.

**Determination of experimental reaction rates**

The gamma-rays from the irradiated foils were measured repeatedly by two calibrated HPGe detectors of 23 and 50 % efficiency and of FWHM 1.8 keV at 1.3 MeV. Activated isotopes were identified on the basis of $T_{1/2}$, γ-ray energies and intensities (Table 2). The experimental reaction rates (RR) were calculated from the specific activities corrected to the decay during irradiation.

***Table 1.*** *Dosimetry reaction for energy region 1 – 18 MeV*

| Foil | Reaction | Energy region |
|---|---|---|
| **In** | $^{115}$In(n,n')$^{115m}$In | 3-11 MeV |
| **Al** | $^{27}$Al(n,α)$^{24}$Na | 8-18 MeV |
| **Au** | $^{197}$Au(n,2n)$^{196}$Au | 12-18 MeV |

***Table 2.*** *Characteristics of dosimetry foils.*

| Isotop | $T_{1/2}$ | $E_\gamma$[keV] | $I_\gamma$[%] |
|---|---|---|---|
| $^{115m}$**In** | 4.486 h | 336.24 | 45.83 |
| $^{24}$**Na** | 14.96 h | 1368.63 | 100 |
| | | 2754.03 | 99.94 |
| $^{196}$**Au** | 6.183 d | 355.68 | 87 |
| | | 332.98 | 22.9 |

## Simulation

The simulation was made by MCNP4a code (Monte-Carlo method utilizing the ENDF/B-6 [3] database). The MCNP4a code cannot simulate analytically neutron sources produced by charged particle reactions. Therefore the tabulated data of the spectral neutron yield from source reaction p(19MeV)+Be [2] were used as the input in a simulation of external neutron field in the space of the module. In the calculations, the neutron source was considered as point-like, the number of simulated neutron events was $10^7$. Due to the missing neutron yield

data below 0.9 MeV, the model calculation was carried out for fast neutron energy region only neglecting the contribution of epithermal neutrons in the source reaction and from room background as well.

## Discussion and Conclusion

### Test of neutron source simulation

To test the neutron source flux at the front of the module and to verify the simulation procedure, the set of foils was located at the same positions that were then repeated for measurement under presence of module. The calculated RR were normalized to measured RR of the $^{27}Al(n,\alpha)^{24}Na$ reaction at the first position (2 cm radial distance). The Figure 3 shows the yield data are well reproduced for the first three positions (correspond to the angle 5°, 21° and 34°) but reflect a systematical overestimate (10-20%) for the position 48° and 55°, which results from a large angular gap in tabulated p+Be data in this angular region. Analytical interpolation procedure for more reliable simulation of source is now under progress.

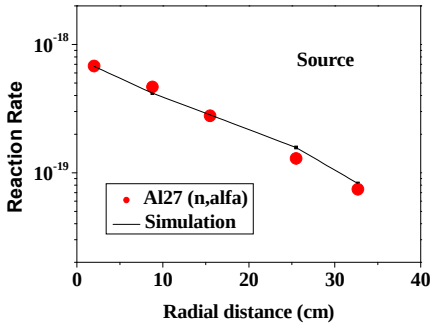


***Figure 3a.*** *The radial distribution of the reaction rates of the $^{27}Al(n,\alpha)$ reaction initiated by neutron flux of the p+Be source. The measured and simulated data are shown.*

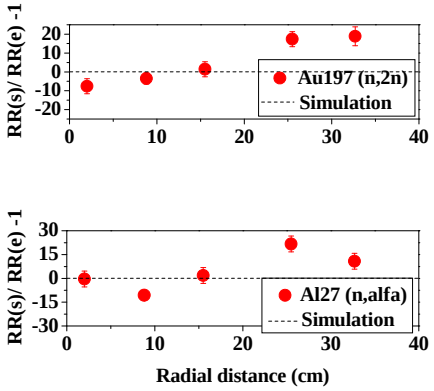


***Figure 3b.*** *The ratio of simulated to experimental reaction rates for the $^{27}Al(n,\alpha)$ and $^{197}Au(n,2n)$ reactions The data are normalized to the experimental reaction rate of the $^{27}Al(n,\alpha)^{24}Na$ for the first position (2 cm radial distance).*

### The neutron response of the module

About two-order difference in measured neutron flux at entry and exit surface of the module was measured with high statistical accuracy (< 10 %) comparable to the accuracy of simulating calculations.

Neutron field measured on the entry side of module corresponds to composed contribution from the source and from secondary emitted neutrons. Secondary neutron flux determined from the ratio of module -in and -off measurements stands for 5-10 % and 25-50 % of primary

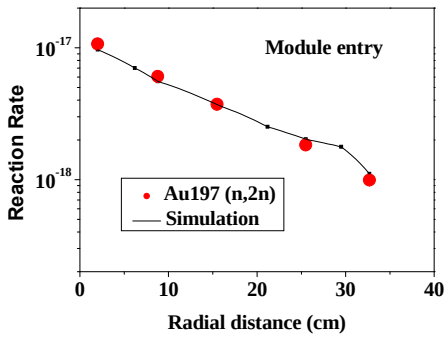


***Figure 4a.*** *The distribution of the reaction rates of the $^{197}Au(n,2n)$ reaction measured on the front side of the module.*

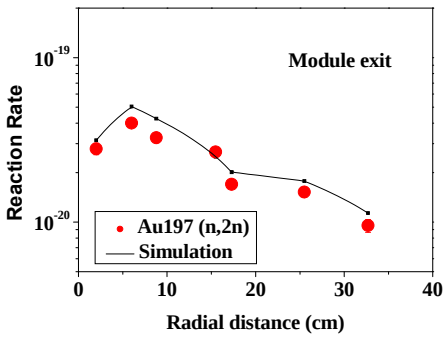


***Figure 4b.*** *The distribution of the reaction rates of the $^{197}Au(n,2n)$ reaction measured on the back side of the module.*

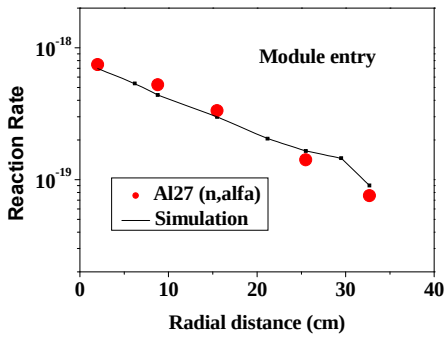


***Figure 5a.*** *The distribution of the reaction rates of the $^{27}Al(n,\alpha)$ reaction measured on the front side of the module.*

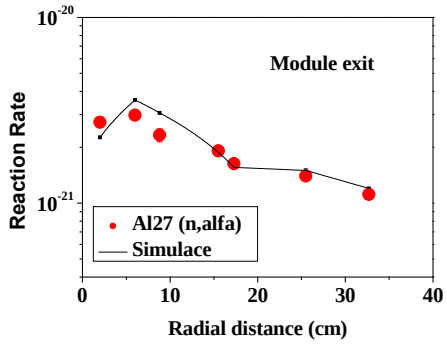


***Figure 5b.*** *The distribution of the reaction rates of the $^{27}Al(n,\alpha)$ reaction measured on the back side of the module.*

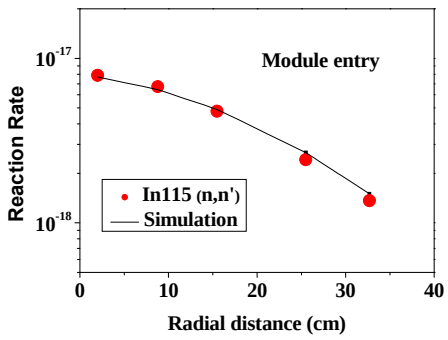


***Figure 6a.*** *The distribution of the reaction rates of the $^{115}In(n,n')$ reaction measured on the entry side of the module.*

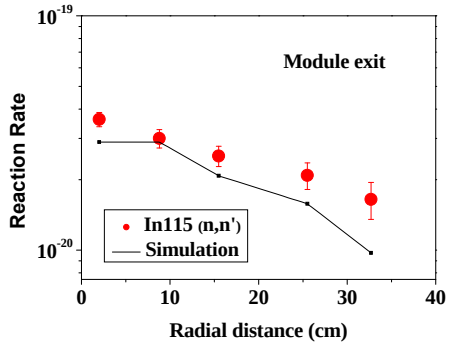


***Figure 6b.*** *The distribution of the reaction rates of the $^{115}In(n,n')$ reaction measured on the exit side of the module.*

field at higher and lower energy part of investigated energy region, respectively. This ratio which is less affected by non-complete describing of source-yield data at large angles is in good agreement with simulating calculations.
Within the statistics of (2 - 3 σ), the systematic deviation of measured and calculated reaction rates at exit surface of module is observed. This difference could be accepted as the benchmark test of data files, computing procedure and projected configuration of the module unless the reliable interpolation procedure for complete simulation of source neutron flux is carried out.

**Acknowledgements**
This work was performed under Contract No 2007/025 between Radioactive Waste Repository Authority (SÚRAO/RAWRA) of Czech Republic and the Nuclear Physics Institute.

**References**

[1] M. Hron, “Project sphinx spent hot fuel incinerator by neutron flux”, Prog. Nucl. Energy. 47(2005), p.347 (ISSN 0149-1970).
[2] H.J.Brede et al., Neutron yields from thick Be targets bombarded with deuterons and protons, Nucl. Instr. And Methods A274 (1989)332
[3] J.F. Briefmeister (editor), MCNP – a general Monte Carlo n-particle transport code, version 4a, manual RSIC Computer Code Collection, CCC – 200, Oak Ridge, (1993).

# Measurements of cross-sections of neutron threshold reactions and their usage in high energy neutron measurements

*O. Svoboda[1,2], A. Krása[1,2], A. Kugler[1], M. Majerle[1,2], V. Wagner[1,2]*

1) Nuclear Physics Institute of the Academy of Sciences of the Czech Republic PRI, 250 68 Řež near Prague
2) Faculty of Nuclear Sciences and Physical Engineering, Czech Technical University, Břehová 7, 115 19 Prague

svoboda@ujf.cas.cz

***Abstract:*** We measured the neutron cross-sections of various threshold reactions using different quasi-monoenergetic neutron sources in the range 20 – 100 MeV. Our motivation comes from the "Energy plus Transmutation" project (E+T), at which Au, Al, Bi, In and Ta activation detectors are used, but almost no experimental cross-section data for observed threshold (n,xn) reactions are available at neutron energies above 20 MeV.
We prepared a few studies to measure the (n,xn) cross-sections using the neutron sources on NPI ASCR cyclotron in Řež and on TSL cyclotron in Uppsala (EFNUDAT program). Quasi-monoenergetic neutrons from p+Li reaction irradiated above mentioned foils and iodine samples (also used at "E+T" experiments). The experiments were already carried out at NPI with 20 and 25 MeV protons, next irradiations are planed for near future to cover whole available neutron energy region (10 - 37 MeV) from this source. In June 2008, measurements at TSL were carried out with proton energies 25, 50, and 100 MeV. Methodology of the measurements and first results are presented in detail.

## Motivation

Our motivation for the cross-section measurements comes from the "Energy plus Transmutation" project [1] being performed at JINR Dubna. In this international project we use the neutron activation foils for measurements of the high energy neutron field, which is produced during the proton or deuteron irradiation of a thick lead target surrounded by a natural uranium blanket. Au, Al, Bi, In, and Ta foils are used as activation neutron detectors, but unfortunately almost no experimental cross-section data for most of observed threshold (n,xn) reactions are available for higher neutron energies.

## State-of-the-art of the neutron cross-section libraries

The present status of knowledge of cross-sections for the (n,xn) reactions is poor. Fig1 and 4 show measured (from EXFOR [2]) cross-sections for (n,xn) reactions in Bi and Au.

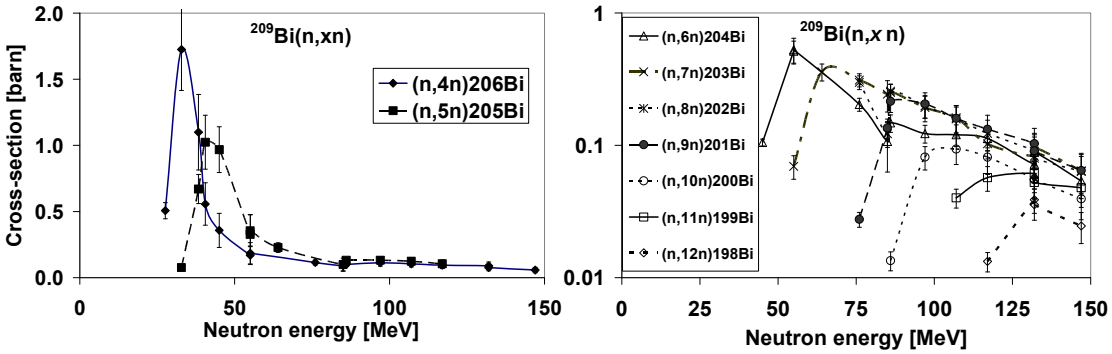


***Figure 1.*** *Neutron cross-section for the Bi (n,xn) threshold reactions. Data are from the EXFOR [2].*

In the case of bismuth, reactions from (n,4n) until (n,12n) were measured already (Figure 1.), but there are values from one experiment only [3]. There are no evaluated data available. In

the case of gold, only (n,2n) reaction was measured in detail and by more authors (Figure 4. left), (n,4n) reaction was measured only for small neutron energies (Figure 4. right). Other (n,xn) reactions were not studied at all. The situation for Al, In, and Ta is similar to Au. Therefore, it is still necessary to perform new cross-section measurements to fill in the gaps and estimate possible systematic errors at already measured values.

## Cross-section measurements

For cross-section measurements by the means of activation analysis one need firstly a good high energy neutron source with quasi-monoenergetic well known spectrum. Due to low cross-section values and limited weight of the samples these sources must furthermore be quite intensive. This reduces the number of suitable neutron sources to few in whole world. For measurements of activated samples one need a spectroscopic laboratory with $\gamma$ and X-Ray detectors of suitable resolution. Finally, wide range of spectroscopic corrections must be applied.

### Cross-section estimation

During planning of the irradiation it is necessary to have at least some knowledge about the possible cross-section course and values. We calculated the threshold energies (Figure 2.) and roughly estimated the course of cross-sections. It is necessary to stress that these $E_{thresh}$ are only illustrative and $\sigma(E)$ reaches its maximum at energy about 10 MeV bigger than $E_{thresh}$ and can have important influence even at energy of 20 MeV bigger, see for example Figure 1. For most of the isotopes it was possible to make a convolution of evaluated (estimated) cross-sections and neutron spectra. We roughly calculated yields of most isotopes and with the knowledge about the detector efficiency we planned the weights of the foils in order to get enough activated nuclei.

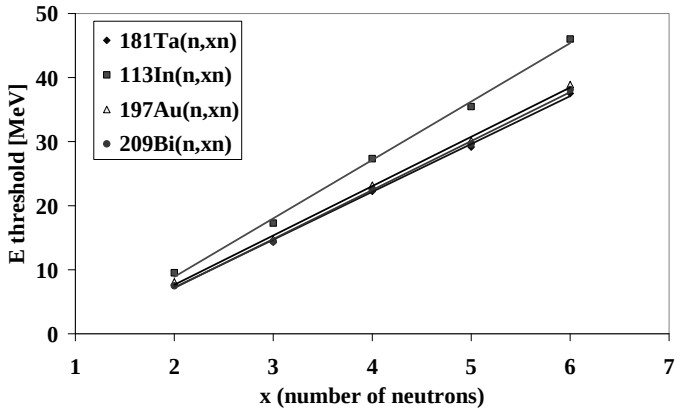


***Figure 2.*** *The threshold energies of (n,xn) reactions in Au, Bi, In, Ta. The values of threshold energies were calculated as the difference between outgoing and incoming particles masses (using mass excesses values from [4]).*

### Neutron sources

In the frame of the EFNUDAT program [5] we performed cross-section measurements at The Svedberg Laboratory (TSL) in Uppsala. In this laboratory quasi-monoenergetic 11 - 175 MeV neutron source based on the $^{7}Li(p,n)^{7}Be$ reaction is available [7]. High energy protons from the cyclotron at TSL are directed to a thin, lithium target, the neutron flux density can be up to $5.10^{5}$ $cm^{-2}s^{-1}$. The half of intensity is in the peak with FWHM = 1 MeV (corresponds to the ground state and first excited state at 0.43 MeV in $^{7}Be$) and half of intensity is in continuum in lower energies (corresponds to higher excited states, multiple-particle emission etc.) Fig4-left. Proton energy loss in the target amounts to 2-6 MeV depending on the incident beam energy and target thickness. Downstream the target, the proton beam is deflected by a magnet and guided onto a graphite beam dump. The neutron beam is formed by an iron collimator (50 cm in diameter and 100 cm long) with a hole of variable size and shape.

Second neutron source that we use is in Nuclear Physic Institute – Academy of Sciences of the Czech Republic in Řež. Protons from the cyclotron are directed to the lithium target and quasi-monoenergetic neutrons in the range 10 – 37 MeV can be produced (Figure 4.-right).

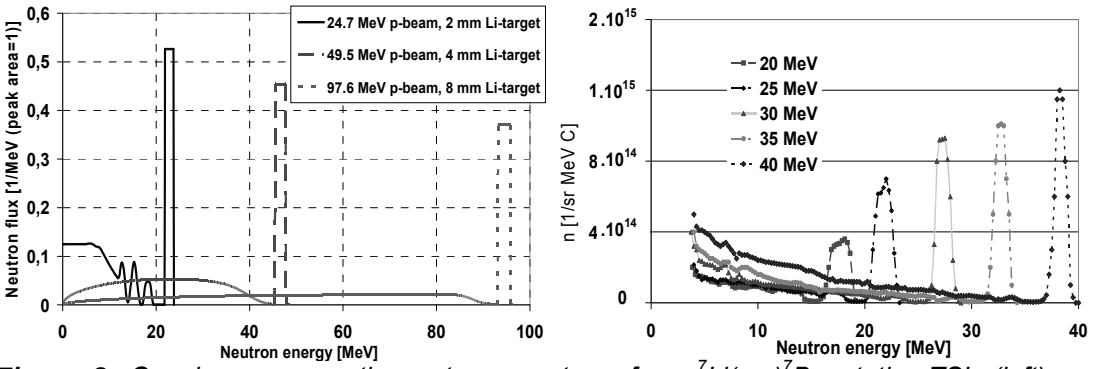


***Figure 3.*** *Quasi-monoenergetic neutron spectrum from $^{7}Li(p,n)^{7}Be$ at the TSL (left) and cyclotron Řež (right).*

**Yield of produced isotopes**

We used Au, Al, Bi, In, I and Ta samples. Materials were except the iodine in form of foils with dimensions of 20x20x0.05-1 mm$^3$, weights of the foils were from 0.2–7 grams depending on the foil type and beam energy. Foils were wrapped in paper to avoid isotope transport between foils and detector contamination. Iodine samples were in form of solid $KIO_4$ tablet packed hermetically in plastic. Samples were irradiated by neutrons in Uppsala with proton beam energies 25, 50, and 100 MeV and in Řež with proton beam energies 20 and 25 MeV. Typical irradiation time was 8 hours, transport from the irradiation hall to the spectrometer took approximately 2 minutes in Uppsala, 10 minutes in Řež .

After irradiations, activated foils were measured on HPGe detectors in Uppsala and Řež. Gained gamma-spectra were evaluated in the DEIMOS-32 code [6]. Yields of observed isotopes were calculated according to equation (1) (scaled to one gram of target material).

We applied various spectroscopic corrections to catch up all possible systematic errors. Beside the standard ones we included following corrections: the self absorption correction was determined to be in extreme case up to the factor of 2 because of big thickness of some foils and low energy of some γ-lines (at most cases typically 1.05). Square-emitter correction was determined with the help of MCNPX to be up to the factor of 0.96 because of the close detector geometry.

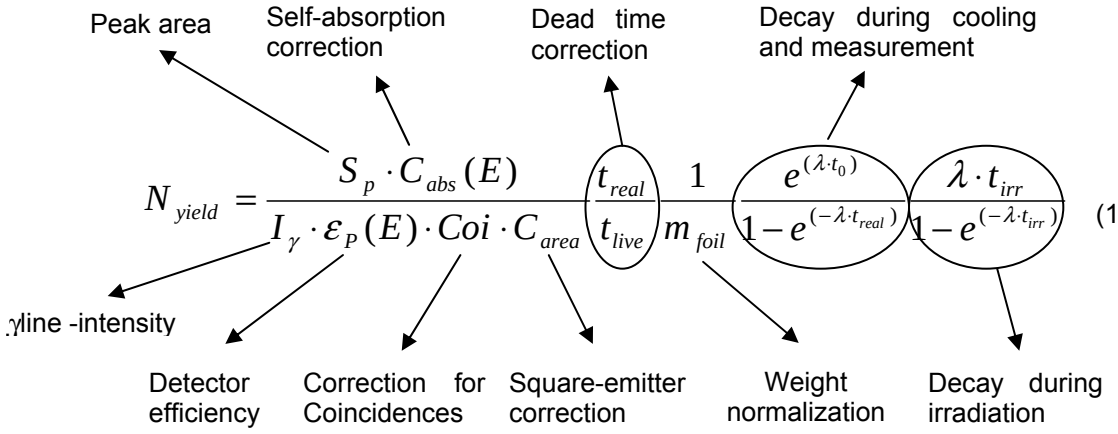


$$N_{yield} = \frac{S_p \cdot C_{abs}(E)}{I_\gamma \cdot \varepsilon_P(E) \cdot Coi \cdot C_{area}} \left(\frac{t_{real}}{t_{live}}\right) \frac{1}{m_{foil}} \left(\frac{e^{(\lambda \cdot t_0)}}{1-e^{(-\lambda \cdot t_{real})}}\right) \left(\frac{\lambda \cdot t_{irr}}{1-e^{(-\lambda \cdot t_{irr})}}\right) \quad (1)$$

With the knowledge of yield we calculated cross-section value $\sigma = \frac{N_{yield} \cdot S \cdot A}{N_n \cdot N_A}$ for respective beam energy (S – foil area, A – molar weight, $N_n$ – number of neutrons in peak, $N_a$ - Avogadro‘s number). This was purposeful only for such isotopes, where most of their amount was produced by the peak neutrons (isotope production by the background neutrons is zero or could be neglected).

**Preliminary results**

Irradiations in Řež took place on the 17. May and the 8. August 2008, irradiations in Uppsala were in days 23.-25.6 2008. Up to now we have determined basic yields without some corrections and we are starting to calculate the cross-sections.

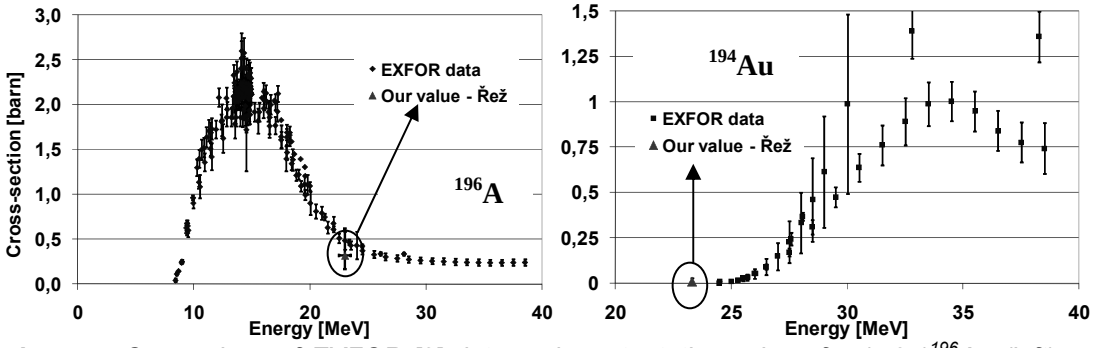


***Figure 4.*** *Comparison of EXFOR [2] data and our tentative values for (n,2n)$^{196}$Au (left) and (n,4n)$^{194}$Au (right).*

Well-known σ(E) for $^{197}$Au(n,2n)$^{196}$Au will be used to check if we get appropriate results. When we divide the yield of $^{196}$Au only by the number of neutrons in the main peak, we get the results like in Fig6-left ($^{196}$Au production by the background neutrons cannot be fully neglected), but we are still near to EXFOR data. On the other hand, $^{194}$Au is produced only by neutrons from the peak and its value corresponds with the EXFOR data very well (Fig6-right). These results are only tentative!

## Conclusion

During the "Energy plus Transmutation" project we realized there are significant voids in the cross-section libraries of (n,xn) threshold reactions. We performed a few experiments, in which we measured (n,xn) cross-sections at Au, Al, In, Bi, Ta, and I under the neutron energies 20, 25, 50, and 100 MeV. Preliminary results show we are close to the known cross-section values, but the data processing is still in progress. In the future we will continue with these measurements to cover whole available energy interval of used neutron sources.

**Acknowledgements**
We would like to thank to the staff of the TSL Uppsala (especially to Alexander Prokofiev and Lars Einarsson) and to the staff of the cyclotron in Řež for great support and excellent beams. Our special thanks belong to Marek Fikrle from the Nuclear Spectroscopy Department (NPI ASCR, p.r.i.) for the help with the set up of the samples. We would like also to thank to Pavel Bém and Eva Šimečková for possibility to joint their irradiations.
This work was supported by the EFNUDAT program [5].

**References**

[1] Křízek F. et al. The study of spallation reactions, neutron production and transport in a thick lead target and a uranium blanket during 1.5 GeV proton irradiation, Czechoslovak Journal of Physics 56 (2006) 243-252.
[2] Experimental Nuclear Reaction Data (EXFOR/CSISRS), http://www.nndc.bnl.gov/exfor, 1.9.2008.
[3] Kim E. et al., Measurements of Neutron Spallation Cross-Sections of $^{12}$C and $^{209}$Bi in the 20 to 150 MeV Energy Range, Nuclear Science and Engineering 129 (1998) 209
[4] Audi G. et al., The NUBASE Evaluation of Nuclear and Decay Properties, Nuclear Physics A 729 (2003) 3-128
[5] European Facilities for Nuclear Data Measurements, www.efnudat.cz, 4.9.2008
[6] Frána J., Program DEIMOS32 for Gamma-Ray Spectra Evaluation, Journal of Radio-analytical and Nuclear Chemistry, V.257, (2003), No. 3 P. 583-587
[7] Prokofiev A. V. et al., The TSL Neutron Beam Facility, Radiation Protection Dosimetry, 126 (2007) 18-22

# AMS measurements in nuclear physics and astrophysics at VERA

*A. Wallner, O. Forstner, R. Golser, W. Kutschera, A.Priller and P.Steier*

VERA Laboratory, Isotope Research, Faculty of Physics, University of Vienna, Währinger Str. 17, 1090 Wien
anton.wallner@univie.ac.at

***Abstract:*** Accelerator mass spectrometry (AMS) represents a powerful technique with excellent sensitivity for the detection of long-lived radionuclides through ultra-low isotope ratio measurements. Research activities using AMS cover a wide variety of domains, e.g. $^{14}$C-dating, geological, biomedical applications, environ-mental and climate studies, and also nuclear physics related measurements.
The Vienna Environmental Research Accelerator (VERA) represents a state-of-the-art AMS facility active in a wide range of such applications. In particular, a substantial part is devoted to nuclear physics and astrophysics applications. AMS being independent on half-lives offers a powerful technique for such investigations. The measurement of neutron and proton capture cross-sections has become one main research topic at VERA. Various samples have been irradiated for that purpose. After the activation the amount of longer-lived radionuclides was quantified using the technique of AMS. In a fusion environment particularly long-lived activation products may lead to significant long-term waste disposals. For such nuclides production cross-sections and induced activities are key parameters for safety and design analyses. The quantification of actinides via AMS is not affected by isobaric molecular interferences. Different kinds of sources producing actinides are reflected in different signatures of e.g. Pu isotopes, like isotopic ratios and concentration levels. This information allows to identify human activity and to reconstruct its neutron history in environmental samples. Also, AMS is applied for searching for feeble traces of long-lived radionuclides as signatures of recent close-by supernova explosions.
An overview on recent research activities at VERA with respect to nuclear physics and nuclear astrophysics is presented. In addition, the actual detection limits for long-lived radionuclides are given.

## Technique of Accelerator Mass Spectrometry

Accelerator mass spectrometry (AMS) is a mass-spectrometric technique based on a tandem-accelerator, commonly used for quantifying long-lived radionuclides within a wide range of applications [1,2]. AMS has been utilized for the measurement of minute concentrations of isotopes over the whole mass range and is characterized by a low measurement background and high detection efficiency. In contrast to other mass spectrometric techniques, like e.g. ICP-MS, AMS is not affected by isobaric molecular interferences.
In most cases, negatively charged ions are produced in a Cs-sputter source. To this end, solid sputter targets have to be produced from the sample to be analyzed by AMS (new developments use also gaseous samples for $^{14}$C applications). The typical sample masses are of the order of mg per sputter sample. The sample material itself is used up during the measurement. Negative ions are pre-accelerated, energy- and mass-selected by passing an electrostatic deflector and an injection magnet, respectively. The ions are injected into a tandem accelerator. At the terminal a gas or foil stripper is utilized to strip-off electrons. The negatively charged ions then leave the accelerator positively charged after being accelerated a second time. With the stripping process, molecules are destroyed and only atomic particles with different charge states are produced. A second analyzing magnet is used to select a specific positive charge state. VERA is based on a 3-MV tandem accelerator, which produces particle energies between 10 and 25 MeV.
Currents are measured for stable isotopes with off-line Faraday cups (see Fig. 1) positioned at both sides, the low-energy side after the mass-selective injection magnet (e.g. $^{209}Bi^-$ or $^{12}C^-$ and $^{13}C^-$), and after the analyzing magnet ($^{209}Bi^{5+}$ or $^{12}C^{3+}$ and $^{13}C^{3+}$). The radionuclides are directly counted with a particle detector (count-rate of $^{210}Bi^{5+}$ or $^{14}C^{3+}$). AMS provides isotope

ratios, the count-rate ratio of radionuclide and stable isotope (e.g. $^{210}Bi/^{209}Bi$, $^{14}C/^{12}C$ or $^{14}C/^{13}C$) with current and count-rate measurements performed sequentially.

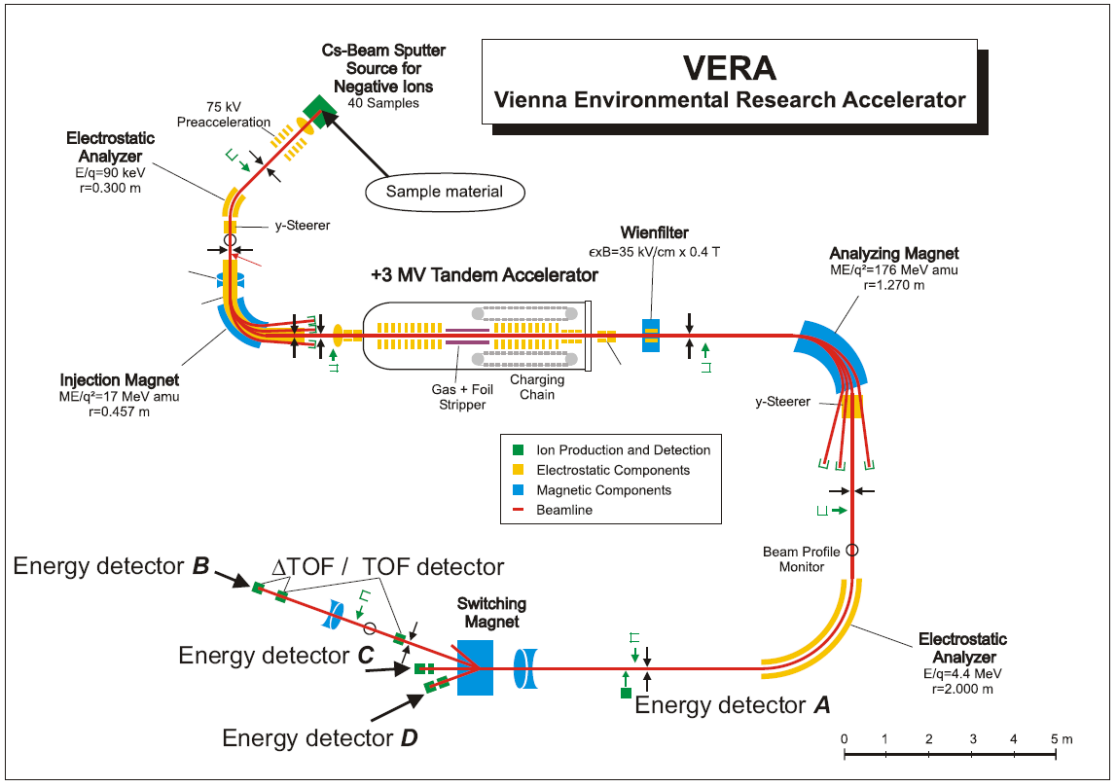


***Figure 1.*** Schematic layout of the VERA facility. Currents of stable ions are measured in sequential mode with Faraday cups positioned after the injection magnet (low-energy section, negative ions) and after the analyzing magnet (high-energy section, positive ions). Various detectors are available for counting rare isotopes (detectors A to D): The heavy-ion beamline (which is also used for $^{236}U$ and $^{210}Bi$-detection) consists of time-of-flight (TOF) detectors and an ionization chamber (E).

In contrast to other mass-spectrometric techniques, the acceleration and the stripping process leads to the destruction of molecular isobars. With the use of the second mass spectrometer at the high-energy side, the beam is free of molecular interference (the molecule $^{209}BiH$ is destroyed and break-up products are deflected by the second magnet when measuring the radionuclide $^{210}Bi$).
Isotopic interference is still possible due to charge-exchange reactions in the residual gas (e.g. “leaking” $^{209}Bi$ in case of $^{210}Bi$ detection, i.e. $^{209}Bi$ is injected as $^{209}BiH^-$ into the tandem, charge exchange at the high-energy side allows the break-up product $^{209}Bi$ to enter the particle detector although the setup is tuned for mass 210). Such interferences are strongly reduced by additional filters. At VERA a Wien-filter, a double-focusing electrostatic analyzer and additional magnetic deflectors are available for this purpose. However, a finite number of isotopic background particle still enter the detector. Time-of-flight (TOF) technique is applied to discriminate isotopic interferences: different masses with the same energy (constricted by the preceding filters) are distinguished by their different flight time.
Atomic isobars (e.g. $^{210}Po$ is the isobar to $^{210}Bi$) cannot be removed from the beam by selective filtering. However, further reduction of isobaric and isotopic interferences for lower masses can be achieved by a dedicated particle detection system. The different energy-loss of isobars is utilized for that purpose: The now widely-used silicon nitride membranes (SiN) offer an unprecedented homogeneity. New developments in compact ionization chambers with significantly improved energy resolution, allow a substantial reduction of isobaric interferences.

The typical isotope ratios in AMS are between $10^{-11}$ and $10^{-16}$, depending on the radionuclide under investigation. This ultra-sensitivity allows quantifying natural concentrations of long-lived radionuclides in our environment (the natural concentration of $^{14}C$, $^{14}C/^{12}C = 1.2\times10^{-12}$). It is also this dynamical range, which makes AMS a versatile tool for many applications. The detection limit in most cases is given by the machine or sample-background signal registered with the particle detector and varies strongly with the specific radionuclide measured. Together with samples of unknown isotope ratios, reference materials with well-known ratios are measured in periodic intervals as well. They serve as standards to check long-term drifts of the beam transmission through the beamline and provide the absolute scaling factor for the final ratios. Another important parameter is the overall-efficiency, i.e. the fraction of particles detected relative to those available in the sputter sample. It depends on the negative ion formation probability and the transmission of the particles through the AMS facility up to the particle detector and varies strongly for different isotopes, and ranges between $10^{-4}$ and up to 10% (see Table 1).

***Table 1.*** *Basic features of some radionuclides measured at VERA*

| Radio-nuclide | Half-life (yr)[1] | Overall efficiency[2] | Detection limit[3] | Precision | Remark |
|---|---|---|---|---|---|
| $^{10}Be$ | $(1.36 \pm 0.05)*10^6$ | $> 1\times10^{-3}$ | $<10^{-15}$ | < 2 % | isobar $^{10}B$ |
| $^{14}C$ | $(5730 \pm 40)$ | $1\times10^{-1}$ | $< 3\times10^{-16}$ | < 0.5 % | no stable isobar* |
| $^{26}Al$ | $(0.71 \pm 0.02)*10^6$ | $3\times10^{-4}$ | $< 6\times10^{-16}$ | < 1.0 % | no stable isobar* |
| $^{36}Cl$ | $(3.0 \pm 0.02)*10^5$ | n.m. | $< 10^{-13}$ | 2-5 % | isobar $^{36}S$ |
| $^{41}Ca$ | $(1.03 \pm 0.05)*10^5$ | n.m. | $< 10^{-13}/ 10^{-15}$ | 2-5 % | isobar $^{41}K$ $CaF_2$/ $CaH_2$ |
| $^{55}Fe$ | $(2.73 \pm 0.03)$ | n.m. | $< 1\times10^{-15}$ | < 2 % | no stable isobar* |
| $^{129}I$ | $(15.7 \pm 0.4)*10^6$ | $1\times10^{-2}$ | $2\times10^{-14}$ | 2 % | no stable isobar* |
| $^{182}Hf$ | $(8.90 \pm 0.09)*10^6$ | $1\times10^{-4}$ | $1x10^{-11}$ | 10 % | isobar $^{182}W$ |
| $^{210m}Bi$ | $(3.04 \pm 0.06)*10^6$ | n.m. | $< 5\times10^{-12}$ | 10 %[4] | no isobar |
| $^{236}U$ | $(23.42 \pm 0.03)*10^6$ | $5\times10^{-4}$ | $< 2\times10^{-12}$ | 3 % | no isobar |
| $^{244}Pu$ | $(80.0 \pm 0.9)*10^6$ | $5\times10^{-4}$ | --[5] | 3 % | no isobar |

* no stable negatively charged isobar is extracted from the source (e.g. $^{14}N^-$ is not stable).
[1] see e.g. Ref. [13]
[2] atoms detected per atoms in sample; 'n.m.' means 'not measured'.
[3] expressed as isotope ratio
[4] detection of $^{210m}Bi$ is under development.
[5] $^{244}Pu$ background is less than 1 count per hour measuring time.

AMS measurements are performed for radionuclides with half-lives between a few years and up to hundred million years. It reflects that this technique offers a powerful tool through ultra-low isotope-ratio measurements irrespective of half-lives and decay schemes of reaction products. In combination with the very low masses needed, AMS measurements of long-lived radionuclides represents a technique with a much higher sensitivity compared to decay-counting techniques. This can easily be seen from the following calculations: 1 mg of carbon contains $5\times10^{19}$ $^{12}C$ atoms. At natural levels, the isotope ratio of $^{14}C/^{12}C = 1.2*10^{-12}$ converts into a total of 60 million $^{14}C$ atoms in 1 mg carbon. An overall efficiency of 5 percent (see Tab. 1), corresponds to a total of 3 million $^{14}C$ counts in principle to be registered. At natural levels a $^{14}C$ count rate of 100 per second is measured with the particle detector in AMS. In order to get a statistical uncertainty of 1% only 100 seconds of counting time are needed. If decay counting is used, and assuming a detection efficiency of 100%, a count rate of $3\times10^{-4}$ (i.e. an activity of 0.3 mBq) is measured. To get the same statistical uncertainty, a counting time of

more than 1 year is needed! To summarize, AMS is orders of magnitude more efficient for long-lived radionuclides compared to decay counting techniques. This is mainly a consequence of the long half-life and the small sample masses needed.
For some radionuclides Table 1 lists basic features of interest in AMS for the specific facility VERA: Their half-lives span a range from 2.7 years ($^{55}$Fe) to 80 million years ($^{244}$Pu). Overall efficiency means the fraction of particles in a sample, which can be counted with the particle detector. The next column in Fig. 1 depicts the detection limit, either determined by isobaric interferences or by the instrumental background. Also listed is the precision of the AMS measurement if not limited by counting statistics.
The dedicated AMS facility VERA provides the ability for quantifying nuclides over the whole mass range [3]. Measured radioisotopes include $^{10}$Be, $^{14}$C, $^{26}$Al, $^{36}$Cl, $^{41}$Ca, $^{55}$Fe, $^{129}$I, $^{182}$Hf, $^{210m}$Bi, $^{236}$U and $^{244}$Pu. AMS facilities based on larger tandems allow to quantify a few additional isotopes in the medium mass range where suppression of isobaric interferences asks for higher particle energies.

## Comparison of AMS with other techniques for cross-section measurements

In particular, well-established data on production-rates and cross sections of long-lived radionuclides are often highly desired. Especially long-lived radionuclides have often been inaccessible to decay counting techniques, e.g. because of low activity or an unfavorable decay scheme. Cross-section measurements can be classified into two complementary techniques: direct and indirect methods. The direct method makes use of the detection of the prompt and characteristic radiation associated with the production of a specific nuclide, or selectively detects the reaction product itself by means of the recoil separator technique. This method is characterized as an on-line technique. A second and independent method makes use of the activation technique, with sample irradiation and subsequent measurement of the reaction product. After the irradiation the number of produced radioactive nuclei can be quantified either by decay-counting or by mass spectrometric methods. This method is mostly restricted to radioactive products; however, it represents a very sensitive technique due to potential long irradiation periods.
AMS represents an independent and complementary method to the above mentioned direct measurements. A comparison of AMS results allows studying systematic contributions to the total uncertainty associated e.g. with direct methods, which otherwise are hard to quantify. In contrast to other mass spectrometric techniques, like e.g. ICP-MS, AMS is characterized by a low measurement background and, most important, it is not affected by isobaric molecular interferences.

## Applications of AMS in nuclear physics and nuclear astrophysics

Improved and highly accurate nuclear data are urgently required for the design of advanced reactor concepts (Gen IV, ADS) or for the design of nuclear fusion devices, like ITER. The determination of cross sections via the combination of the activation technique and AMS represents an important indirect method. Similarly, there is a clear need for more data to support our understanding of nucleosynthesis processes in astrophysical scenarios. One important contribution to the study of nuclear processes occurring in stars can be provided by measurements of nuclear reactions at accelerator based facilities in combination with AMS.
AMS is also used to quantify absolute concentrations of long-lived radionuclides in a bulk material: Concentrations of rare radionuclides in our environment have the potential to provide unique information. The measurement of such radionuclides allows tracing anthropogenic activities or environmental processes. Similarly, spurious amounts of extra-terrestrial input into terrestrial archives can be investigated by AMS. In the following, with a few examples related to nuclear physics and nuclear astrophysics, a sketchy overview of AMS applications in this field is given.

### $^{235}$U(n,$\gamma$)$^{236}$U – a prime example for actinide measurements

Existing data for the capture channel of $^{235}$U have been measured by time-of-flight techniques via detection of the prompt capture $\gamma$-rays. A major difficulty in these experiments is the safe discrimination against the strong $\gamma$-background from the competing fission channel, therefore those data might suffer from systematic uncertainties. Using AMS, any interference from the fission channel is completely excluded. Activations can be performed with very small samples of natural uranium. This method for measuring the neutron-capture cross section of $^{235}$U has

the advantage that the involved systematic uncertainties are in no way correlated with the uncertainties inherent to the TOF technique. In particular, measurement methods for the detection of the long-lived radionuclides were established at VERA, where suppression of isobars is not required (no stable isobar for $^{236}$U detection) [4]. To suppress interference from neighboring masses (isotopic interference by $^{235}$U and $^{238}$U), the resolution of VERA was recently increased, both by improving the ion optics of existing elements and by installing a new electrostatic analyzer after the analyzing magnet. Interfering ions which pass all beam filters are identified with a high-resolution time-of-flight (TOF) system. In collaboration with various neutron-producing facilities, AMS measurements are performed for neutron energies between thermal and 500 keV.

**$^{209}$Bi(n,γ)$^{210m}$Bi – of interest for ADS and nuclear astrophysics**

The reaction $^{209}$Bi(n,γ) leading to the short-lived $^{210g}$Bi ($t_{1/2}$ = 5 days) and the long-lived isomer $^{210m}$Bi ($t_{1/2}$ = 3.0 Myr) is studied at VERA for thermal energies and in the keV energy range. In the design of future high-power spallation sources a eutectic Pb-Bi target is envisaged, also Pb-Bi may be used as a coolant for accelerator driven systems. The neutron capture reactions on Pb and Bi were considered of key relevance for the design of such systems. In addition, the neutron capture reaction $^{209}$Bi(n,γ) terminates the s-process in nucleosynthesis, because no stable or sufficiently long-lived nuclide can further be produced via slow neutron capture processes (see e.g. [5,6]). Although no stable isobar exists for $^{210}$Bi, the decay product of $^{210g}$Bi, $^{210}$Po ($t_{1/2}$ = 138.4 days), with a much higher negative ionization yield, interferes with $^{210m}$Bi in AMS measurements. The low cross-section value requires suppressing efficiently interference from the neighbouring mass $^{209}$Bi (like for $^{236}$U measurements, see above). Measurements have been started first to investigate the thermal cross section [7].

**Neutron-capture reactions in the keV energy range for s-process studies**

The measurement of neutron and proton capture cross-sections relevant to nuclear astrophysics has become one main research topic at VERA. This work continuous and adds to previous measurements e.g. performed at Rehovot, Argonne and Munich [8-10]. Various samples have been irradiated for that purpose at Forschungszentrum Karlsruhe [11]. After the activation the amount of longer-lived radionuclides is quantified using the technique of AMS. Examples are $^{9}$Be(n,γ)$^{10}$Be, $^{13}$C(n,γ)$^{14}$C, $^{14}$N(n,p)$^{14}$C, $^{40}$Ca(n,γ)$^{41}$Ca and $^{54}$Fe(n,γ)$^{55}$Fe in the neutron energy range from thermal to keV [12,13]. These reactions are of interest in Big-bang nucleosynthesis and in the slow-neutron capture process (s-process) in stars.

**Long-lived radionuclides as activation products in a fusion environment**

In a fusion environment particularly long-lived activation products may lead to significant long-term waste disposals and radiation damage. Many of these production cross sections are not well-known making it difficult to calculate concentration limits [14]. With the high neutron flux in a fusion reactor also impurities in structure materials may lead to significant or dominating activations. For such nuclides production cross-sections and induced activities are key parameters for safety and design analyses. At VERA a program to measure cross sections for various long-lived radionuclides in the neutron energy range relevant for nuclear fusion is ongoing. Within that program, in collaboration with various neutron-producing facilities (e.g. IRMM Geel, Forschungszentrum Dresden-Rossendorf, Forschungszentrum Karlsruhe), cross sections are measured for reactions like $^{14}$N(n,p)$^{14}$C, $^{27}$Al(n,2n)$^{26}$Al, $^{54}$Fe(n,np+d)$^{53}$Mn, $^{56}$Fe(n,2n)$^{55}$Fe, $^{60}$Ni(n,2n)$^{59}$Ni, etc. for neutron energies from 13 to 20 MeV [15,16].

**AMS measurements in environmental samples for nuclear forensic studies**

The concentrations of rare radionuclides in our environment have the potential to provide unique information. The measurement of such radionuclides allows tracing anthropogenic activities or environmental processes. Man-made radionuclides will enter the environment via different processes, e.g. from nuclear weapons tests, as accidental local fallout products, from nuclear-fuel reprocessing plants, or from industrial or medical applications. For the trans-uranium elements like plutonium, by far their largest signals stem from artificial sources. Different kinds of origin are reflected in different signatures like isotopic ratios and concentration levels [17,18]. Its detection represents therefore a proper means for proving human activity. Besides $^{238}$Pu, all other Pu isotopes, i.e. from $^{239}$Pu to $^{244}$Pu, do not suffer from stable isobaric interferences.

**Search for long-lived radionuclides as signatures of a recent close-by supernova explosion**

Some ten years ago, it was pointed out that some radionuclides produced in a supernova explosion might have been incorporated into terrestrial archives [19]. We continue to explore the AMS detection of very feeble natural traces of such long-lived radionuclides, like $^{244}$Pu ($t_{1/2}$ = 81 Ma) and $^{247}$Cm (15.6 Ma). These isotopes may be present on Earth in suitable archives (e.g. deep-sea sediments [20] and deep-sea manganese crusts [21]) as the remnants of supernovae, which happened "close" in space and time (<100 light-years, < 100 million years ago). Such a finding would be of great interest in nuclear astrophysics complementing the recent detection of possibly supernova-produced $^{60}$Fe [22]. The principle of the measurement is similar as for environmental samples. The expected extremely small concentrations makes AMS the favorite method.

**References**


[1] W. Kutschera, Int. J. Mass Spectrom. 242 (2005)145.
[2] C. Tuniz, J.R. Bird, D. Fink and G.F. Herzog, CRC Press, Boca Raton, Boston, London, New York, Washington, D.C (1998).
[3] P. Steier, R. Golser, W. Kutschera, A. Priller, C. Vockenhuber, A. Wallner, S. Winkler, Nucl. Instr. and Meth. B240 (2005) 445.
[4] P. Steier, R. Golser, W. Kutschera, A. Priller, C. Vockenhuber, V. Liechtenstein, Nucl. Instr. and Meth. B 188 (2002) 283.
[5] C. Domingo-Pardo et al, Phys. Rev. C74 (2006) 025807.
[6] A. Borella et al., AIP Conf. Proc. Vol. 769, Proc. Nuclear Data for Science and Technology 2004, Santa Fe, New Mexico (USA), pp. 652-658, 2005.
[7] S. Bisterzo et al., in Proc. Nucl. Data for Science and Technology, 2007, Nice, France, EDP Sciences, 2008, pp. 1333-1336.
[8] H. Nassar, M. Paul et al., Phys. Rev. Lett. 96 (2006) 041102.
[9] M. Paul et al., Nucl. Phys. A718 (2003) 239c.
[10] G. Rugel et al., Nucl. Instr. and Meth. B259 (2007) 683.
[11] W. Ratynski, F. Käppeler, Phys. Rec. C37 (1988) 595.
[12] A. Wallner et al., Journal of Physics G **35** (2008) 014018 ; and A. Wallner et al., Nucl. Instr. and Meth. B259 (2007) 677.
[13] see e.g. Holden, N.E., Pure Appl. Chem. 62, 941 (1990); and http://www-nds.iaea.org/wallet/.
[14] S. Fetter, E.T. Cheng and F.M. Mann, Fus. Engrg. Des. 13 (1990) 239.
[15] A. Wallner et al., AIP Conf. Proc. Volume 769, Proc. Nuclear Data for Science and Technology 2004, Santa Fe, New Mexico (USA), pp. 621-624, 2005.
[16] A. Wallner et al., in Proc. Nucl. Data for Science and Technology, 2007, Nice, France, EDP Sciences, 2008, pp. 1007-1010.
[17] E. Hrnecek et al., J. Radioanal. Nucl. Chem. 276, (2008) 789.
[18] E. Hrnecek, P. Steier, and A. Wallner, Applied Radiation and Isotopes 63 (2005) 633.
[19] J. Ellis, B. D. Fields, and D. N. Schramm, Astrophys. J. 470, 1227 (1996).
[20] M. Paul et al., Astrophys. J. Lett. 558 (2001) L133; and M. Paul et al., Nucl. Phys. A719 (2003) C29.
[21] C. Wallner, T. Faestermann, U. Gerstmann, K. Knie, G. Korschinek, C. Lierse, G. Rugel, New Astr. Rev. 48 (2004) 145.
[22] K. Knie et al., Phys. Rev. Lett. 93 (2004) 171103.

# Author index

European Commission

**EUR 24692 EN – Joint Research Centre – Institute for Reference Materials and Measurements**
Title: NEMEA-5, Neutron measurements, evaluations and applications – Nuclear data for sustainable nuclear energy
Editor: Arjan Plompen
Luxembourg: Publications Office of the European Union
2011 – 126 pp. – 21.0 x 29.7 cm
EUR – Scientific and Technical Research series – ISSN 1018-5593
ISBN 978-92-79-19067-4
doi:10.2787/36236

**Abstract**
The CANDIDE workshop NEMEA-5, Neutron Measurements, Evaluations and Applications, Nuclear data for sustainable nuclear energy was held from 27-29 October 2008 in Ljubljana, Slovenia. These proceedings collect the full papers summarising the contributions to this workshop.

The mission of the JRC is to provide customer-driven scientific and technical support for the conception, development, implementation and monitoring of EU policies. As a service of the European Commission, the JRC functions as a reference centre of science and technology for the Union. Close to the policy-making process, it serves the common interest of the Member States, while being independent of special interests, whether private or national.

JRC
EUROPEAN COMMISSION

LA-NA-24692-EN-C

ISBN 978-92-79-19067-4